Attachment 4

Model Performance Evaluation

This attachment to the Technical Support Document discusses model performance of both the "regular" and "adjusted" base cases.

Model Performance Statistics

The first assessment of model performance is usually an analysis of the standard EPA-recommended performance measures: relative bias, relative gross error, and unpaired peak accuracy. These statistics provide a benchmark for determining what episode days should be used in further analysis, or, more appropriately, provide a measure of the confidence that should be placed on the modeling when using the model to evaluate control strategies. The criteria associated with the statistics do not constitute a pass-fail test for episode days, but are a useful first assessment of model performance. Even when the model performance exceeds the minimum requirements, however, model performance must be judged on a number of additional criteria, which, unfortunately, are much less easily quantified.

Table 1 shows model performance statistics for the unadjusted base case, including the August 24 ramp-up day (model performance was poor on the first two ramp-up days even with meteorological and inventory adjustments). The statistics are calculated for monitors in the eight HGA counties only. Note that September 1, 2000 was not modeled as part of the Base4a series of model runs. This day suffered from serious model performance problems, and to conserve both staff and computing resources it was decided to halt the modeling analysis a day early. The TCEQ will continue to analyze September 1, and if possible include modeling for that day in the Mid-Course Review. Note that the peak observed values in the table have changed since the June 2002 proposal due to inclusion of monitored ozone concentrations at the La Porte airport.

Table 1: Base4a.regular model performance in HGA 8-county area (4 km grid)

Statistic	EPA range	Date							
		8/24	8/25	8/26	8/27	8/28	8/29	8/30	8/31
Normalized Bias (%)	< +/-15	-28.5	-35.1	-12.6	2.9	5.6	-13.1	-11.6	-1.1
Normalized Gross Error (%)	< 35	30.3	37.4	17.4	7.0	12.5	18.8	20.1	13.7
Peak Observed (ppb)		120	194	140	87	112	146	201	176
Peak Pred (ppb)		89	113	115	97	104	102	108	133
Accuracy of Peak (%)	< +/-20	-26.1	-42.0	-18.2	11.4	-7.4	-30.3	-46.2	-24.0

The normalized bias figures in Table 1 show that the model generally underpredicts ozone concentrations on August 24 and 25. Although the model produces acceptable levels of bias thereafter, substantial underprediction is still seen on August 26, 29, and 30. Normalized gross error is quite large on August 24 and 25, primarily owing to the large biases on those days. The model shows moderate gross error for the remainder of the episode.

The major performance issue is the model's inability to produce peak ozone concentrations approaching the high monitored values on August 25, 29, 30, and 31. In fact, the only day in

which an exceedance of the NAAQS was simulated was August 31, with no other day predicting ozone peaks over 110 parts/billion. In general, the model appears to be simulating ozone concentrations reasonably well when the monitors recorded low-to-moderate ozone, but fails to reproduce the highest values.

After running numerous sensitivity analyses, the TCEQ staff picked a model configuration that was both based on measured aerometric data and performed well for the days of primary interest: August 25, 29, 30 and 31. When the PBL and emissions adjustments described in the body of the Technical Support Document are employed, model performance improves substantially for the four days of primary interest. Table 2 shows model performance for the Base4a.pt_o2no_070pbl base case for the 4-km grid, and Table 3 shows model performance in the 1-km flexi-nest grid only. Note that the 1-km grid was only used on August 25 and 29-31.

Table 2: Base4a.pt_o2n2_070pbl model performance in HGA 8-county area (4 km grid)

Statistic	EPA range	Date							
		8/24	8/25	8/26	8/27	8/28	8/29	8/30	8/31
Normalized Bias (%)	< +/-15	-15.0	-15.6	-3.6	18.6	22.4	-2.5	-11.3	1.9
Normalized Gross Error (%)	< 35	22.3	33.8	16.7	19.3	25.8	20.9	21.8	14.3
Peak Observed (ppb)		120	194	140	87	112	146	201	176
Peak Pred (ppb)		107	198	142	124	128	156	149	161
Accuracy of Peak (%)	< +/-20	-10.5	2.0	1.5	42.1	14.1	7.1	-25.7	-8.4

Table 3: Base4a.pt_o2n2_070pbl model performance in 1-km flexi-nest grid

Statistic	EPA range	Date			
		8/25	8/29	8/30	8/31
Normalized Bias (%)	< +/-15	-17.2	2.4	-10.7	2.7
Normalized Gross Error (%)	< 35	34.3	22.6	23.6	14.3
Peak Observed (ppb)		194	146	201	176
Peak Pred (ppb)		209	160	161	173
Accuracy of Peak (%)	< +/-20	7.6	9.6	-19.7	-1.7

Overall, model performance with the Base4a.pt_o2n2_070pbl is seen to be much better than seen with the unadjusted (Base4a.regular) base case. Model performance with the adjusted base case meets the minimum EPA statistical requirements on August 26, 29, and 31 using the 4-km grid, and meets performance specifications on August 29, 30, and 31 when using the flexi-nest grid (note August 26 was not run with flexi-nesting). Additionally, model performance for August 25 narrowly misses because of general underprediction of ozone, even though the peak on that day

is larger than observed. The major performance issue on August 25 appears to be a northerly displacement of the modeled ozone from the area in western Harris County where the majority of ozone exceedances were recorded that day. Had the modeled winds been a rotated a few degrees counterclockwise, it is likely that model performance would have been quite good on August 25. The next section provides plots showing daily peak ozone for each modeled day; the plots for August 25 clearly show the displacement of the peak on August 25.

Daily Peak Ozone Plots and Daily Performance Summaries

The plots in this section show the daily peak ozone modeled in each grid cell for each episode day, excluding ramp-up days. Both the adjusted and unadjusted base cases are presented, and the one-kilometer flexi-nest grid is also shown for the adjusted base case. Note that the 4-km plots are only presented for the western portion of the 4-km grid to provide better resolution in the nonattainment area.

Daily Modeled Peak Ozone for August 24, 2000, Unadjusted Base Case

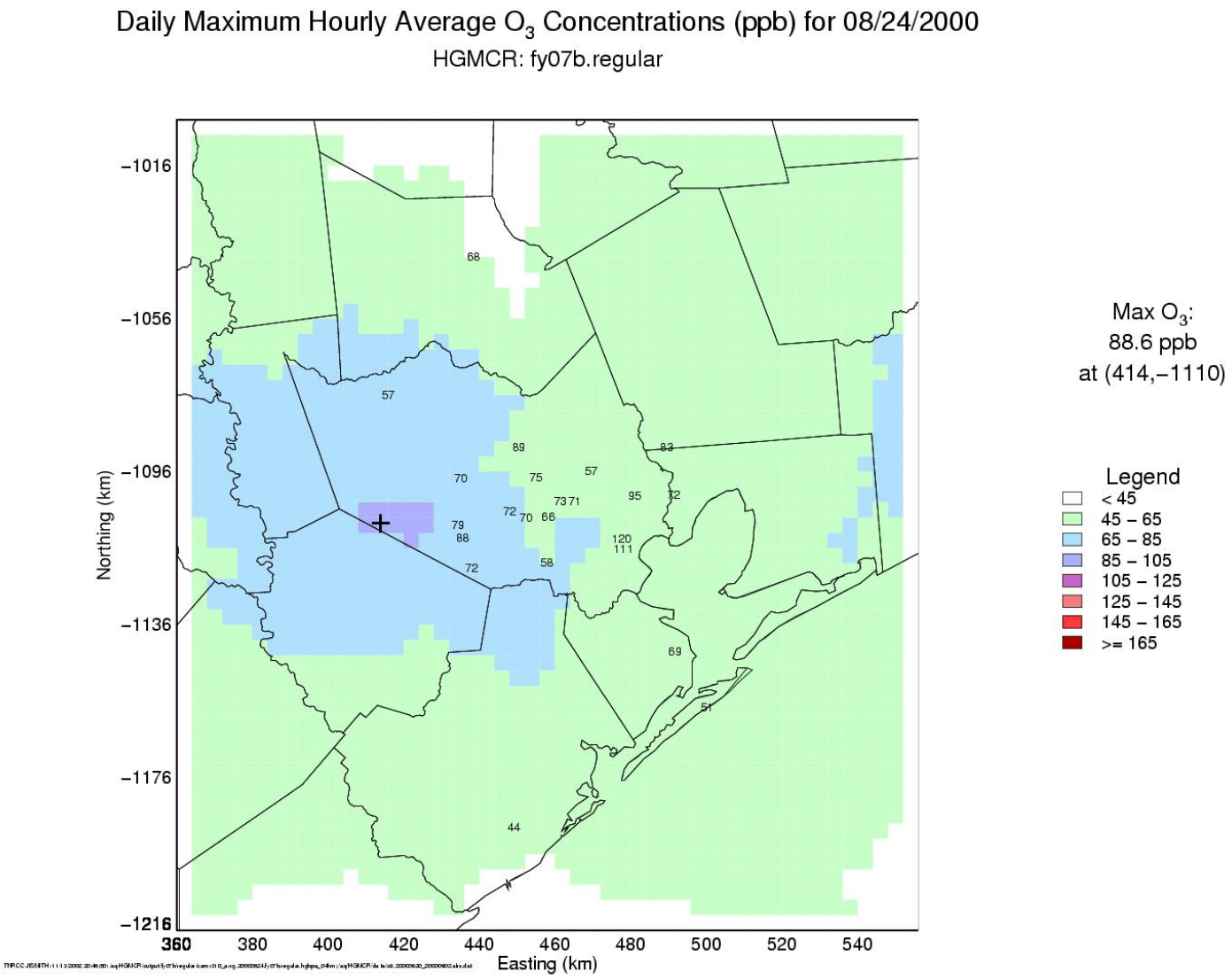

Daily Modeled Peak Ozone for August 24, 2000, Adjusted Base Case

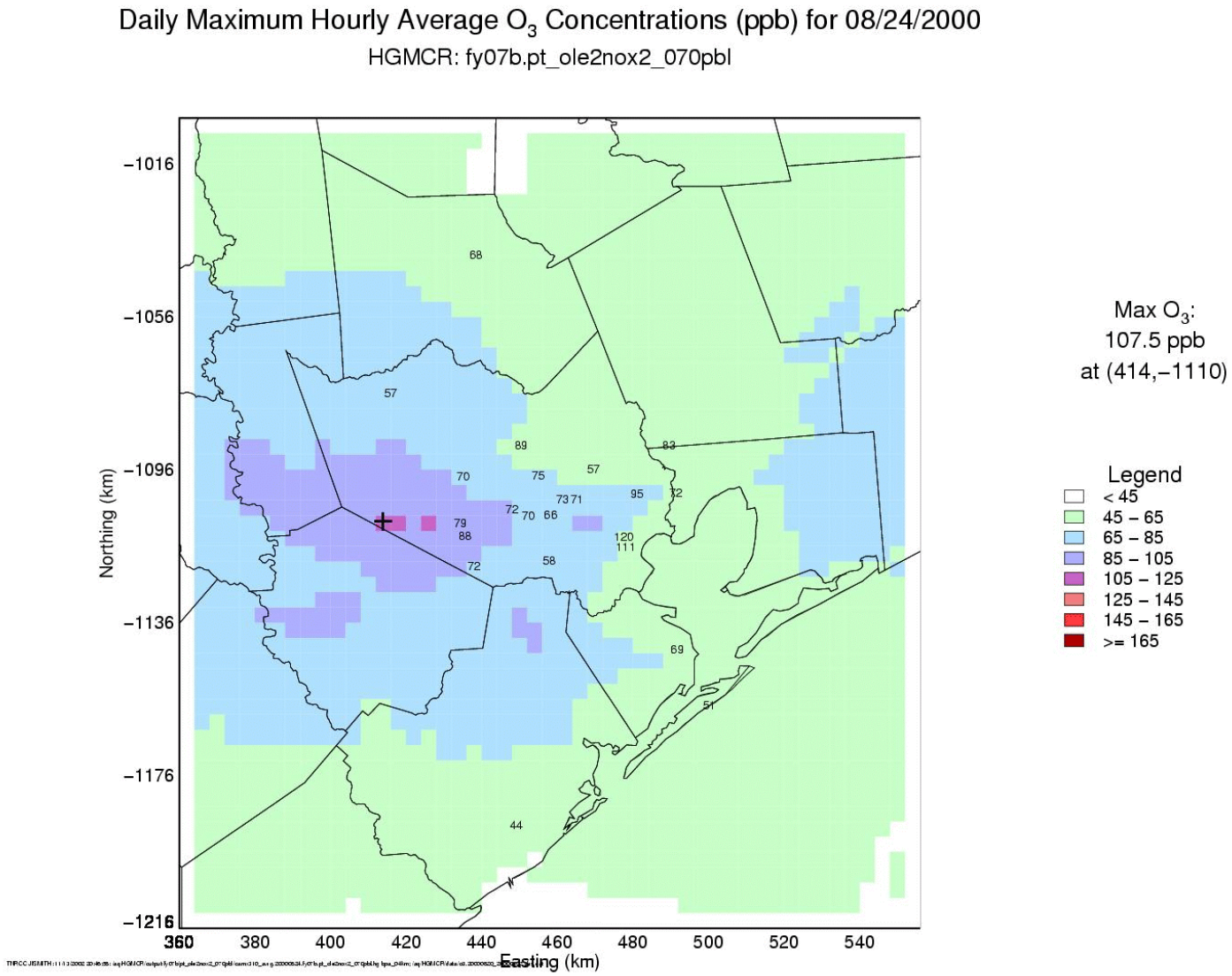

Model performance summary, August 24 ramp-up day: Relatively low ozone was measured this day (120 ppb max). Neither the adjusted nor the unadjusted base case performed well, showing underprediction biases. Modeled peaks were located in western Harris County, whereas the measured peak was in Deer Park area.

Daily Modeled Peak Ozone for August 25, 2000, Unadjusted Base Case

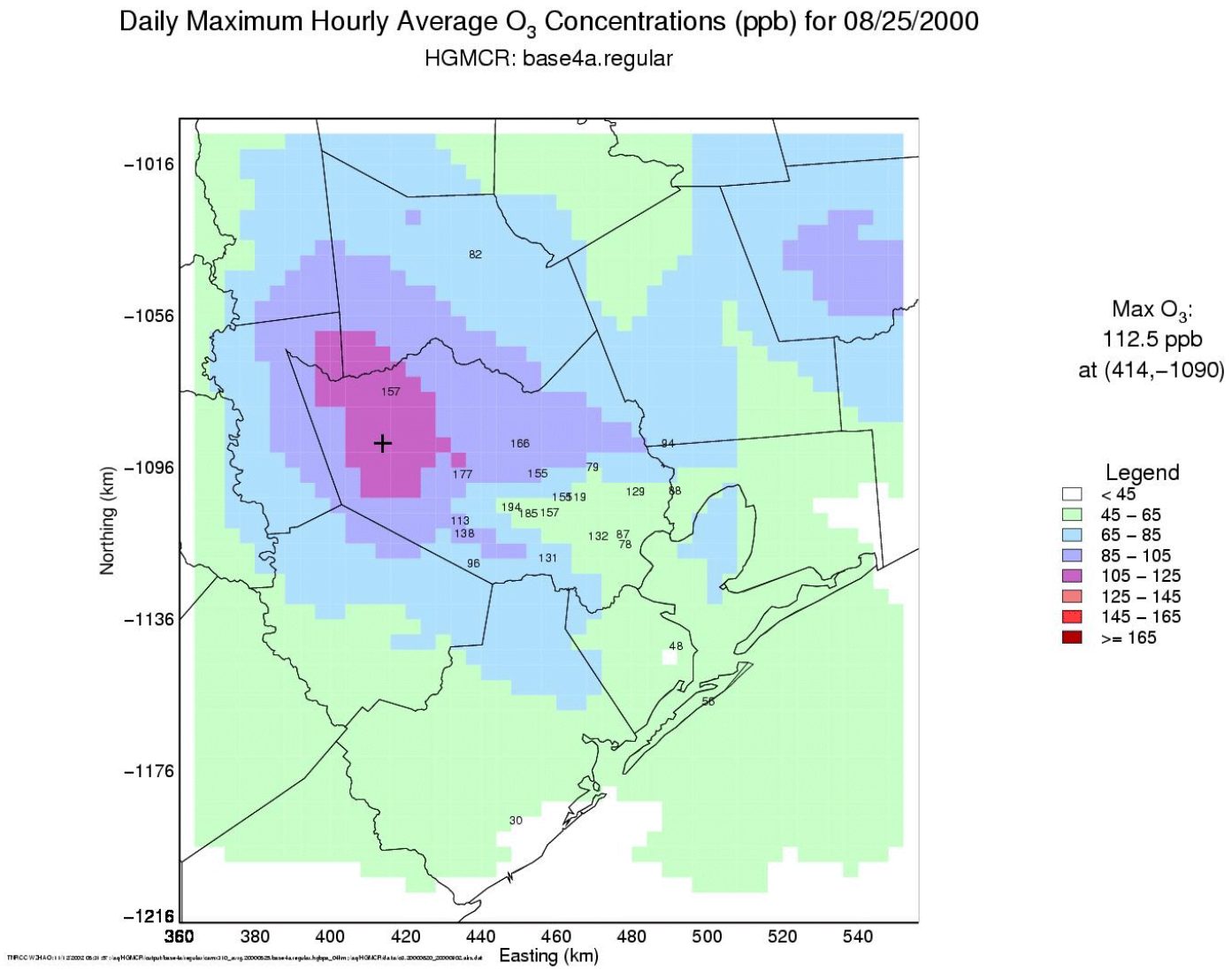

Daily Modeled Peak Ozone for August 25, 2000, Adjusted Base Case

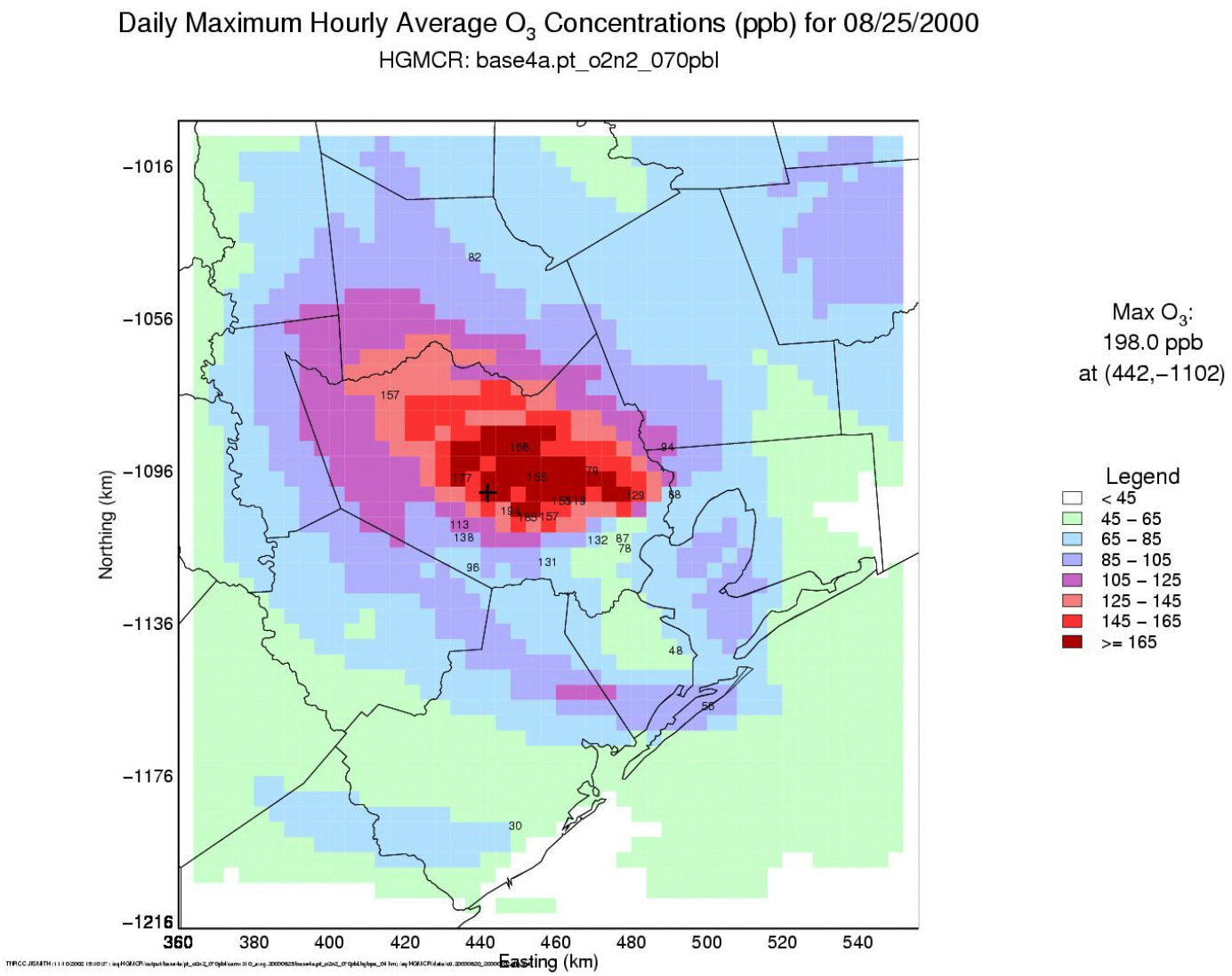

Daily Modeled Peak Ozone for August 25, 2000, Adjusted Base Case, 1 Km Flexi-nest Grid

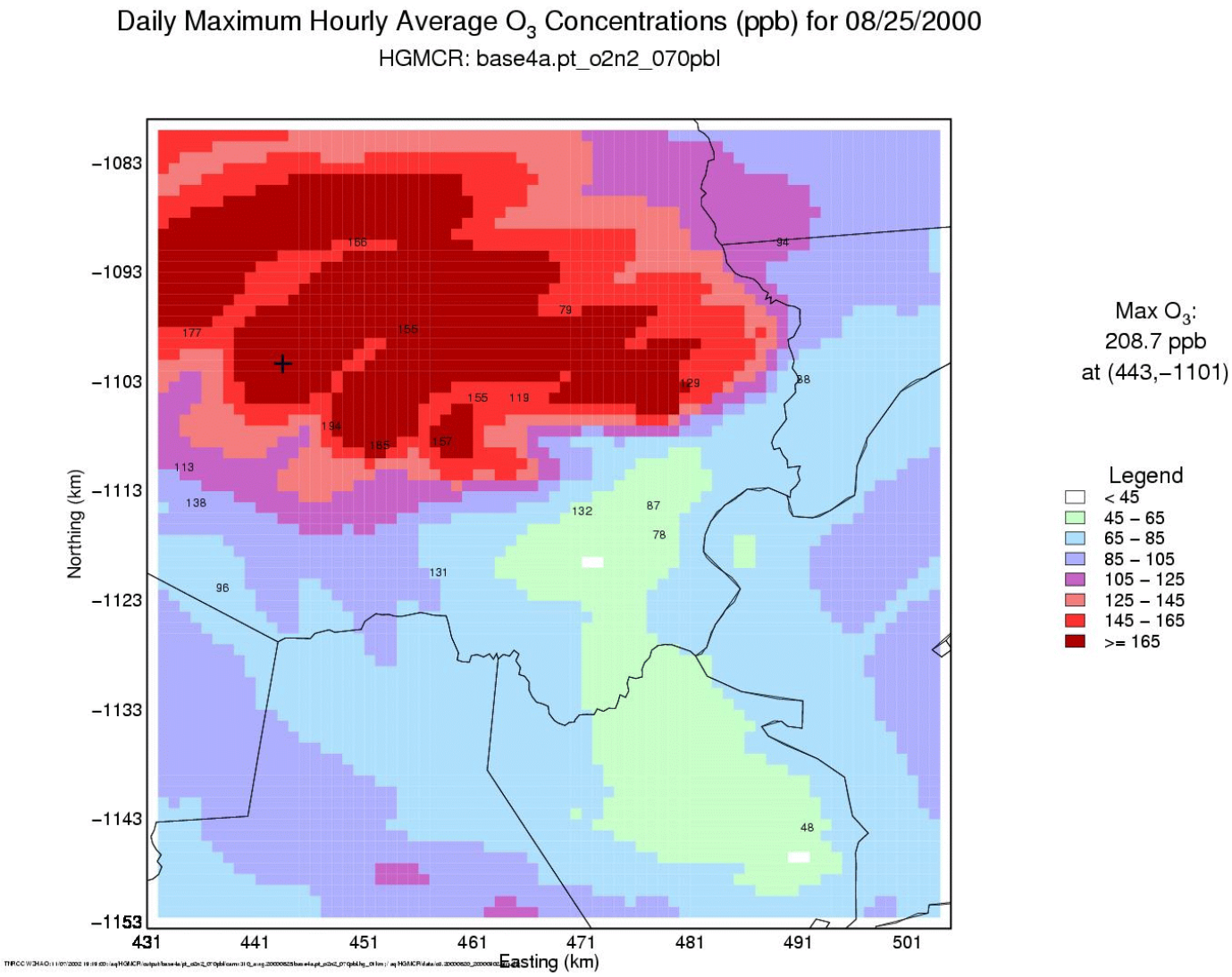

Model performance summary, August 25: The unadjusted base case failed to replicate the extremely high ozone concentrations observed this day. The adjusted base case replicated both the magnitude of the peak and its location very well, but overall suffers from an underpredictive bias. The modeled areas of highest ozone concentration originate in the ship channel and move west-northwest in the afternoon, while the observed ozone plume drifted more westward. It appears that a minor correction in wind direction could greatly improve model performance by bringing the modeled ozone plume across the highest monitors.

Another possible cause for the general underprediction on this day is insufficient emissions on the western end of Ship Channel. Adjustments to the emission of HRVOCs were applied to the modeling inventory, but similay adjustments have not yet been developed for less reactive VOCs

such as butanes. Automatic Gas Chromatograph show that high butane concentrations are often seen on the western end of the Ship Channel, and so the lack of an emission adjustment of these VOCs may result in less ozone in western Houston downwind of the western end of the Ship Channel.

After the La Porte lidar data was used to nudge the winds, the model began creating "spikes" at 07:00, which dissipate the next hour. The data plotted here have been post-processed to remove these "spikes". A discussion of the spike phenomenon, its causes and ramifications is presented in the next section.

Daily Modeled Peak Ozone for August 26, 2000, Unadjusted Base Case

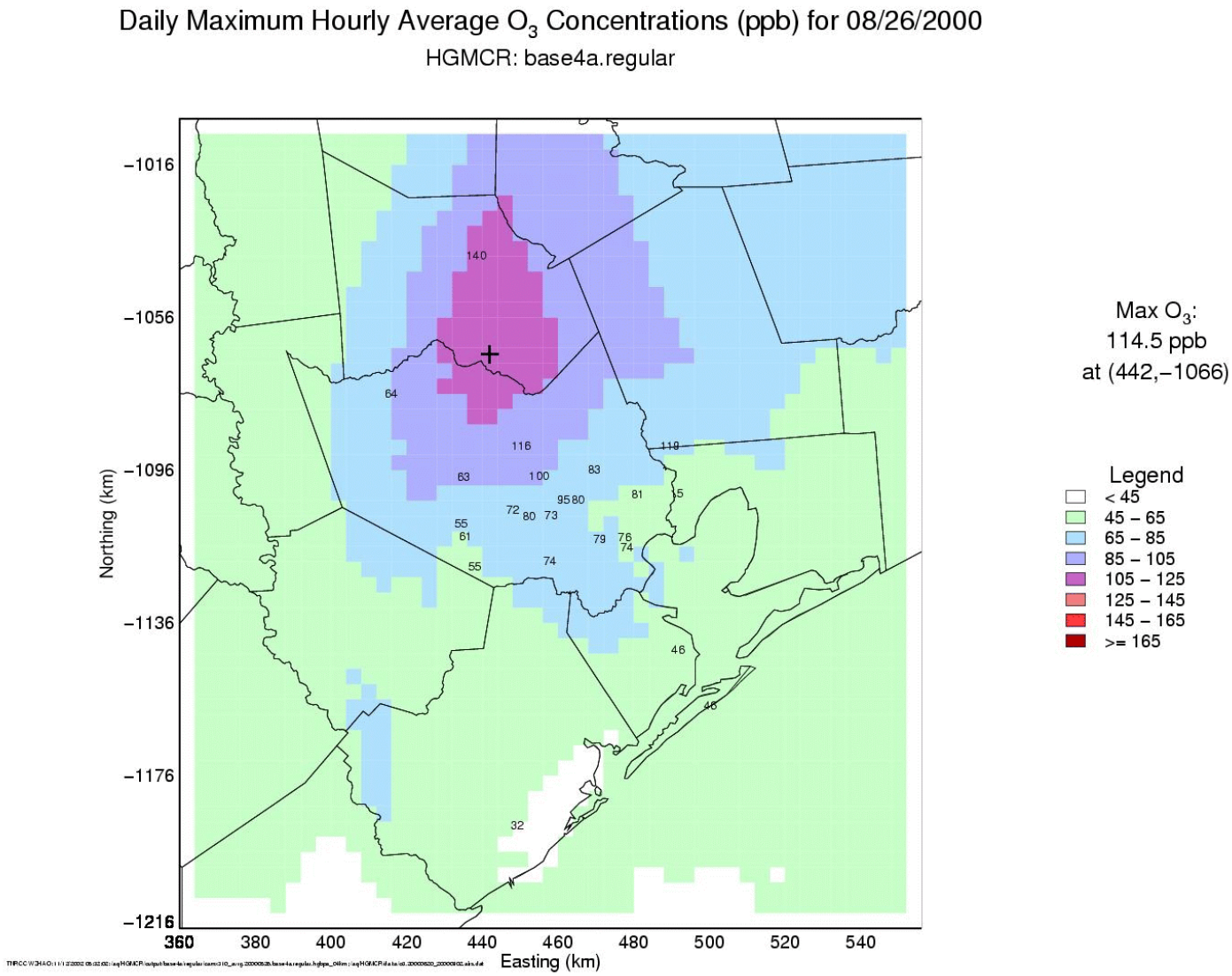

Daily Modeled Peak Ozone for August 26, 2000, Adjusted Base Case

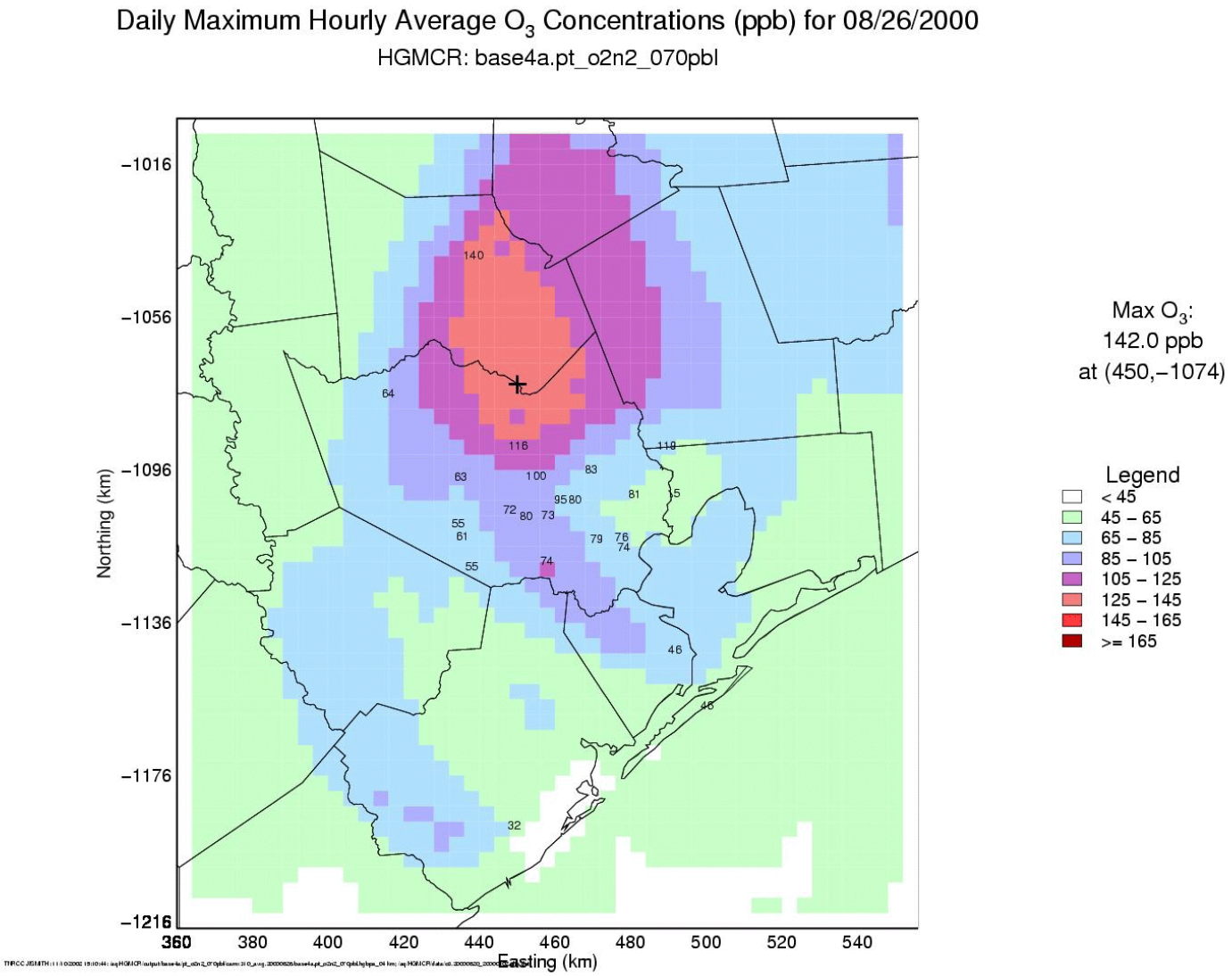

Model performance summary, August 26: Again the unadjusted base case suffered from a significant underprediction bias, but the adjusted base case performed quite well, locating a moderate ozone plume in northern Harris and eastern Montgomery Counties. The modeled peak was close in magnitude to the monitored peak, but occurred about 30 km south of the observed peak.

Daily Modeled Peak Ozone for August 27, 2000, Unadjusted Base Case

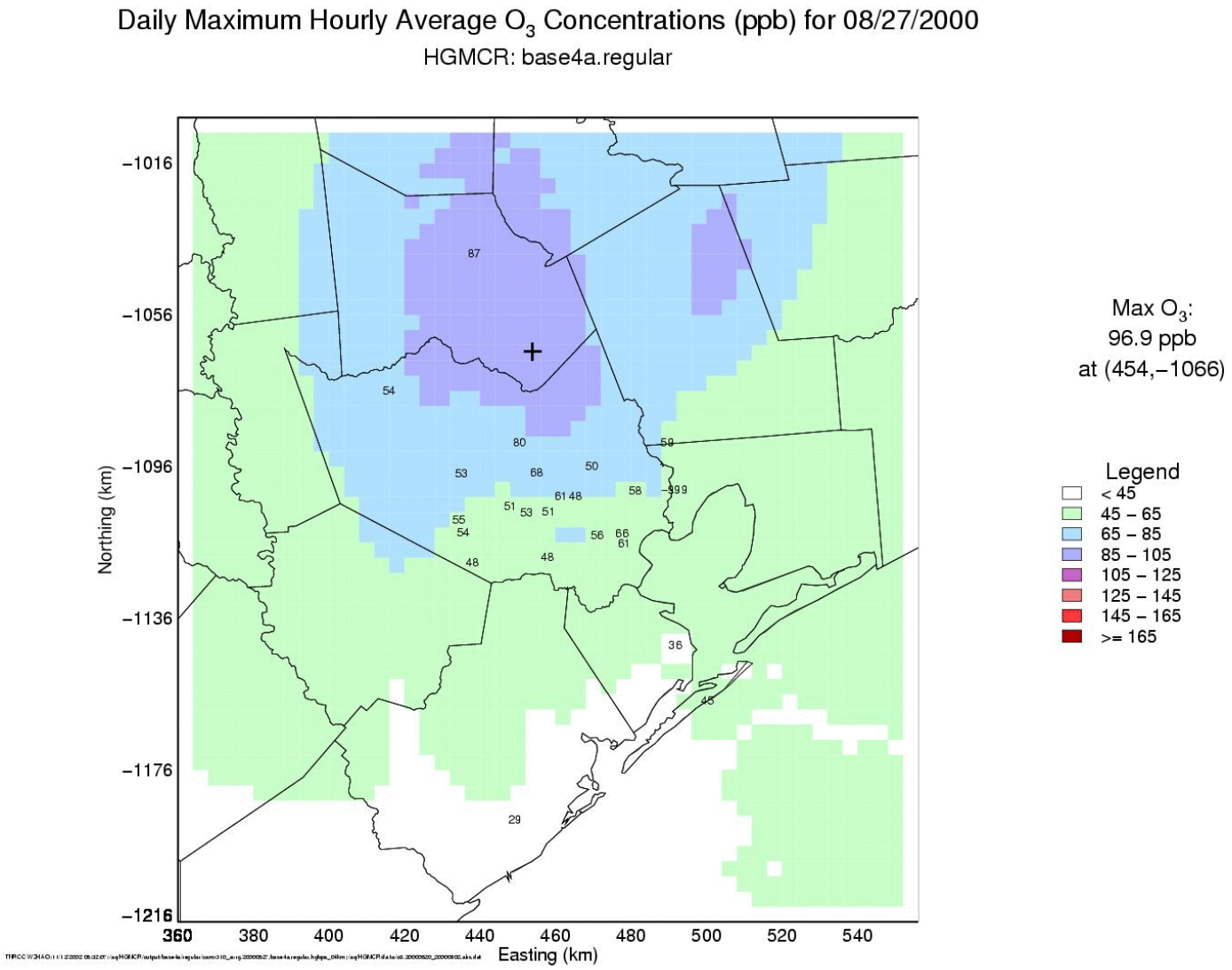

Daily Modeled Peak Ozone for August 27, 2000, Adjusted Base Case

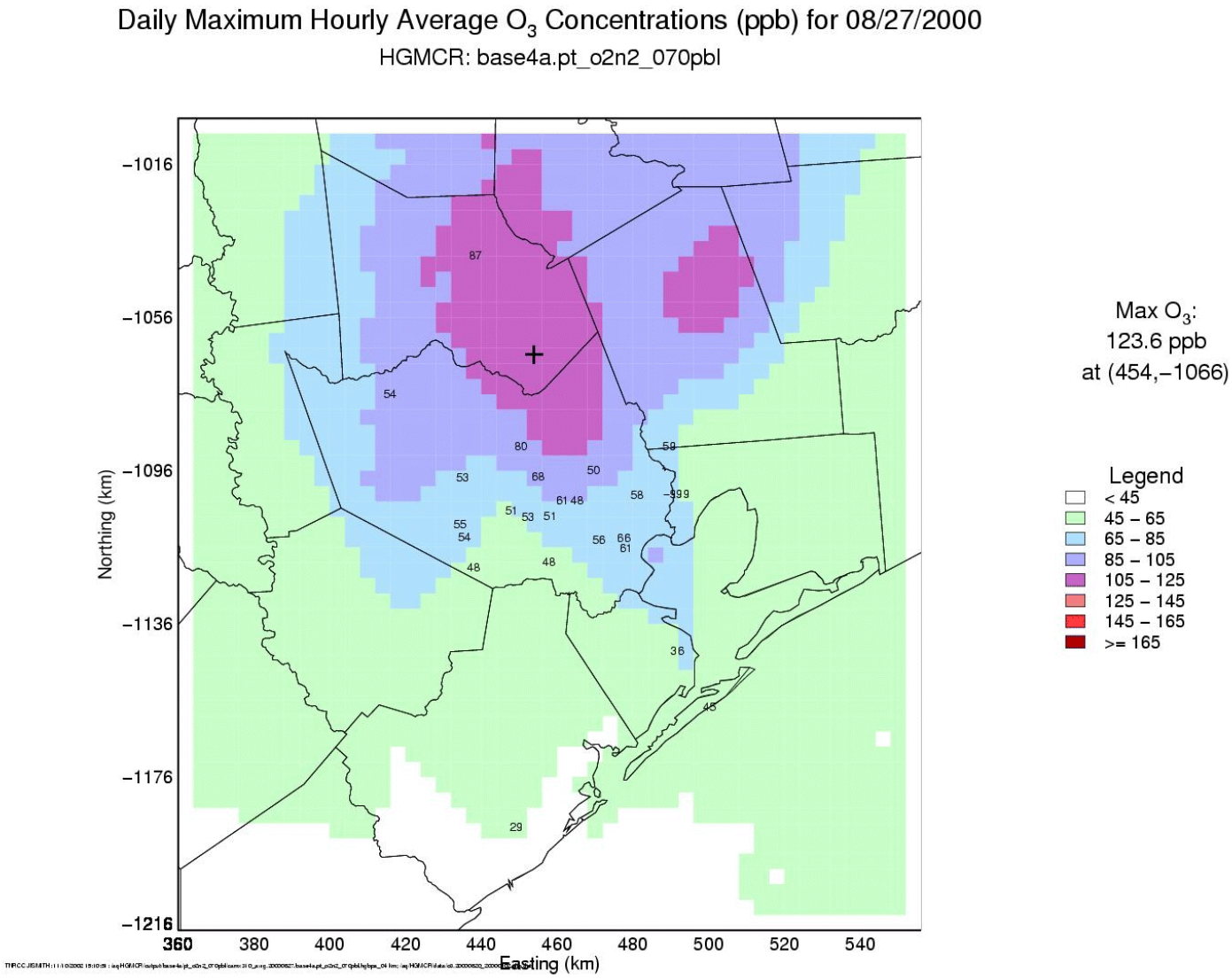

Model performance summary, August 27 & 28: On both the 27th and 28th, no high ozone concentrations were recorded in the area, and in both cases the unadjusted base case performed quite well. In both cases, the adjusted base case tended to generally overpredict ozone concentrations across the area. Persistent onshore flow, combined with deep mixing on these days contributed to the low ozone measurements. The overprediction seen in the adjusted base case may be due to wind speeds that are too low, to an emission adjustment that was too large on these particular days, or both.

Daily Modeled Peak Ozone for August 28, 2000, Unadjusted Base Case

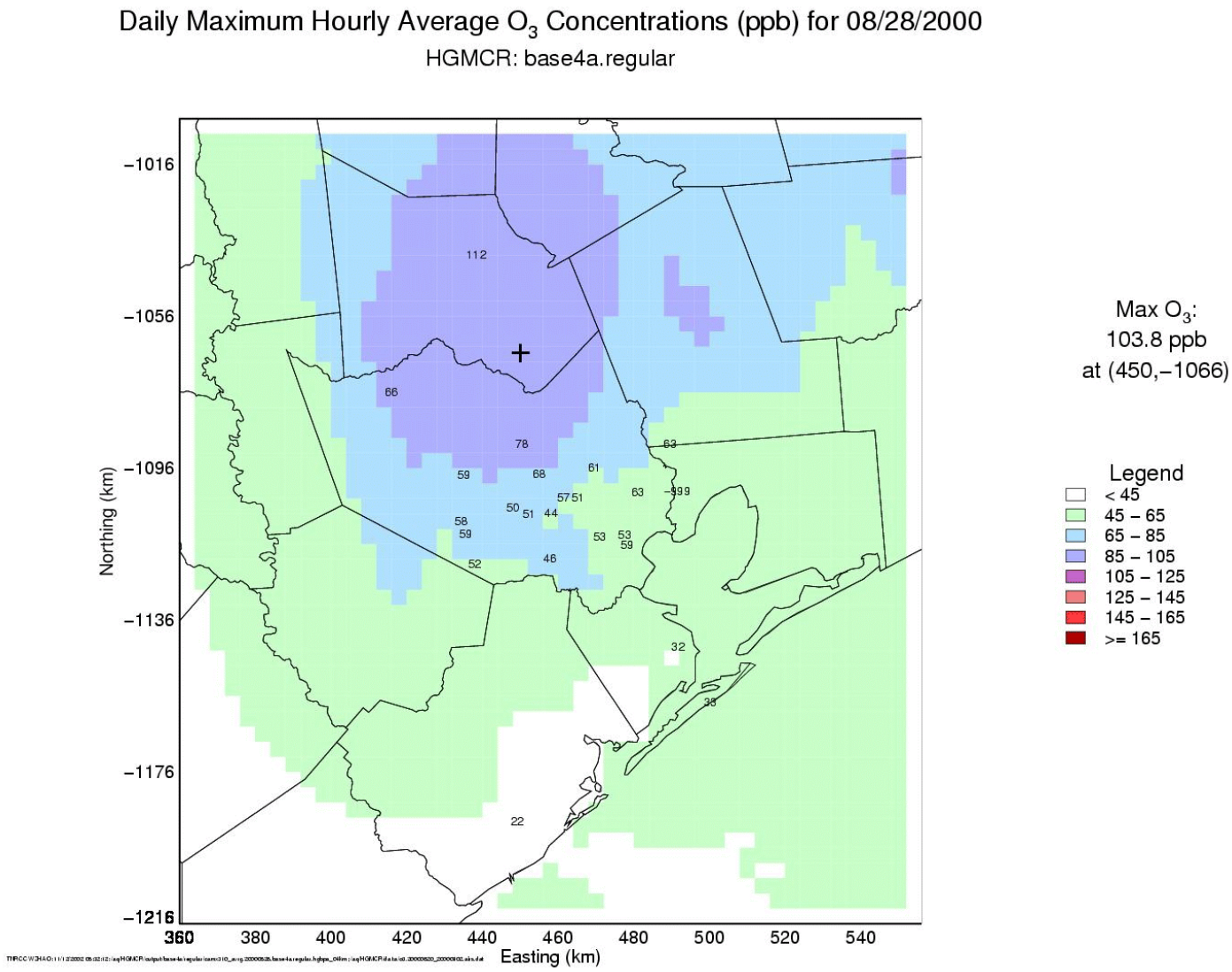

Daily Modeled Peak Ozone for August 28, 2000, Adjusted Base Case

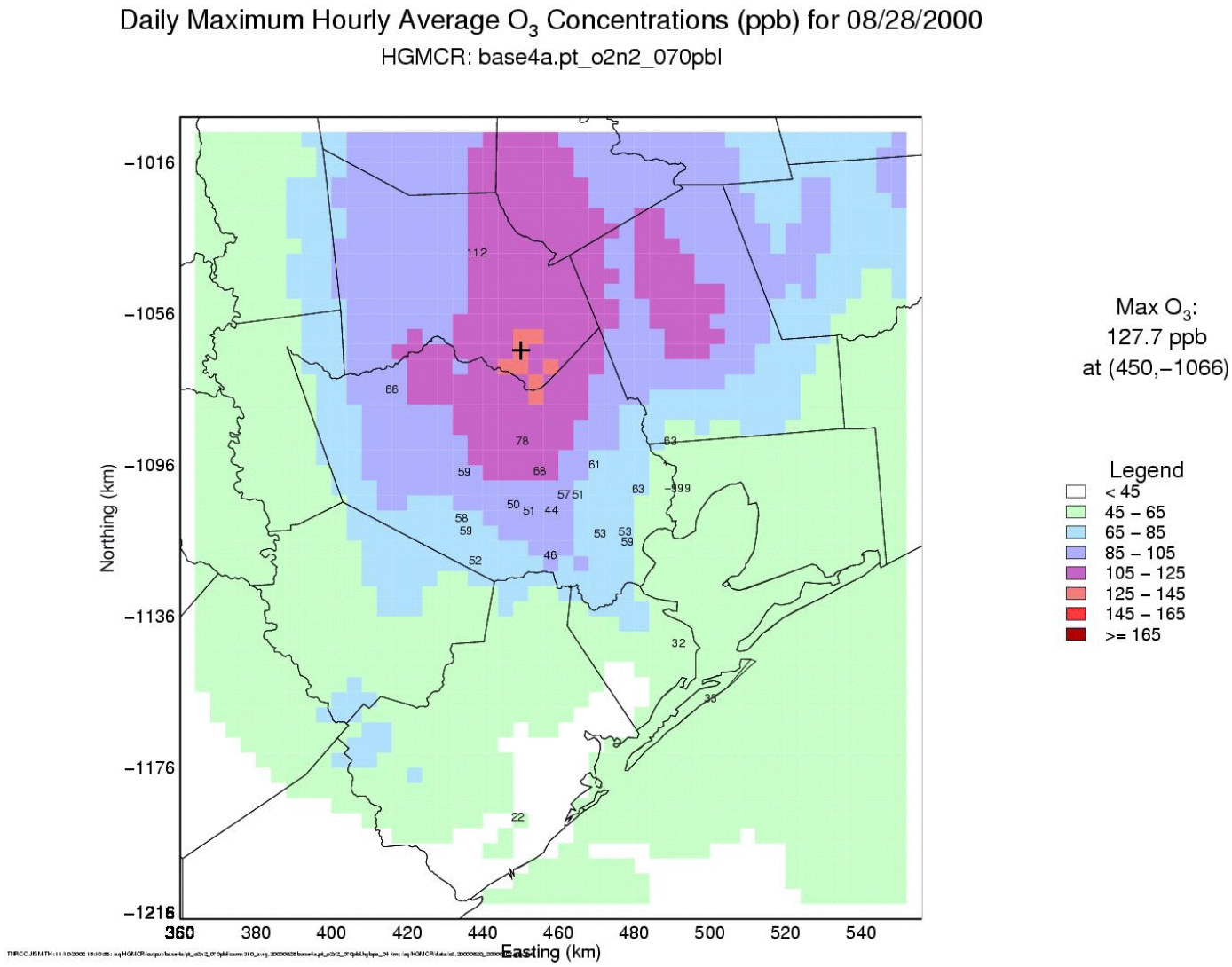

Model performance summary, August 28 - See August 27.

Daily Modeled Peak Ozone for August 29, 2000, Unadjusted Base Case

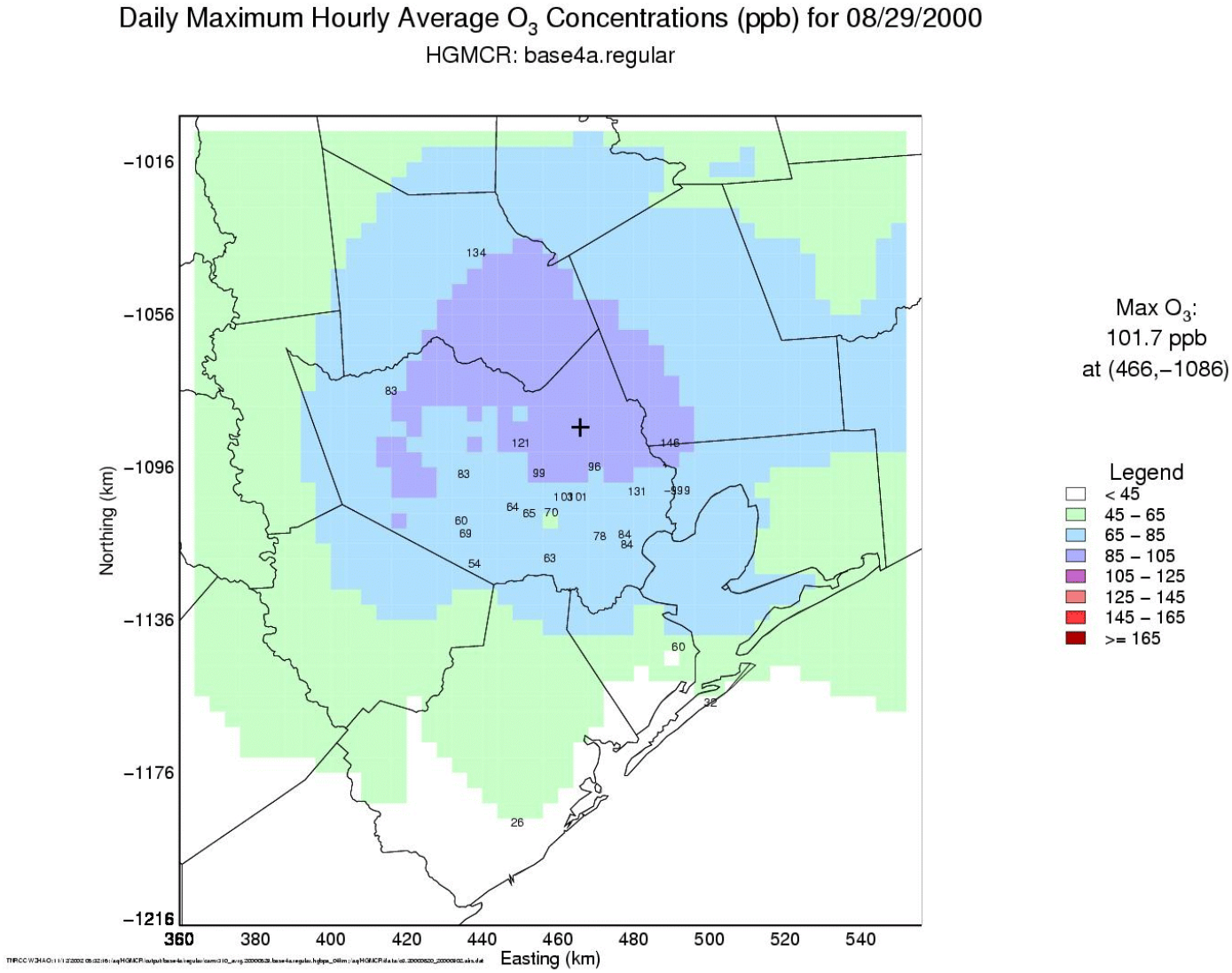

Daily Modeled Peak Ozone for August 29, 2000, Adjusted Base Case

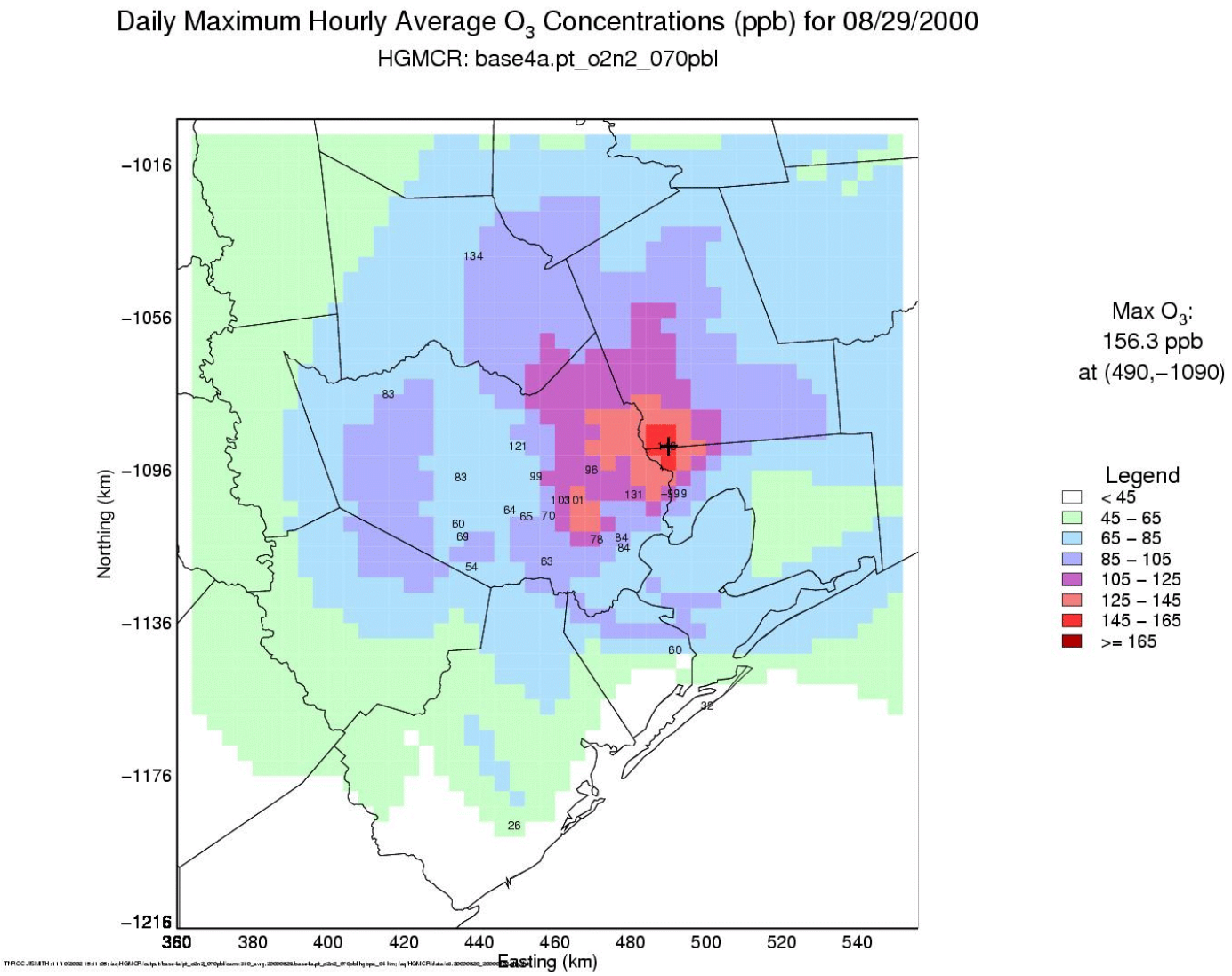

Daily Modeled Peak Ozone for August 29, 2000, Adjusted Base Case, 1 Km Flexi-nest Grid

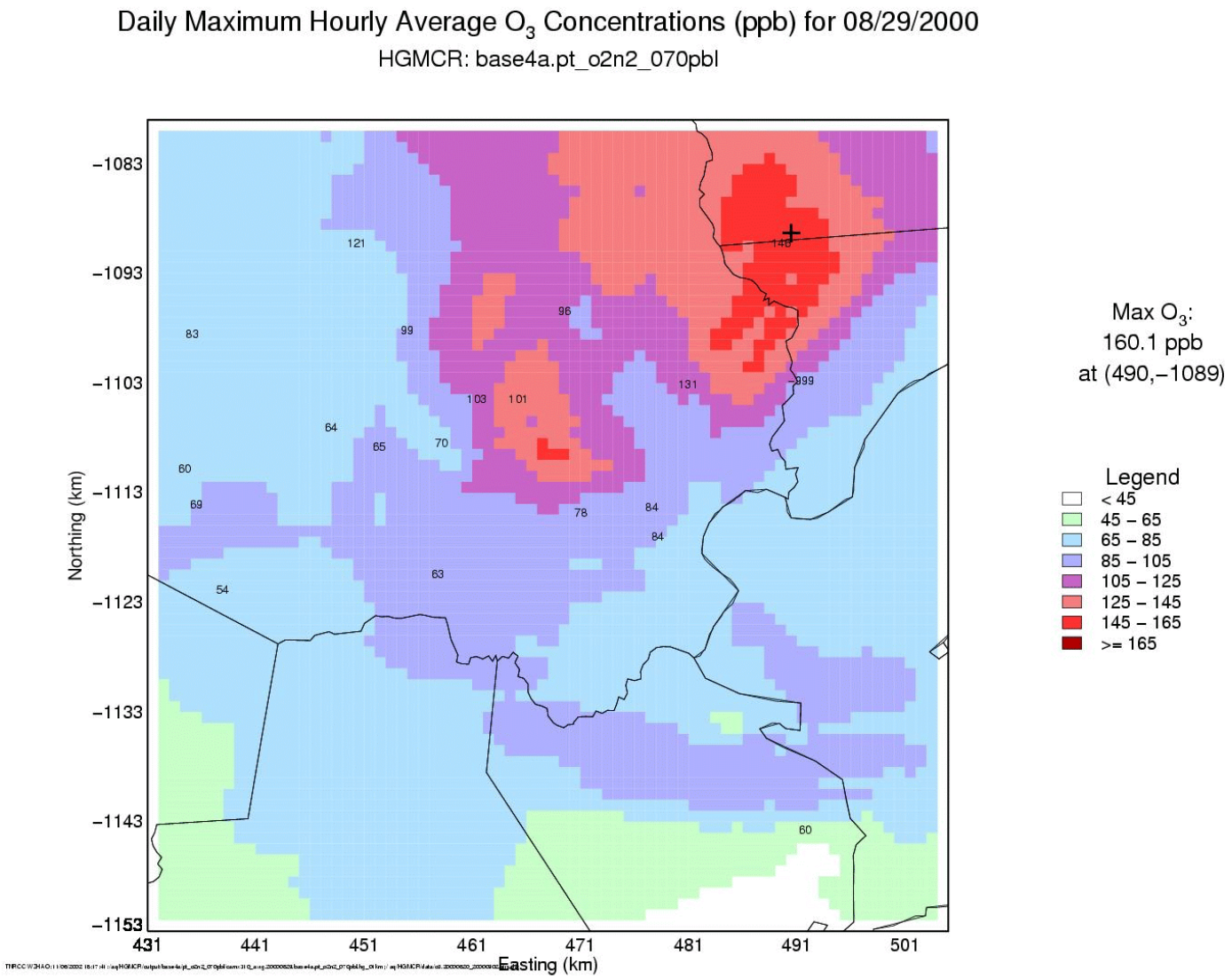

Model performance summary, August 29: Model performance for the adjusted base case is very good on this day, with almost no bias and moderate gross error. The modeled peak was located almost exactly at the location of the measured peak, but was 14 parts/billion higher. The unadjusted base case generally underpredicts ozone.

Daily Modeled Peak Ozone for August 30, 2000, Unadjusted Base Case

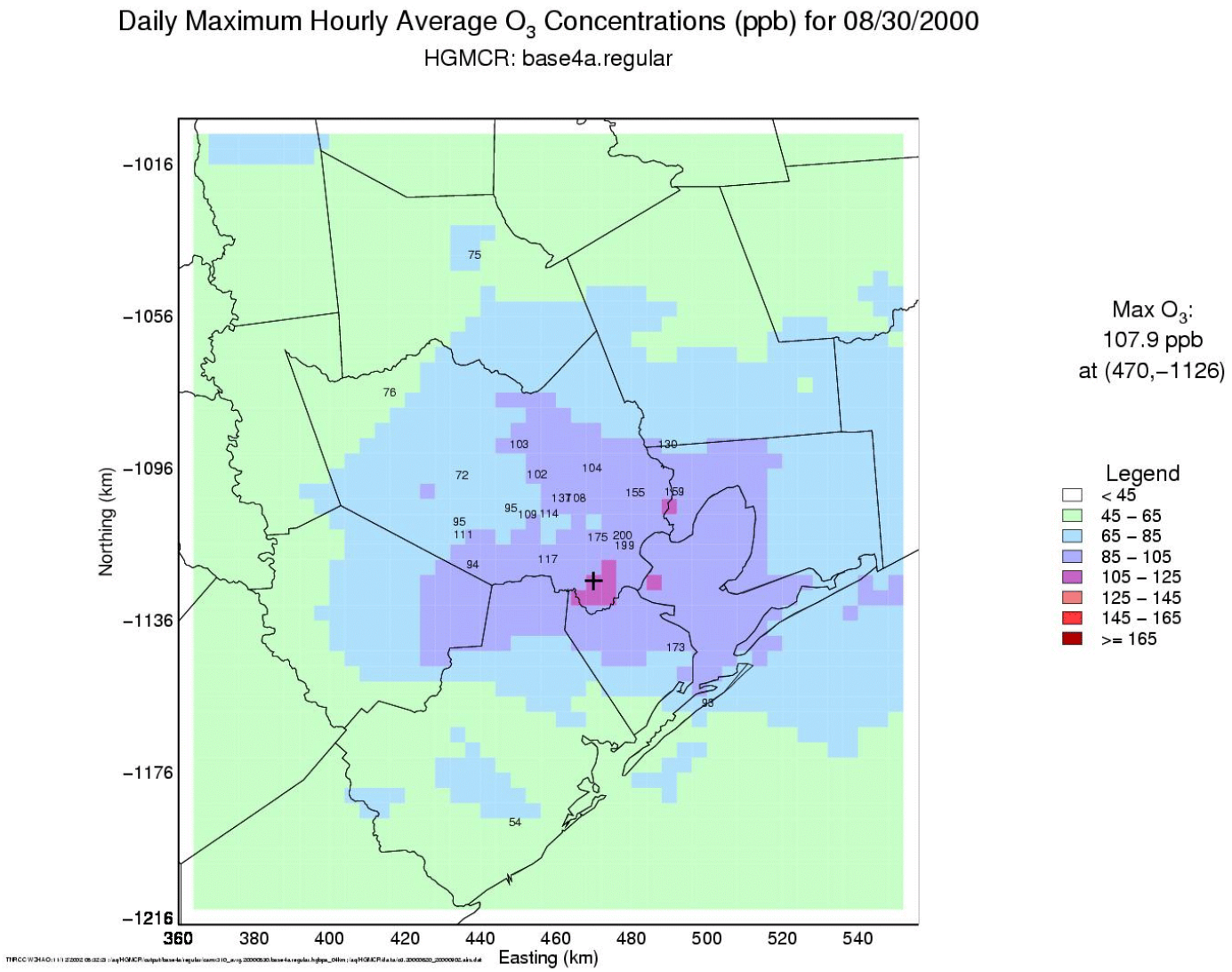

Daily Modeled Peak Ozone for August 30, 2000, Adjusted Base Case

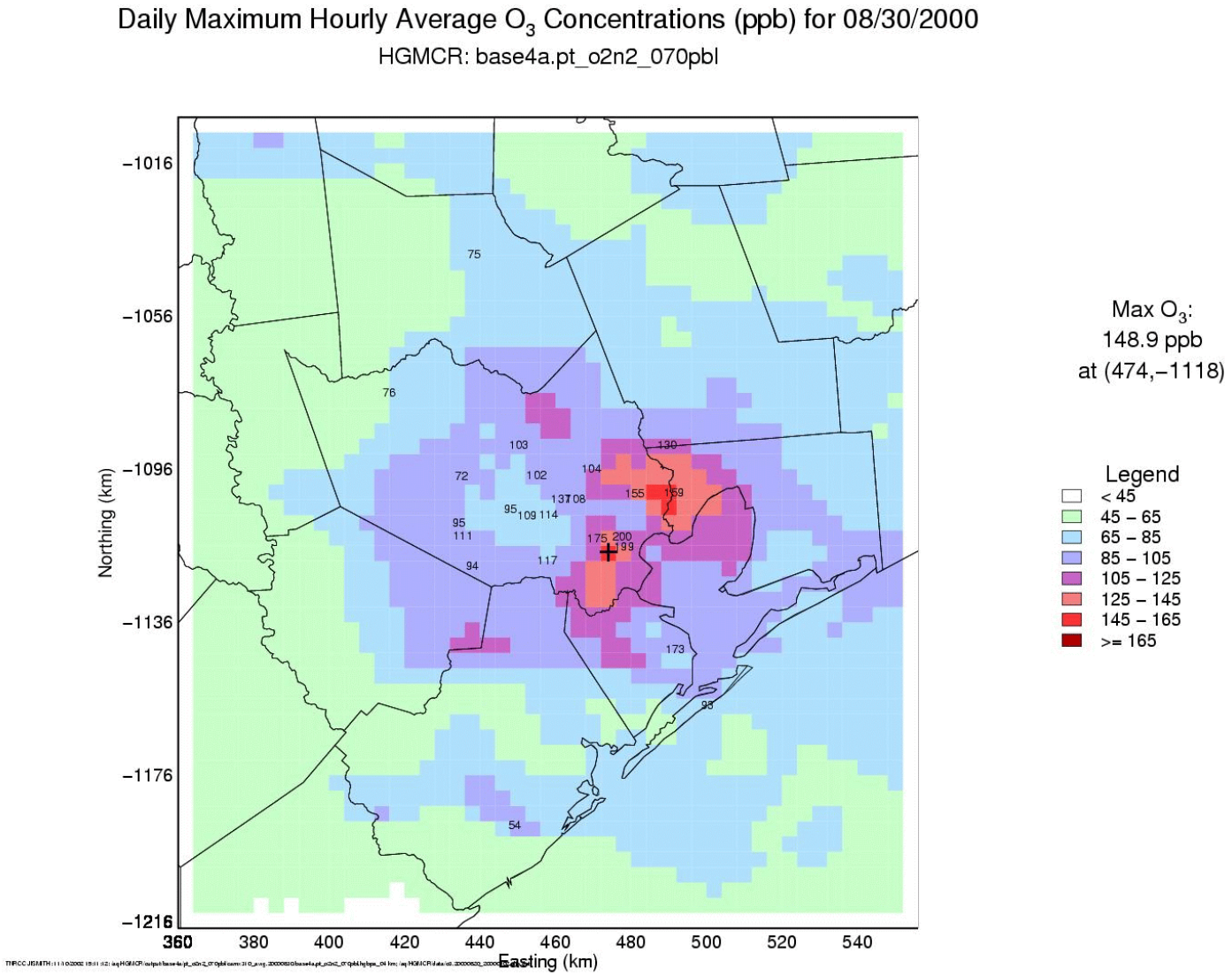

Daily Modeled Peak Ozone for August 30, 2000, Adjusted Base Case, 1 Km Flexi-nest Grid

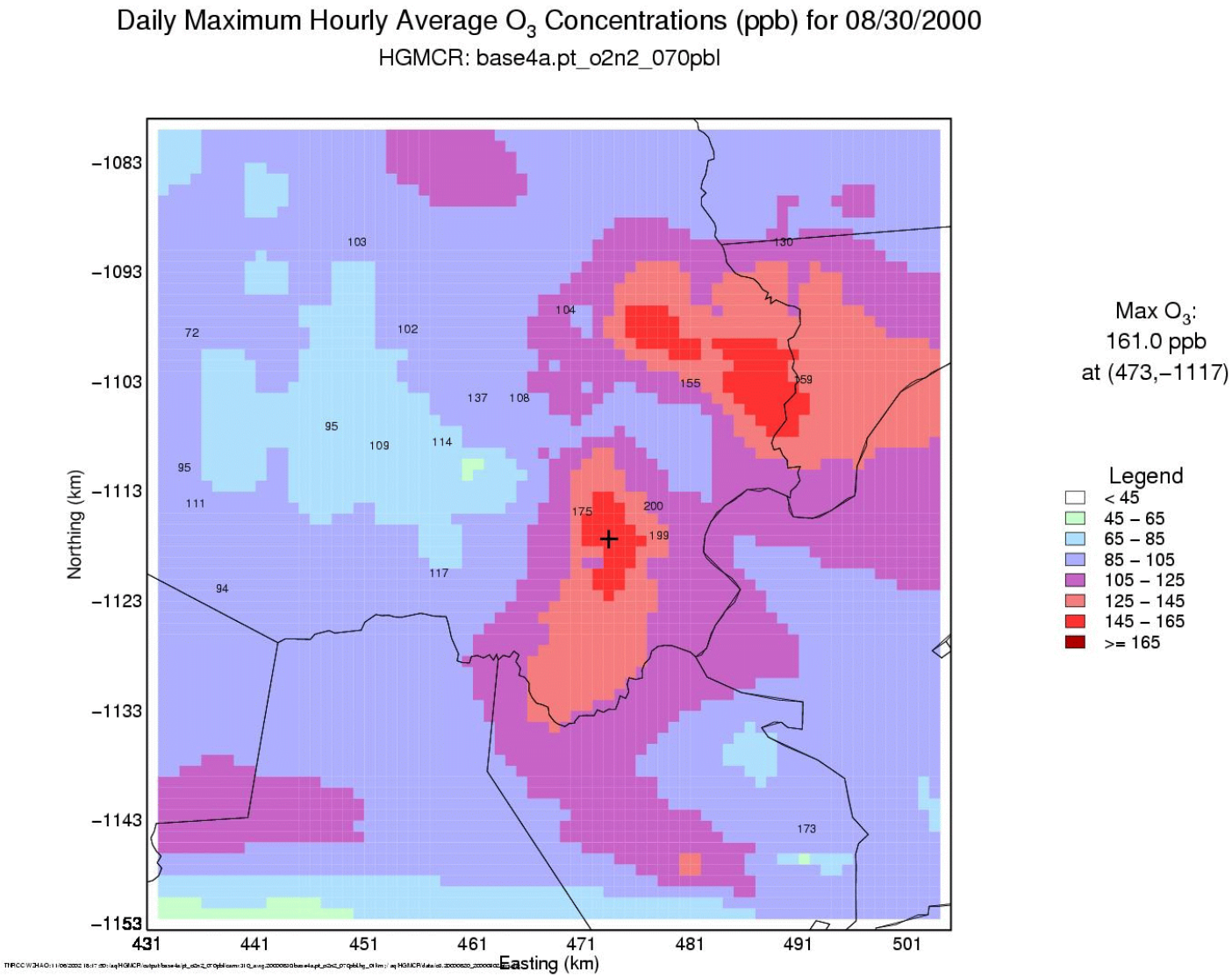

Daily Modeled Peak Ozone for August 31, 2000, Unadjusted Base Case

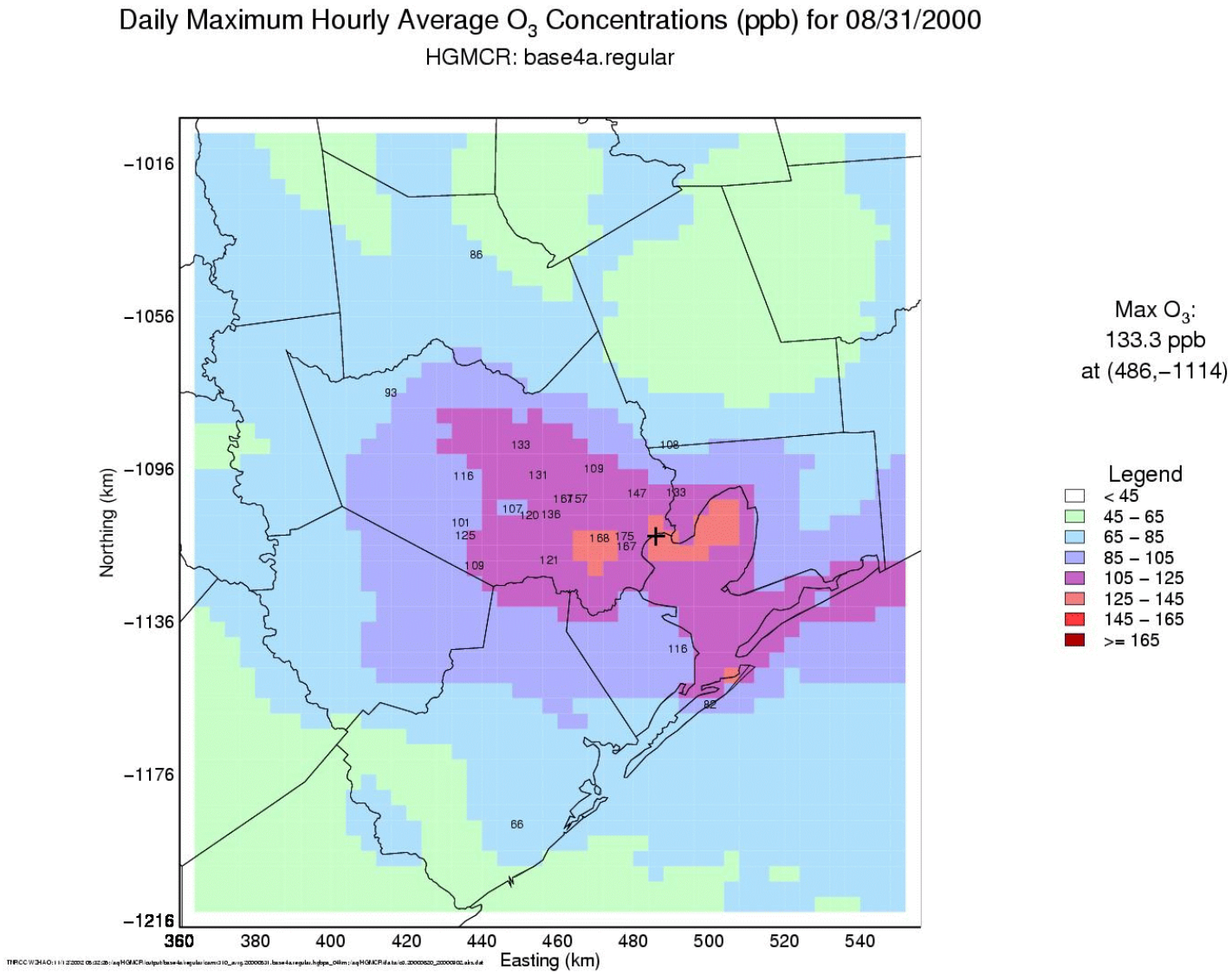

Model performance summary, August 30: On this day, model performance was greatly improved by setting the model's hourly pbl depth to the average of the values observed by the radar profilers operating during the TexAQS, but even so, the adjusted base case still underpredicts ozone and especially the peak concentration. The unadjusted base case performed quite badly.

In the main body of the Technical Support Document the reader can find a description of further sensitivity analysis conducted for this day. The sensitivity includes a set of observationally-derived adjustments, which resulted in very good model performance for August 30.

Daily Modeled Peak Ozone for August 31, 2000, Adjusted Base Case

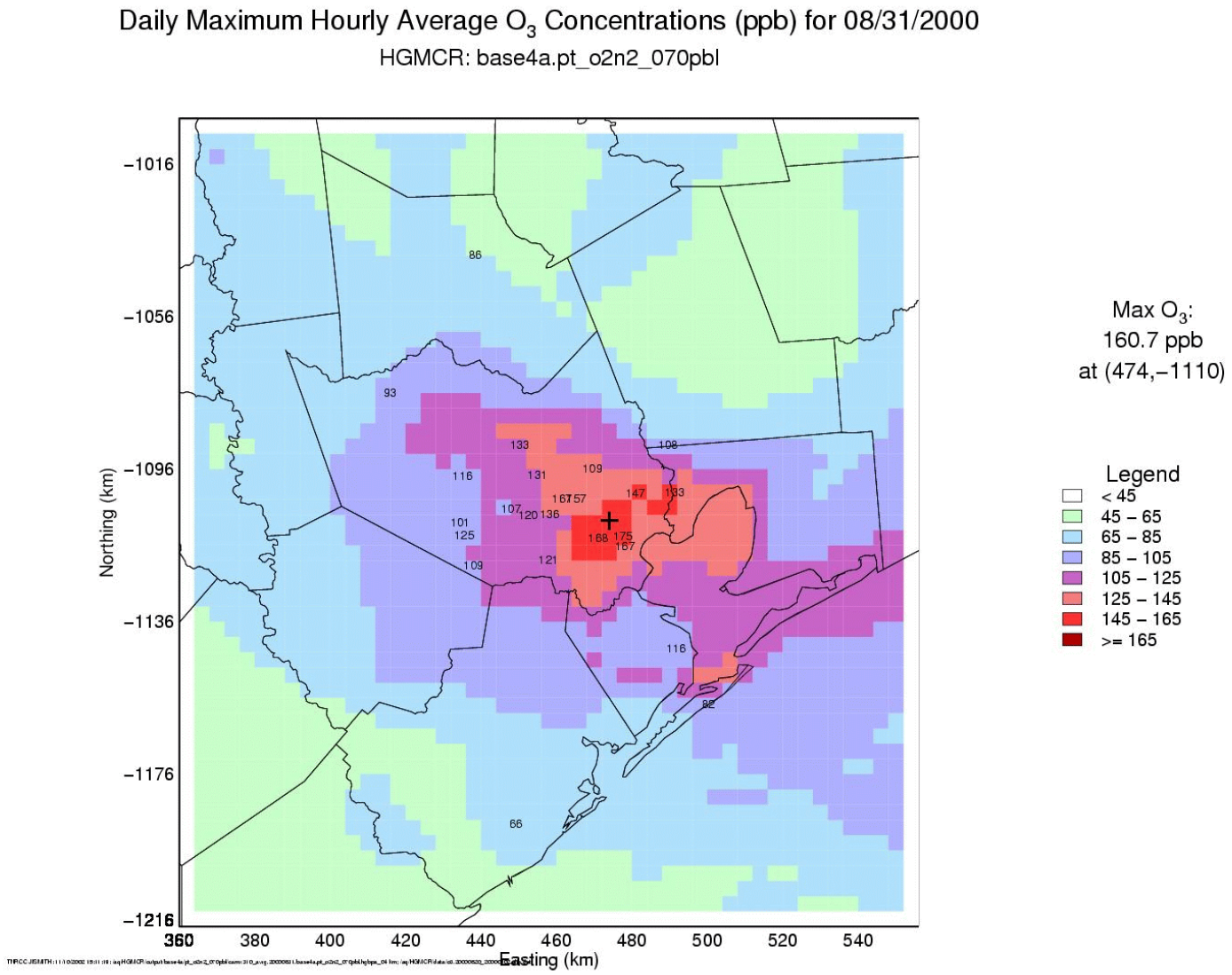

Daily Modeled Peak Ozone for August 31, 2000, Adjusted Base Case, 1-km Flexi-nest Grid

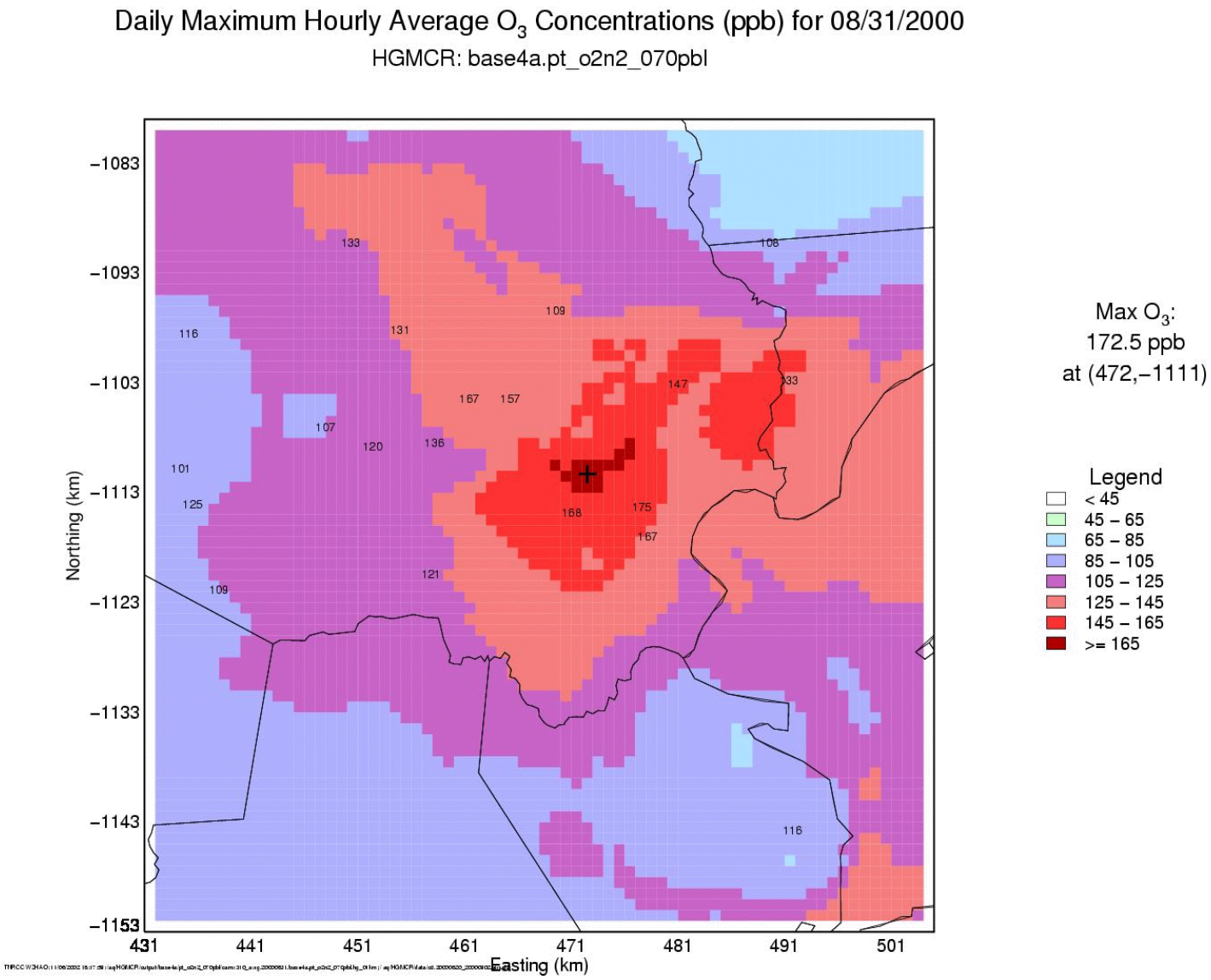

Model performance summary, August 31: Like August 29, model performance for the adjusted base case is excellent on this day, with almost no bias and very low gross error. The modeled peak was located less than ten kilometers from the observed peak concentration, and is within 3 parts/billion of the observed peak value. Unlike August 29, in this case the unadjusted base case actually performed quite well, except for underpredicting the measured peak by about 40 parts/billion. The peak performance of the unadjusted base case might be expected to improve if flexi-nesting were used.

The August 25 Ozone "Spike"

One unusual feature was observed in the model output for August 25th which was not observed on other episode days. This feature was a very localized and transient "spike" of ozone which was first noticed when the wind field nudged by lidar winds replaced the original wind field. The use of the doppler lidar wind data for nudging helped organize the low-level winds and improved model performance later in the day when peak ozone was observed. However, at hour 7 (6:00-7:00 A.M. CST), a one-hour average concentration of over 160 parts/billion was predicted at the HRM 4 monitor. An hour later the ozone concentration had returned to more typical values. This temporal behavior is seen in Figure S-1 below.

Early morning ozone "spikes" similar as the one depicted in the figure below have occasionally been observed in the Houston-Galveston monitoring network, but the magnitude of the modeled "spike" exceeds those typically recorded. The most similar example noted to date was a one-hour increase in ozone concentration of 98 parts/billion recorded at Deer Park at 8:00 AM on September 20, 1999. However, the extreme nature of the modeled "spike", together with the lack of any evidence for such an occurrence at the HRM 4 monitor, may indicate that the "spike" is something of a modeling artifact. In any case, the modeled "spike" is unrepresentative of the wide spread and extensive ozone generally found in the afternoons during a high ozone period.

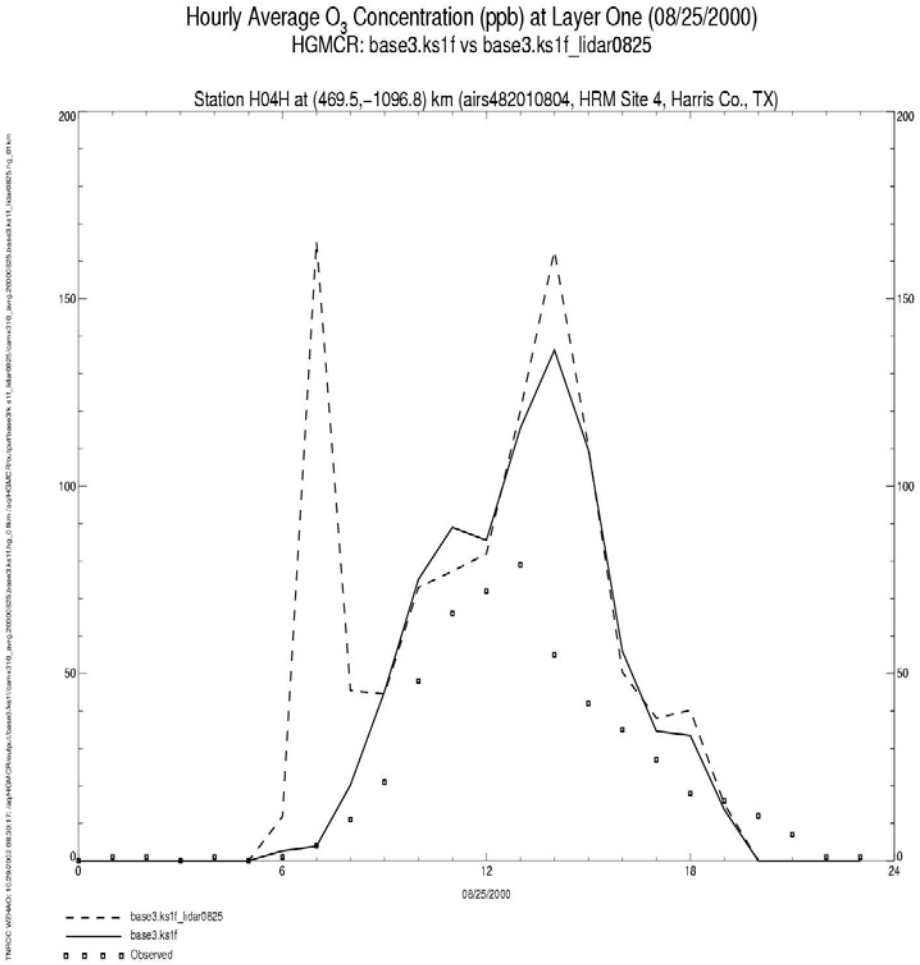

Figure S-1: Modeled ozone concentrations at HRM-4, with and without lidar nudging to winds

The other distinguishing aspect of this feature is the very localized spatial extent of the spike. The high ozone was predominantly found in the first layer and over a one kilometer grid cell which is shown in Figure S-2 below. Upon inspection, although the winds are basically calm, they are calm over a broad portion of Harris County and not just at the "hot spot". MM5 predicted mixing height were approximately 100 meters, and the first level vertical diffusivities (Kv's) were set to the minimum default of 0.1 m^2/s. This amount is a low value, but not necessarily unusual under stable conditions. The default value for the Kv was also assigned over a large part of Harris County. Since the lowest level vertical diffusivity can be influenced by land use, TCEQ staff discussed this feature with ENVIRON staff responsible for the converter program MM5CAMx which calculates the Kv's. ENVIRON provided TCEQ with another program, KVPATCH, which partially adjusts first level Kv's by a land use weighted scheme as well as information about mixing at the second layer. A maximum minimum default Kv is defined to be 1.0 m^2/s over urban industrial areas. Use of this additional program does modify the lowest level diffusivities, and the "spike" is greatly reduced. The TCEQ will continue model development for Phase II of the MCR and will continue to evaluate the use of KVPATCH for later use. For the current application, however, the model output has been simply "filtered" to remove the hour 0700 concentrations in a few cases where this "spike" has produced the daily maximum modeled ozone concentration.

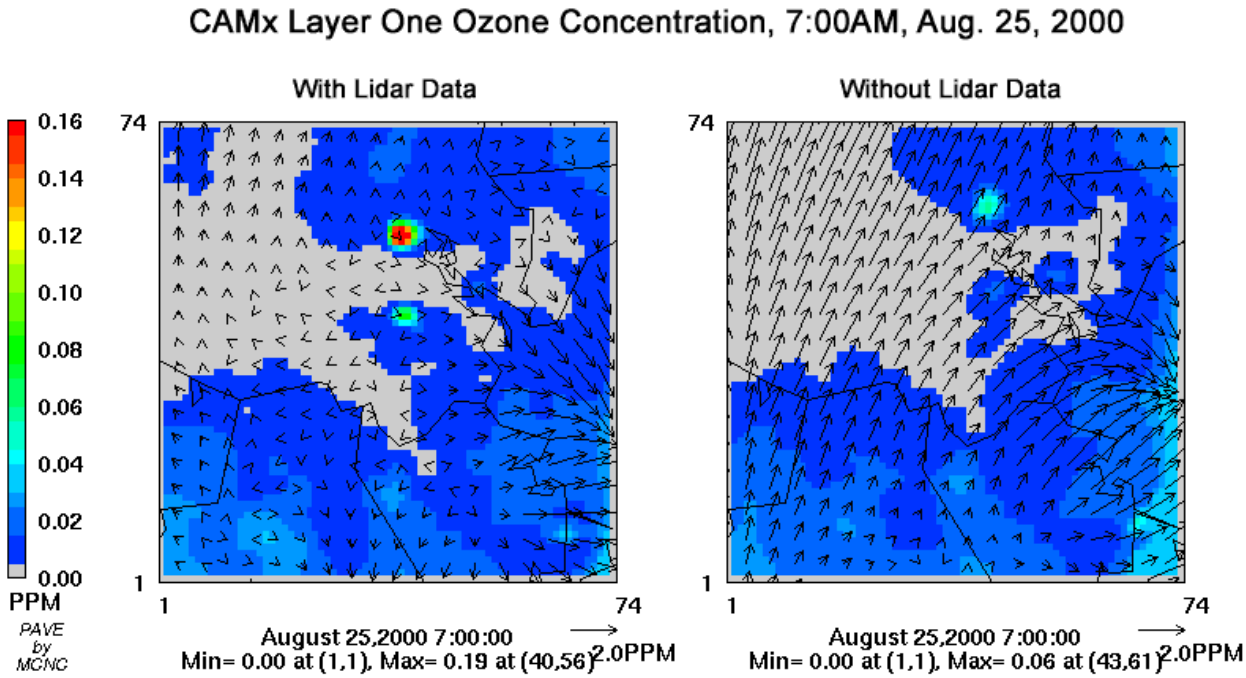

Figure S-2: Modeled 07:00 ozone concentration in 1-km flexi-nest grid, August 25

Process analysis of base4.pt_o2n4_kvnoaa for Aug 25, 2000.

Integrated Process Rate (IPR) process analysis was performed on a subregion of the 1-km domain for August 25, 2000 to determine why the model produced a large early morning ozone spike in the vicinity of Channelview from 7-8 AM CST.

Light olefin emissions were substantially increased above the reported emissions inventory in this modeling scenario, so that the modeling inventory would be more consistent with observations during 2000 and 2001. When the olefins were increased, the modeling generally reproduced the behavior of ozone and ozone precursors in a more accurate manner than the original reported inventory. However, at a few locations where the olefins had been greatly increased, the model produced rapid ozone formation in the early morning hours, beginning at sunrise and then rapidly dissipating. Early morning rapid ozone formation and transient high ozone have been observed in Houston. But in this particular case, rapid ozone formation was not observed in the ambient data. To determine what was happening in the grid cells where the observed and simulated ozone behavior were inconsistent, process analysis was performed on the 1-km flexi-nest grid. Grid cells used were bounded by cells (36, 52) and (44,62) in layer 1. This region encompasses the point sources in the Channelview area.

Figure IPR-1 shows O3, NO, NO2, ETH, OLE, PAR, FORM, ALD2, PAN, and HNO3 concentrations modeled within the subregion, where the Carbon Bond 4 species ETH, OLE, PAR, FORM, and ALD2 represent ethylene, olefins (alkenes), paraffins (alkanes), formaldehyde and larger aldehydes, respectively. Hours are denoted by the ending hour, i.e., 0700 represents the hour beginning at 6:00 AM and ending at 7:00 AM. Note that ETH, OLE, PAR, and NO gradually accumulate during the overnight hours within the grid cells of interest, up until 7 AM, and then level off and drop dramatically between 7 AM and 10 AM. Meanwhile, species that are formed by chemical reaction (O3, NO2, FORM, ALD2, PAN, and HNO3) instead of being directly emitted are relatively low during the overnight hours, and then rapidly increase for a few hours beginning at 7 AM, with the highest increase between 7 and 8. Note that the species formed by reaction also decrease after 0800.

Figures IPR-2 and IPR-3 show that both chemistry and meteorology are causing the spiky behavior. Figure IPR-2 shows that the O3 spike is formed between 6-8 AM completely by chemistry within the selected grid cells. However, the decrease in O3 after 8:00 AM is caused by transport through the top boundary of the selected cells, due to the rising mixing height after sunrise. Figure IPR-3 shows the change in concentrations due to chemistry for all CB4 species of interest. Note that the FORM and ALD2 spikes are also caused by local chemistry. The CB4 mechanism creates FORM and ALD2 quite efficiently from oxidation of ETH and OLE. FORM is not created by oxidation of PAR by OH radicals. ALD2 is created much less efficiently by PAR (yield=0.11 per PAR oxidized) than by ETH (yield=1.56) or OLE (yield=1), so FORM and ALD2 formation seem to be mostly related to ETH and OLE behavior. ETH and OLE accumulate due to decreased vertical mixing until 8:00 AM, and then begin being chemically consumed after 7:00 AM when photochemical reactions begin. The creation of O3, FORM and ALD2 coincide with destruction of ETH, OLE, and PAR. However, the largest decrease in ETH, OLE, and PAR concentrations occurs at 8:00-9:00 AM, and is primarily caused by vertical transport of these compounds out of the lowest layer, presumably when the mixing height rises

and allows mixing through several layers of the lower atmosphere (Figure IPR-4).

The behavior of the nitrogen species is consistent with these explanations as well. The primary emission species NO accumulates like ETH, OLE and PAR before 7:00 AM, decreases a little as photochemical reactions begin, then decreases abruptly as the mixing layer deepens. The secondary species NO2 increases as photochemistry begins, peaking the same hour as O3, HNO3, PAN, and the other photochemical reaction products. All nitrogen species decrease as the mixing layer deepens.

Ozone is formed very efficiently per NO_X oxidized during the period of rapid ozone formation. Figure IPR-5 shows the ratio of ozone production rate to NO_Z production rate for the hours of 6:00 AM to 4:00 pm. During the hour from 6:00-7:00 AM, the ratio is 14 ppb O3 formed per ppb of NO_Z formed, a very efficient rate.

Conclusions.

The early morning O3 spike was created by a combination of chemical and meteorological effects. The rapid rise in O3 concentrations was due to local creation of O3 primarily from the oxidation of ETH and OLE. ETH, OLE, and NO reached high concentrations before sunrise mostly due to a lack of transport during the predawn hours. After sunrise, ozone formation occurred rapidly and efficiently. The rapid fall in O3 concentrations during the following hour was due to the deepening of the mixing layer after sunrise.

The model is able to create ozone at a very rapid and efficient rate when the olefin concentrations are large and there is sufficient NO_X, as has been frequently observed in the Houston area.

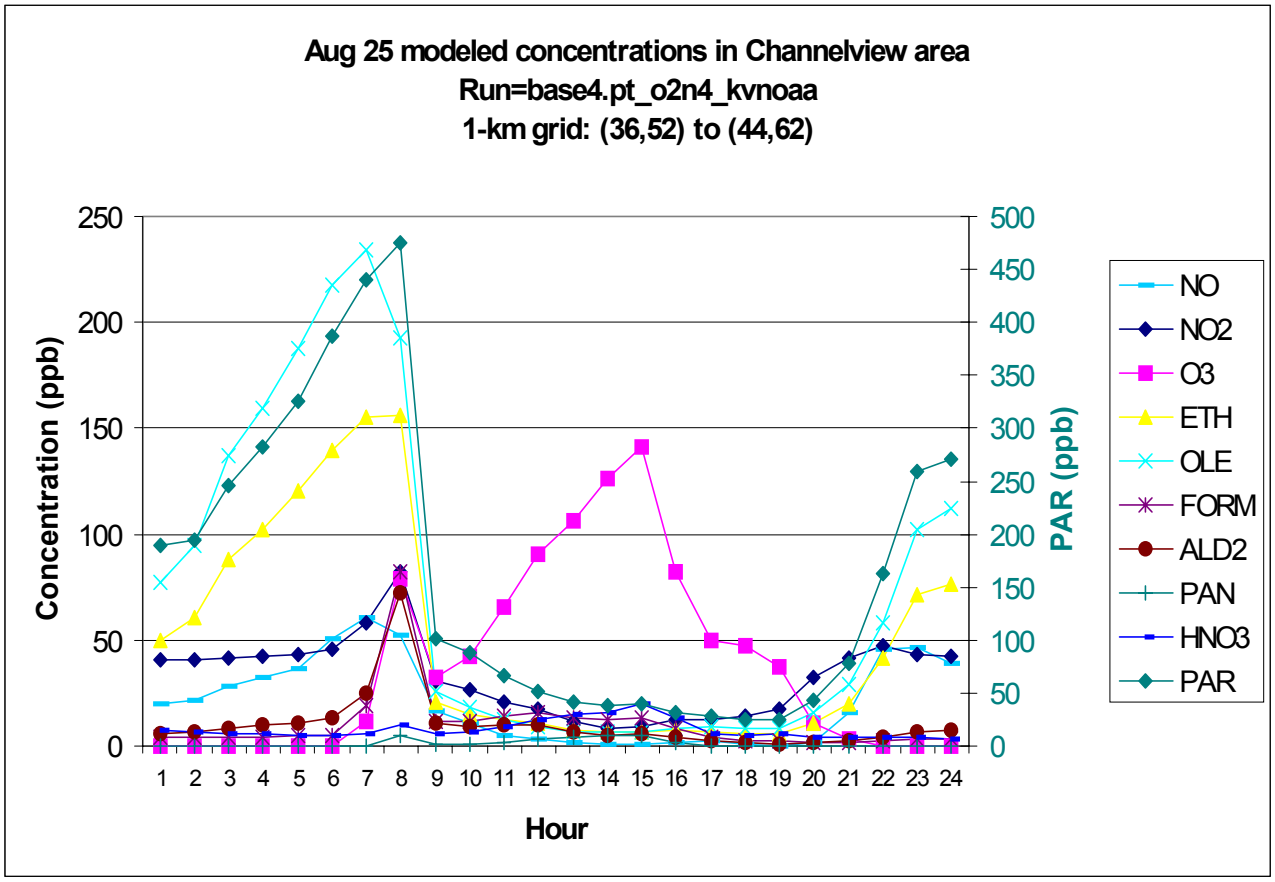

Figure IPR-1. Propylene concentrations as a function of wind direction at Clinton auto-gc. The site clearly sees a distinct signal from the areas with reported propylene emissions.

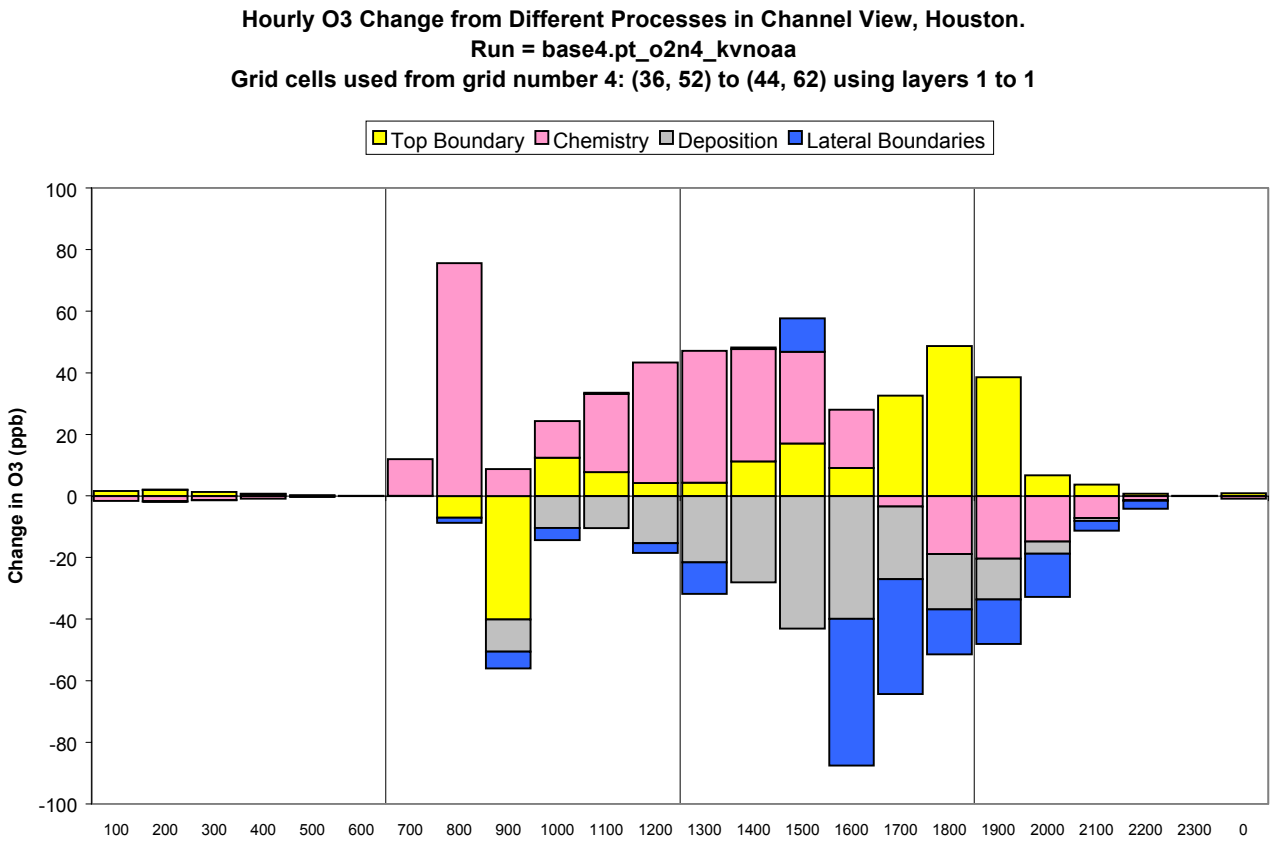

Figure IPR-2. Changes in modeled O3 concentrations for 25 Aug 2000 in the vicinity of Channelview.

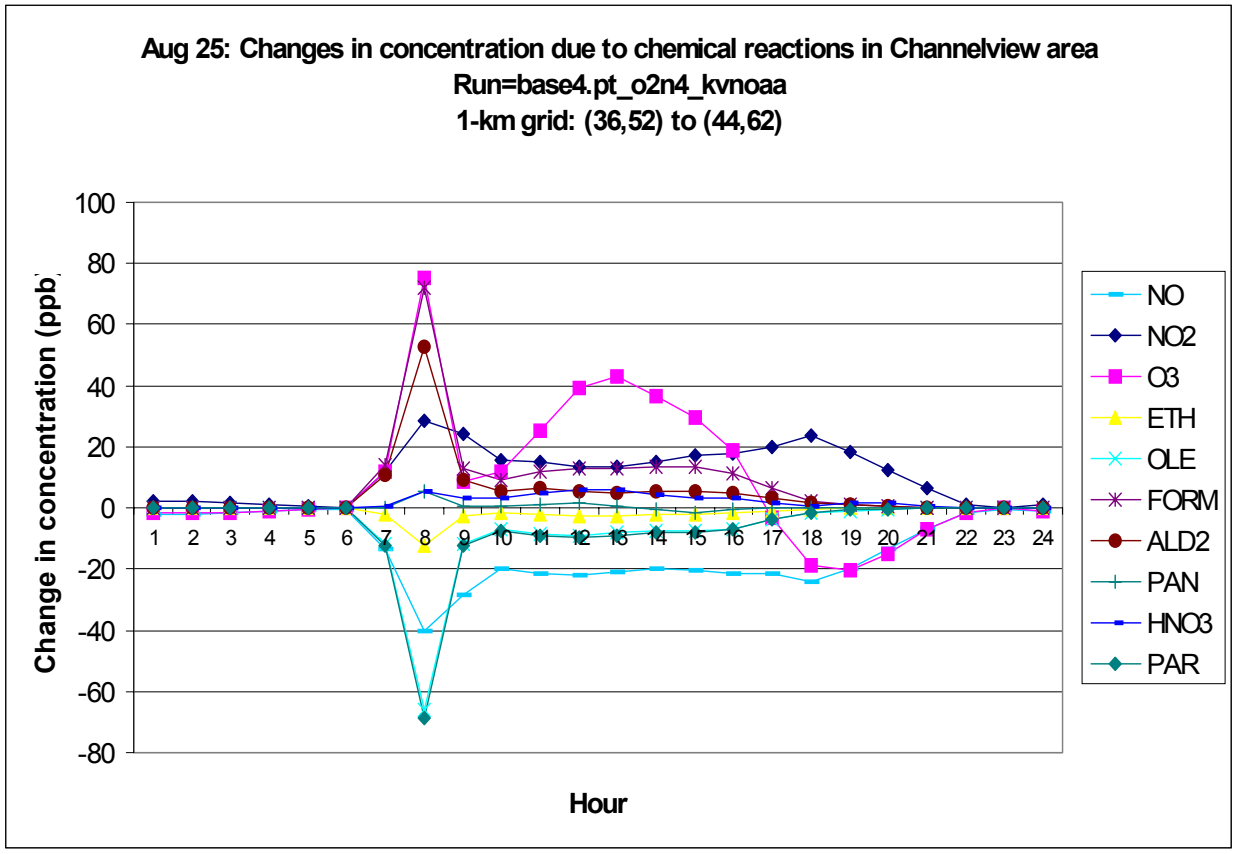

Figure IPR-3. Modeled changes in concentration of selected CB4 species due to chemistry on 25 Aug 2000 in the vicinity of Channelview.

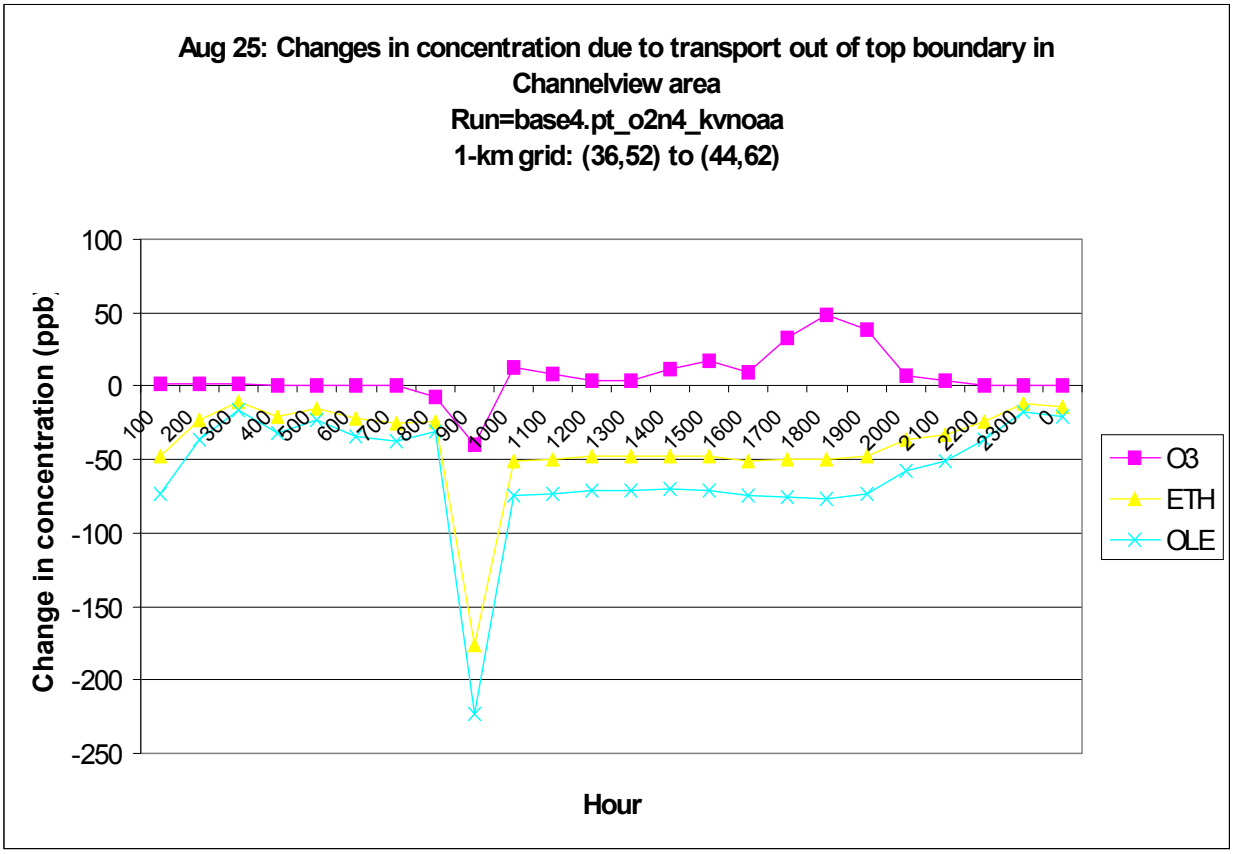

Figure IPR-4. Modeled changes in ETH, OLE and O3 concentrations due to vertical transport out of the top boundary of model layer 1, 25 Aug 2000 in the vicinity of Channelview.

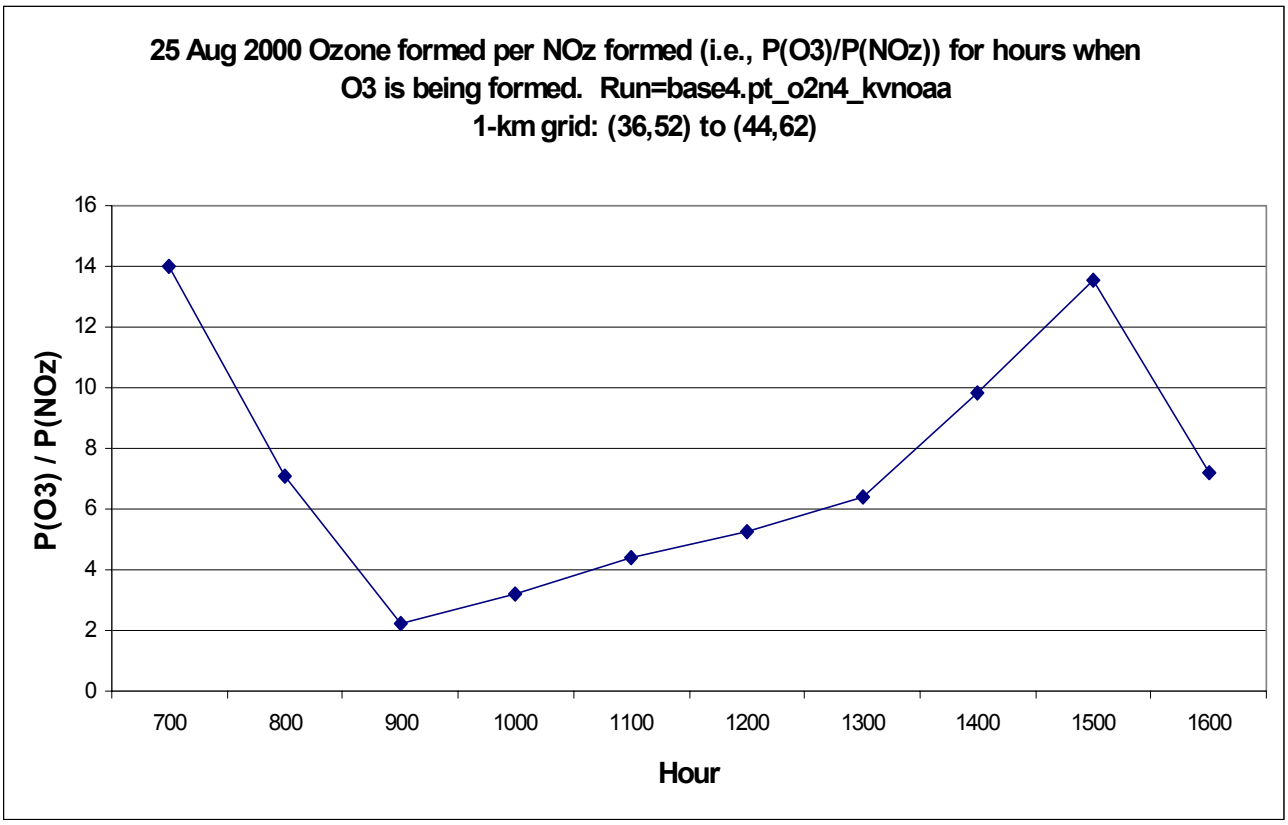

Figure IPR-5. Ozone formed per NO_Z formed.

Time Series for Each Monitoring Site

The following time series represent a comparison of ambient measurements and modeled concentrations at each monitoring site in the eight-county nonattainment area. Each plot shows both the adjusted (Base4a.pt_02n2_00pbl) and unadjusted (Base4a.regular) modeled concentrations. All concentrations are taken from the four-kilometer grid except for the adjusted base case on August 25, 29, 30, and 31, where the concentrations in the one-kilometer flexi-nest grid are plotted. Time series are presented for ozone, NO, NO_2, CO, and VOC where ambient data are available during the episode period.

OZONE TIME SERIES

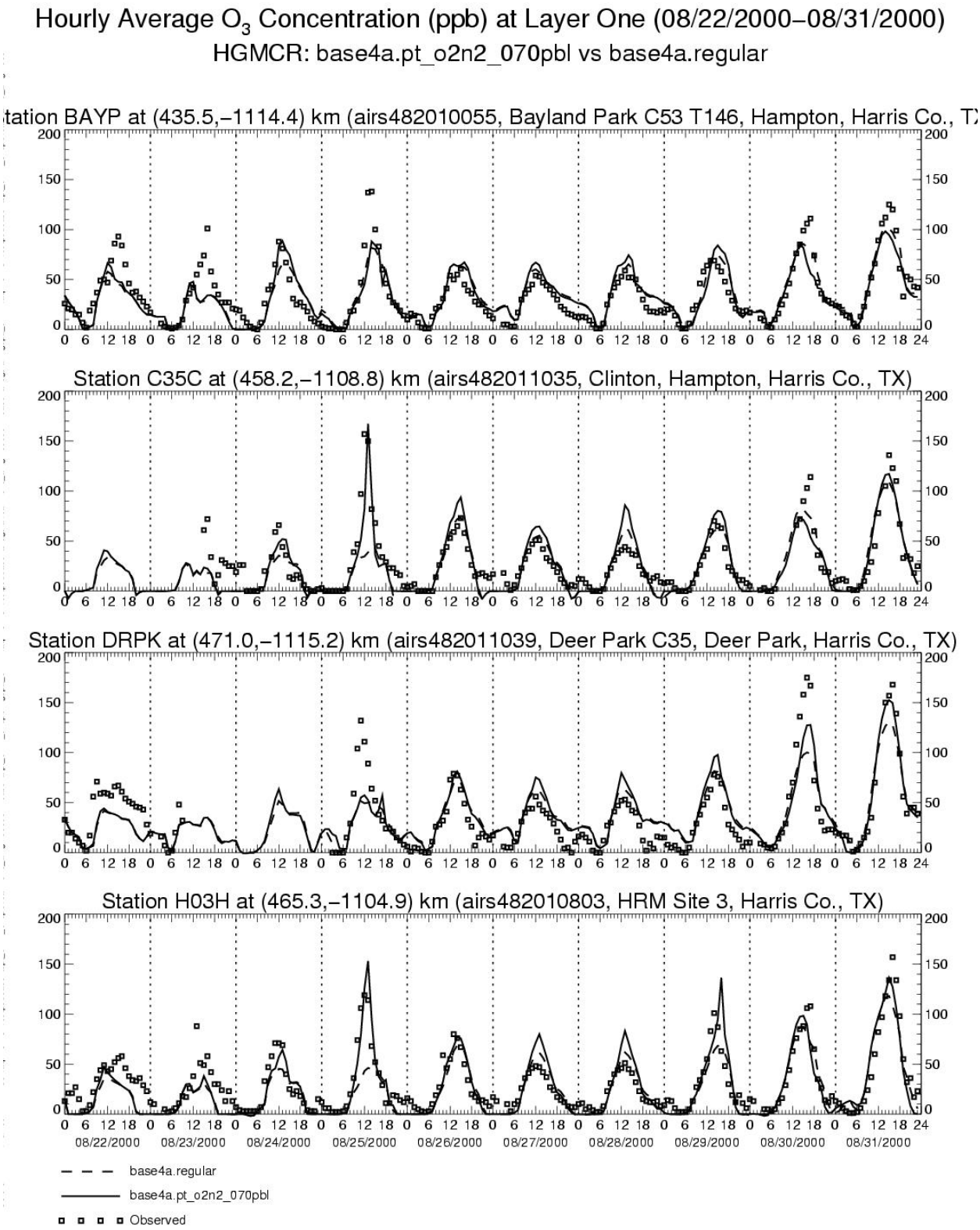

Hourly Average O_3 Concentration (ppb) at Layer One (08/22/2000–08/31/2000)

HGMCR: base4a.pt_o2n2_070pbl vs base4a.regular

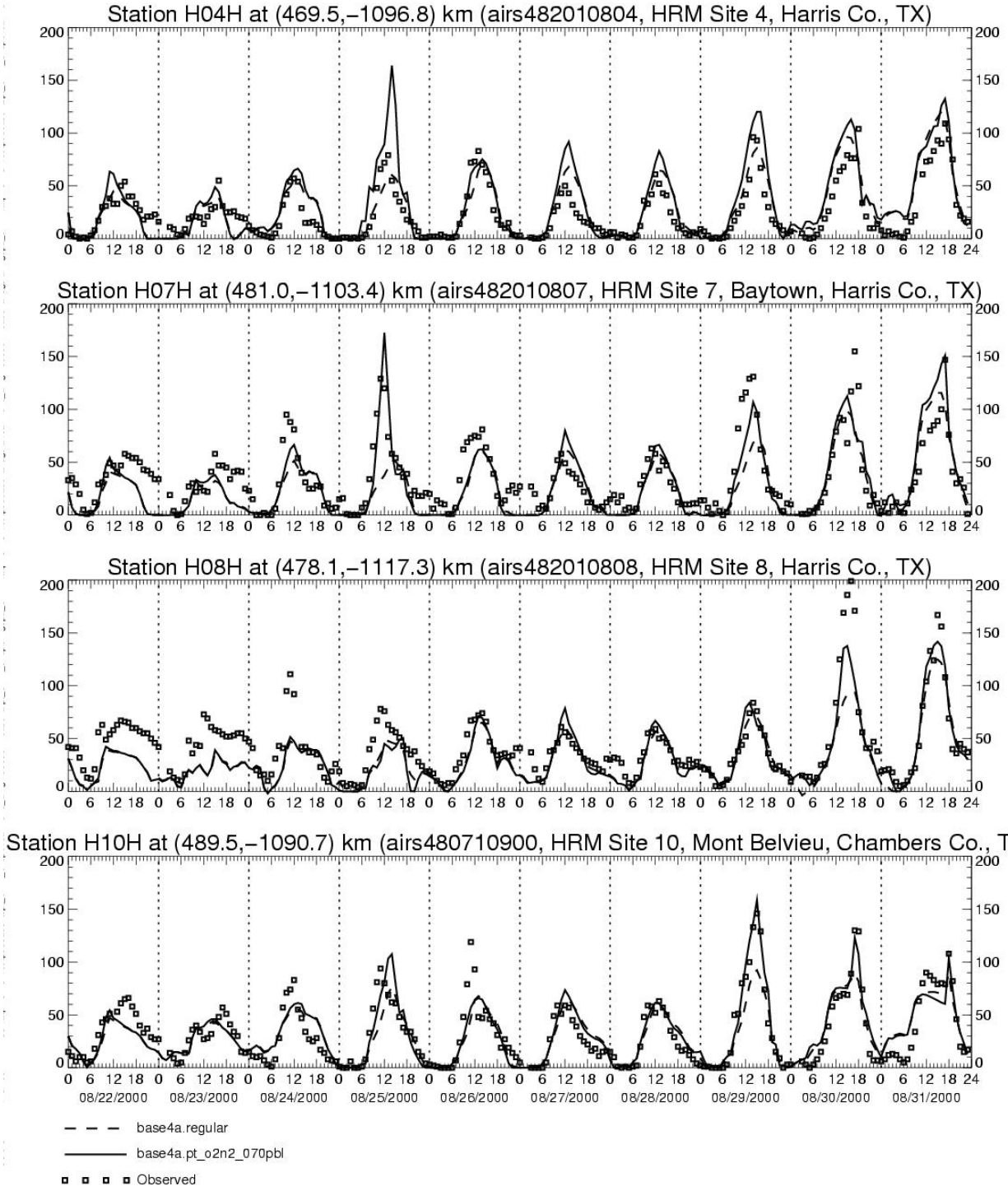

Hourly Average O_3 Concentration (ppb) at Layer One (08/22/2000–08/31/2000)

HGMCR: base4a.pt_o2n2_070pbl vs base4a.regular

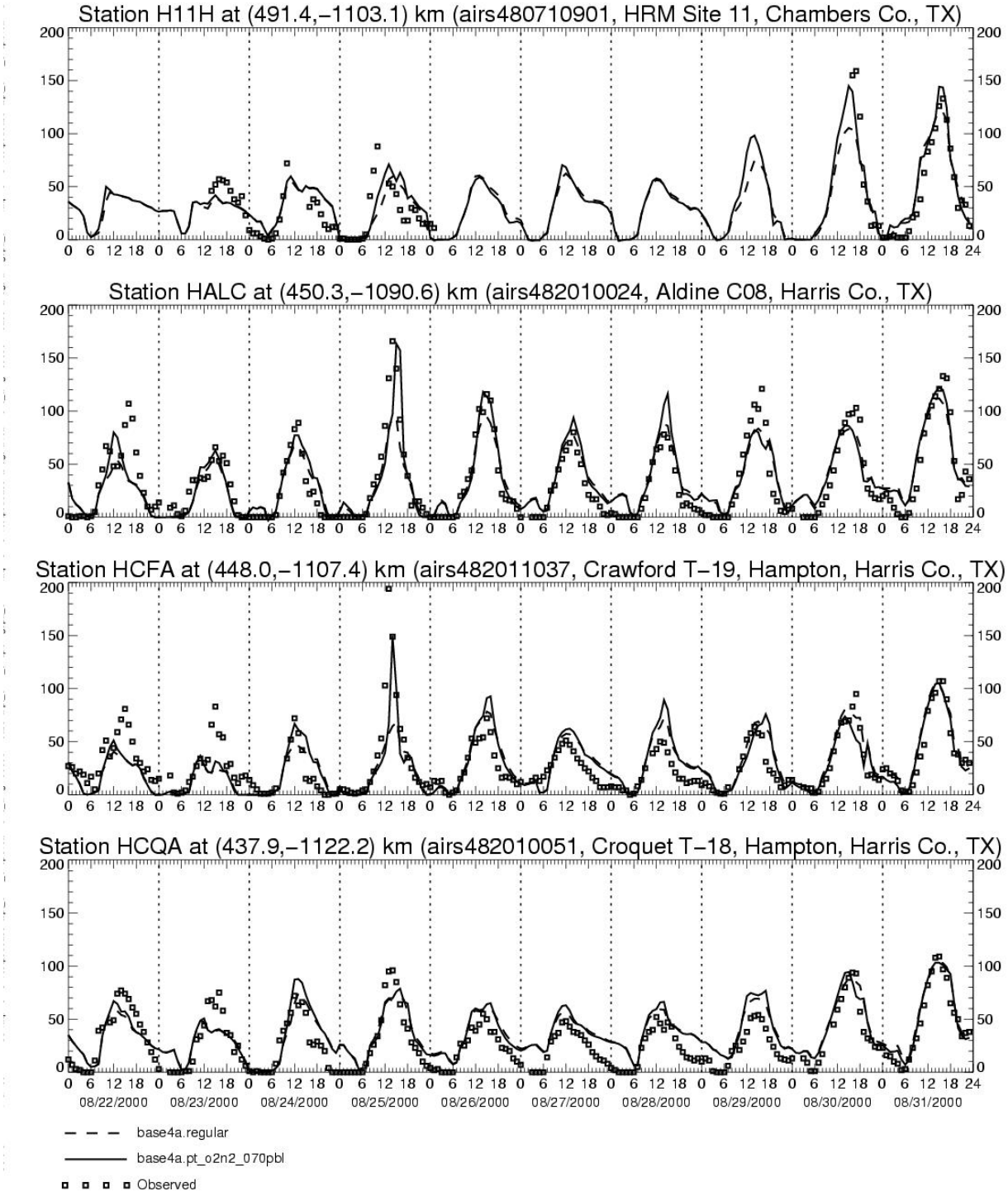

Hourly Average O_3 Concentration (ppb) at Layer One (08/22/2000–08/31/2000)

HGMCR: base4a.pt_o2n2_070pbl vs base4a.regular

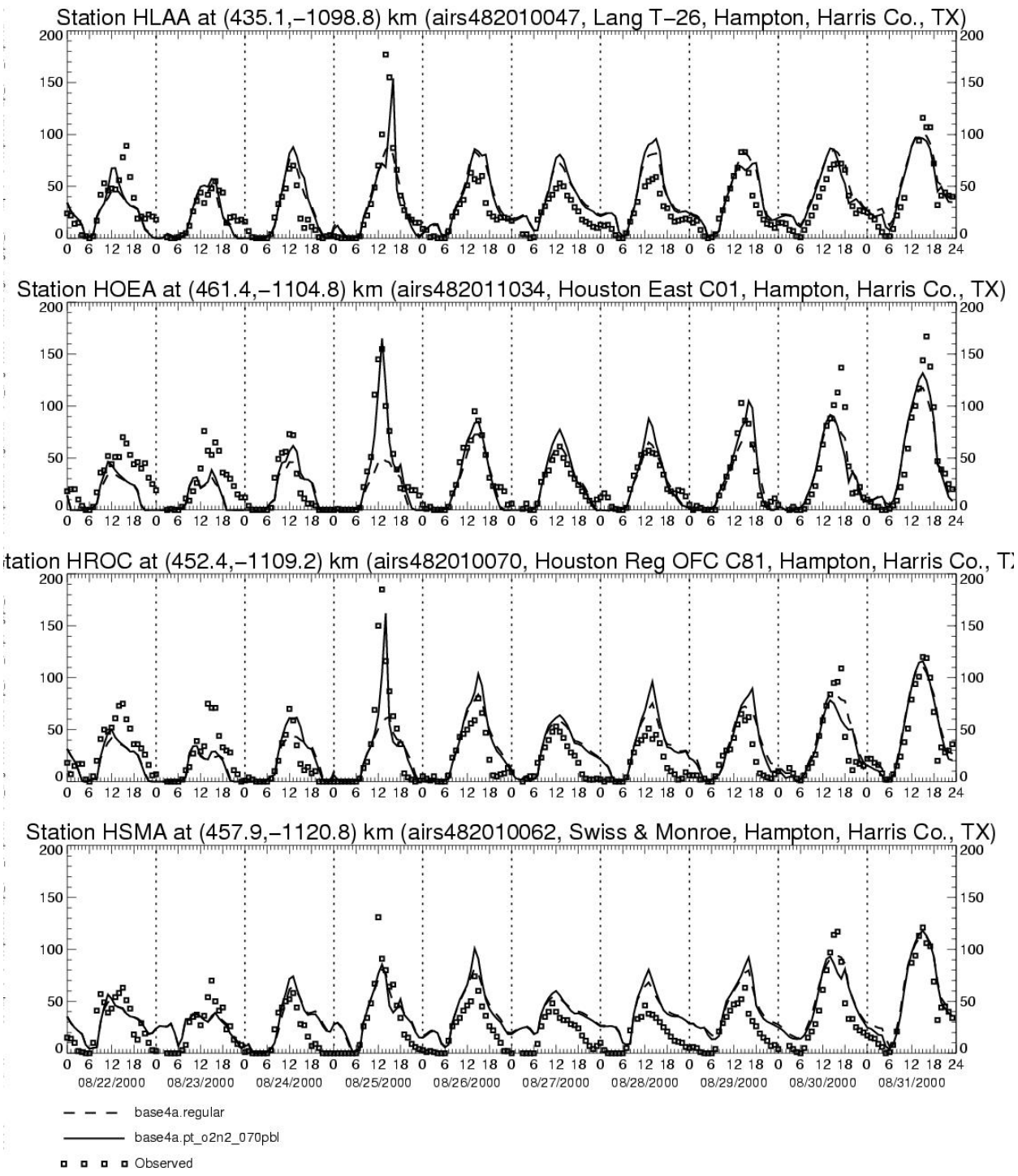

Hourly Average O_3 Concentration (ppb) at Layer One (08/22/2000–08/31/2000)

HGMCR: base4a.pt_o2n2_070pbl vs base4a.regular

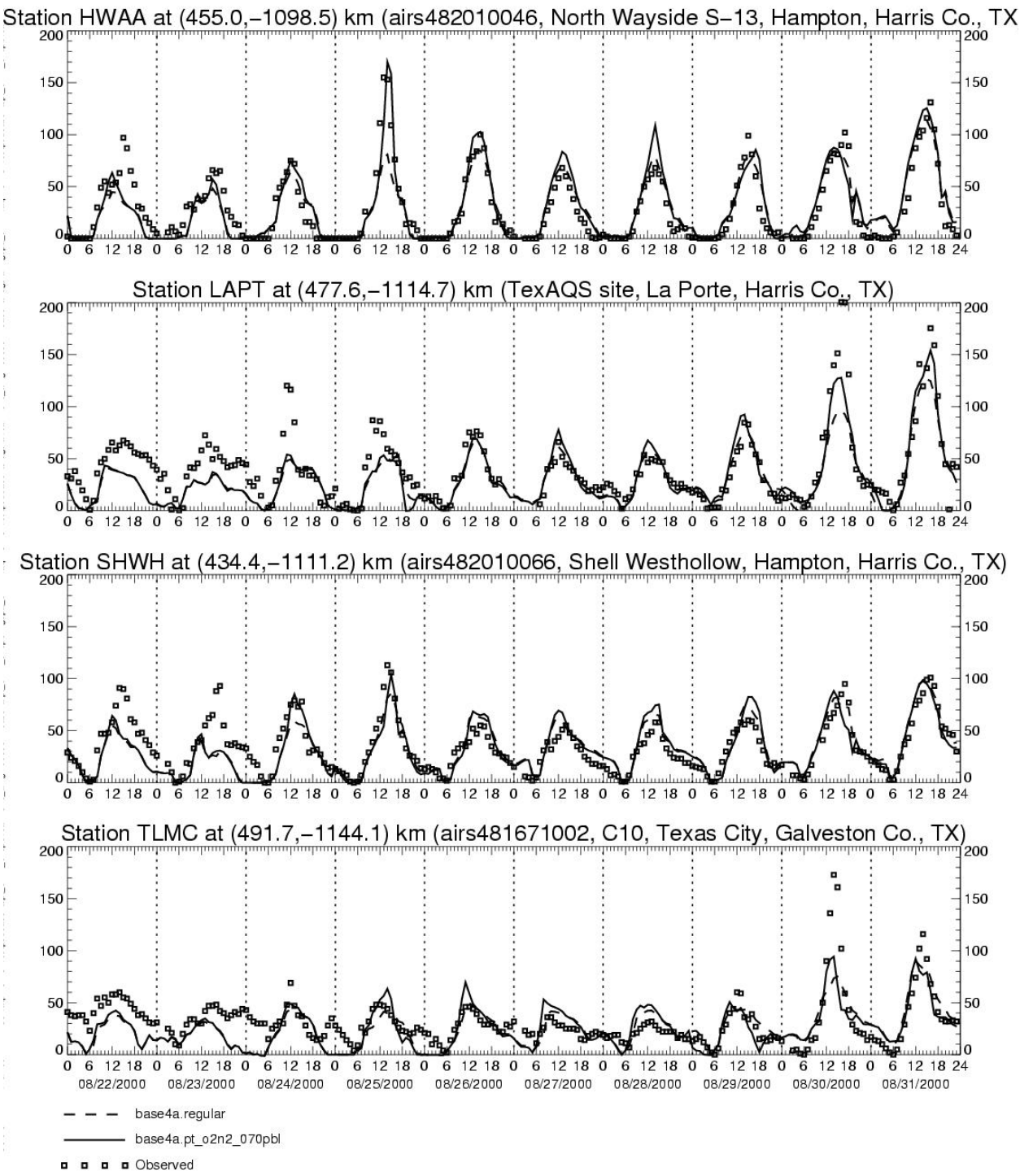

Hourly Average O_3 Concentration (ppb) at Layer One (08/22/2000–08/31/2000)

HGMCR: base4a.pt_o2n2_070pbl vs base4a.regular

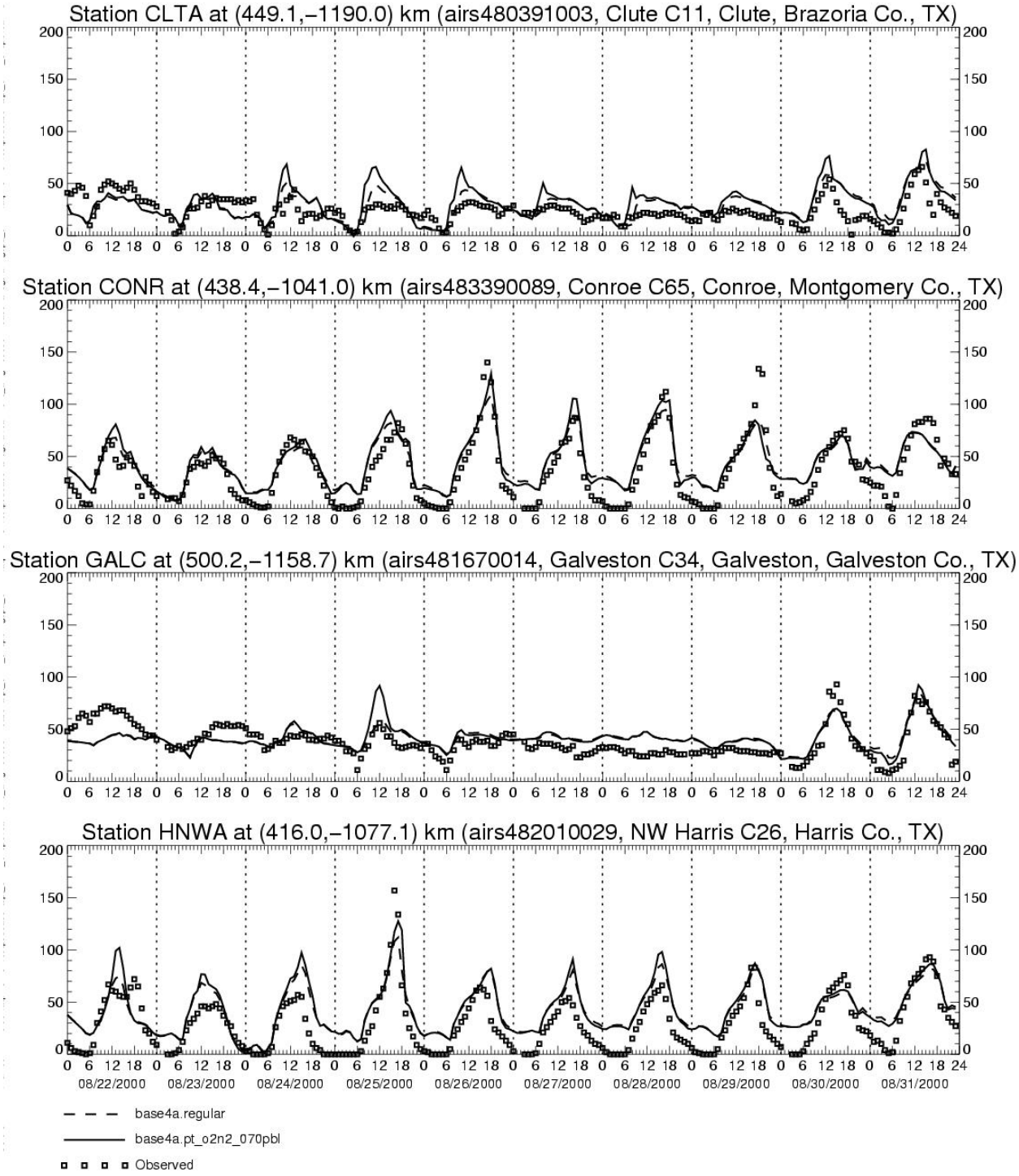

Overall, both the adjusted and unadjusted base cases replicate ozone well, in many cases capturing not only the diurnal rise and fall of the ozone concentrations but also many cases of overnight increases in ozone (see, for example, station HLAA). For a number of sites, the adjusted and unadjusted base cases are almost indistinguishable except for some of the afternoon peak hours, when the adjusted base case, with few exceptions, clearly replicates the peaks better than the unadjusted case.

NO TIME SERIES

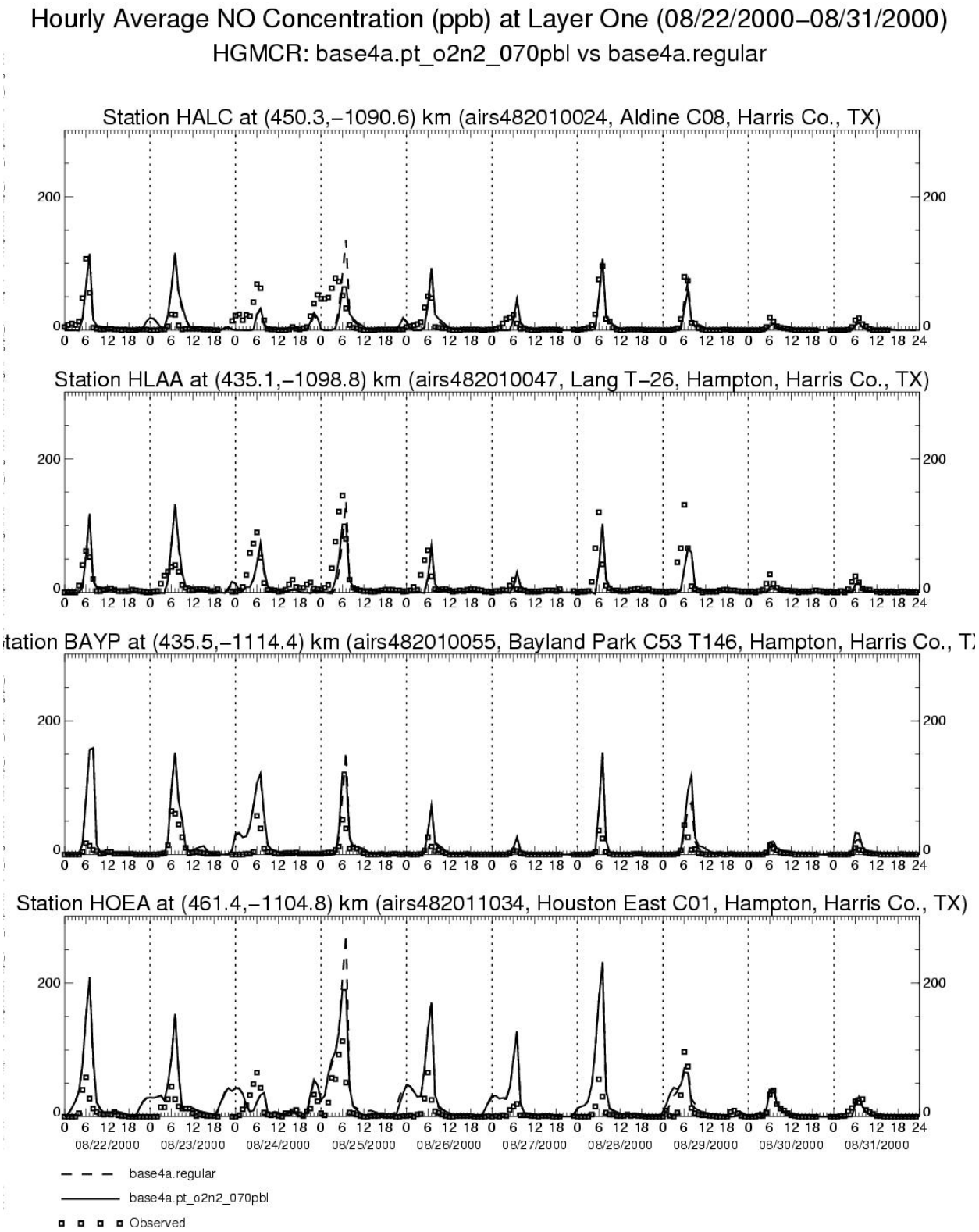

Hourly Average NO Concentration (ppb) at Layer One (08/22/2000–08/31/2000)

HGMCR: base4a.pt_o2n2_070pbl vs base4a.regular

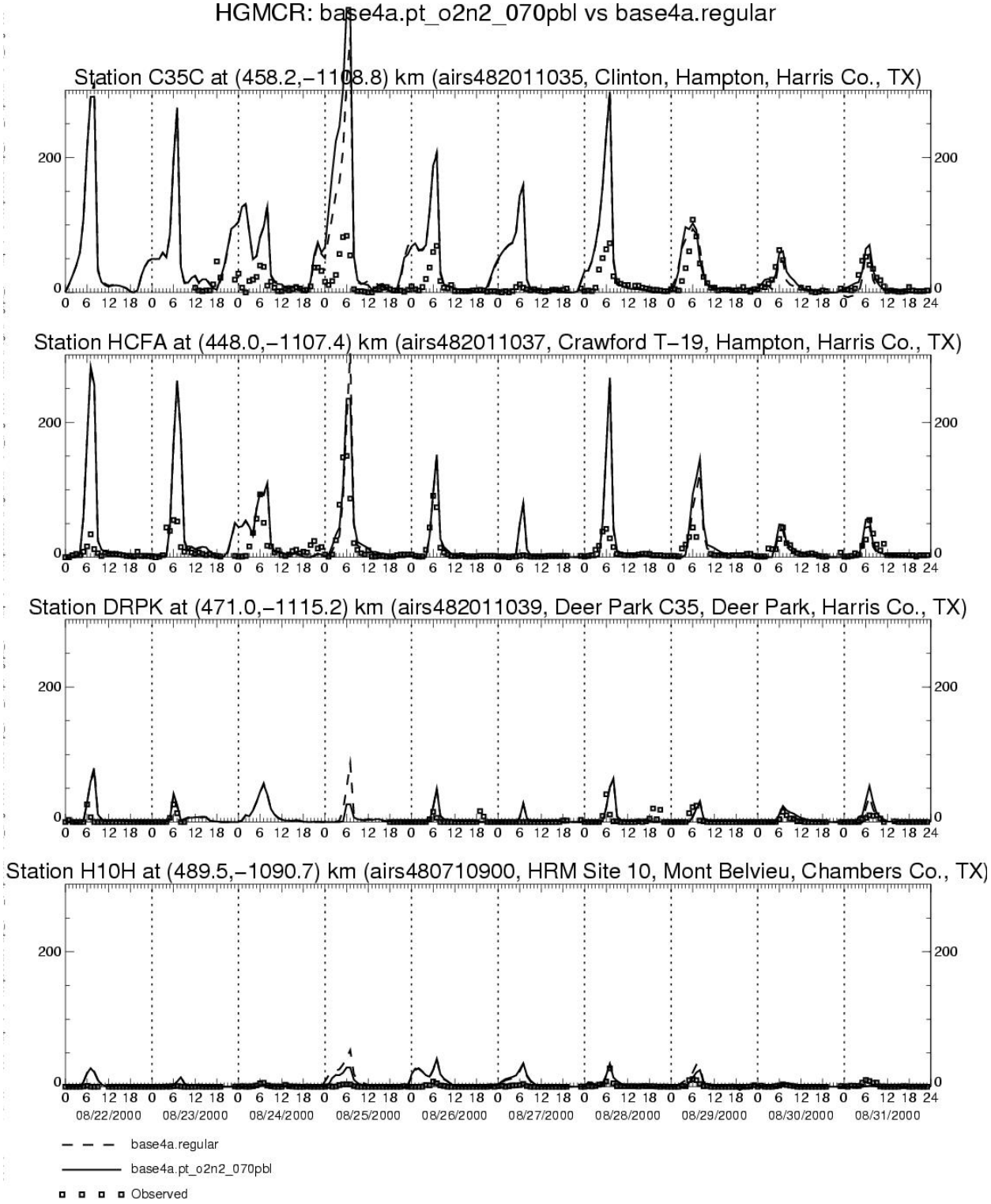

Hourly Average NO Concentration (ppb) at Layer One (08/22/2000–08/31/2000)

HGMCR: base4a.pt_o2n2_070pbl vs base4a.regular

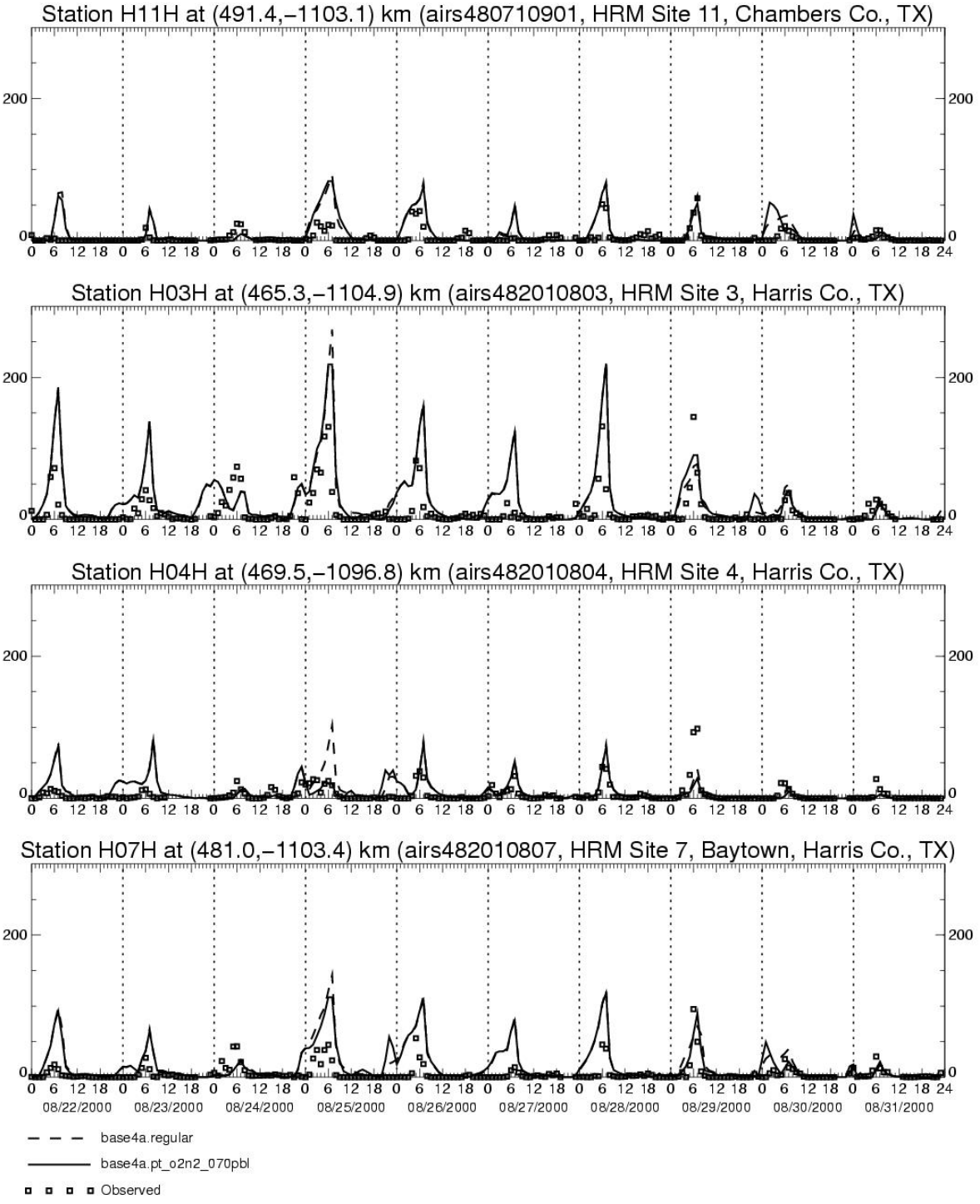

Hourly Average NO Concentration (ppb) at Layer One (08/22/2000–08/31/2000)

HGMCR: base4a.pt_o2n2_070pbl vs base4a.regular

Station H08H at (478.1,–1117.3) km (airs482010808, HRM Site 8, Harris Co., TX)

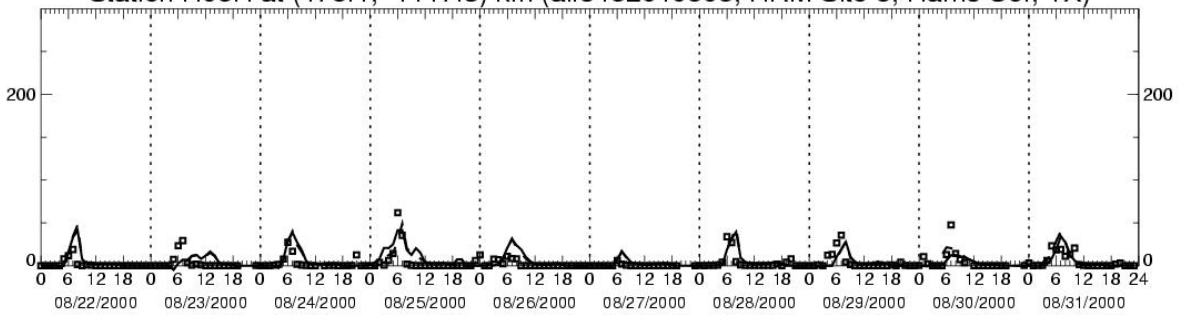

base4a.regular

base4a.pt_o2n2_070pbl

Observed

Hourly Average NO Concentration (ppb) at Layer One (08/22/2000–08/31/2000)

HGMCR: base4a.pt_o2n2_070pbl vs base4a.regular

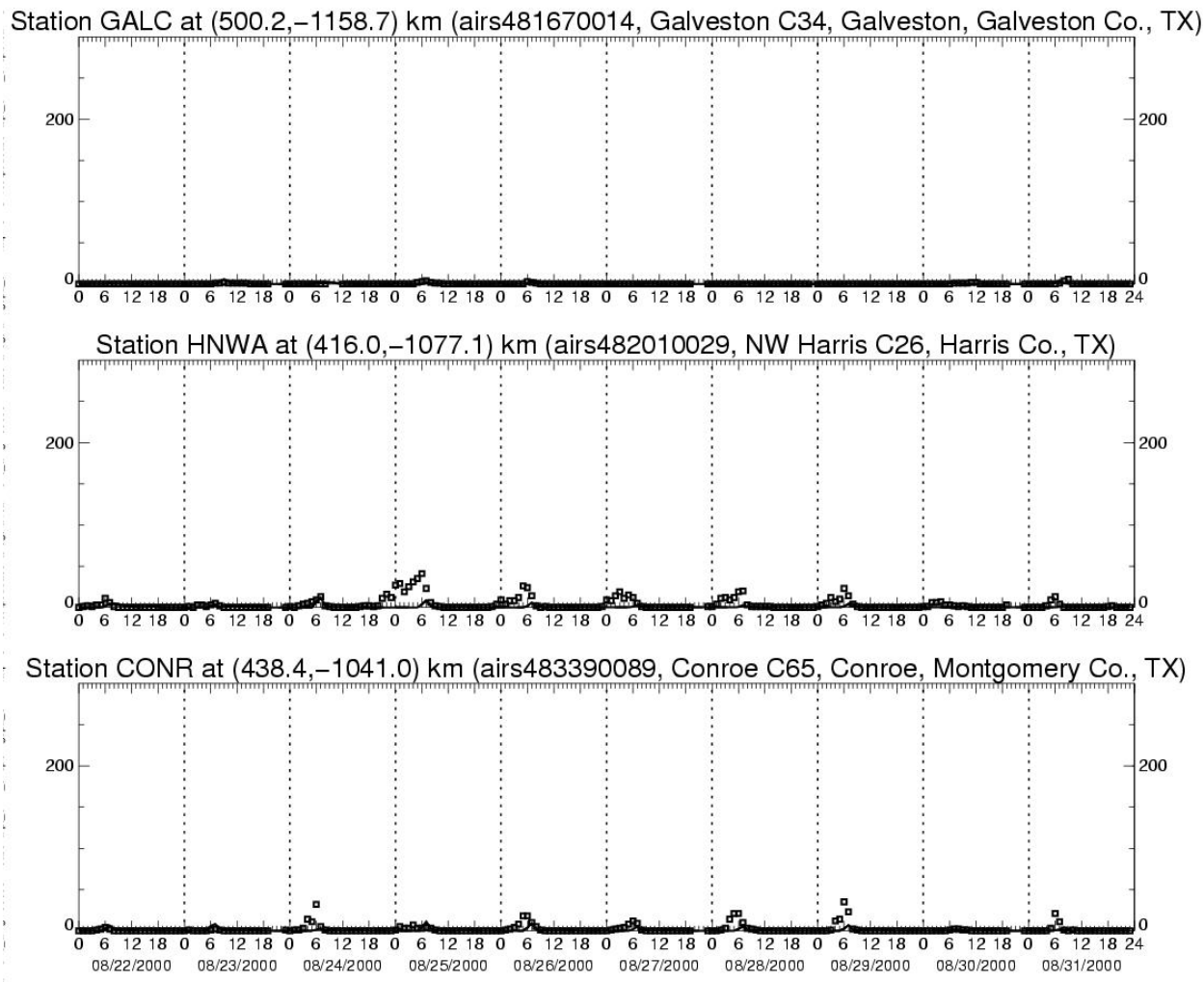

base4a.regular

base4a.pt_o2n2_070pbl

Observed

Overall, again both base cases replicate NO concentrations reasonably well. Comparatively little difference is evident between the two cases. The model tends to predict a sharp NO rise during the morning hours at urban sites, which is mirrored by the measurements in some cases. In others, however, the morning NO peak is considerably larger than the measurements, for example station C35C from August 25 through 28.

NO_2 TIME SERIES

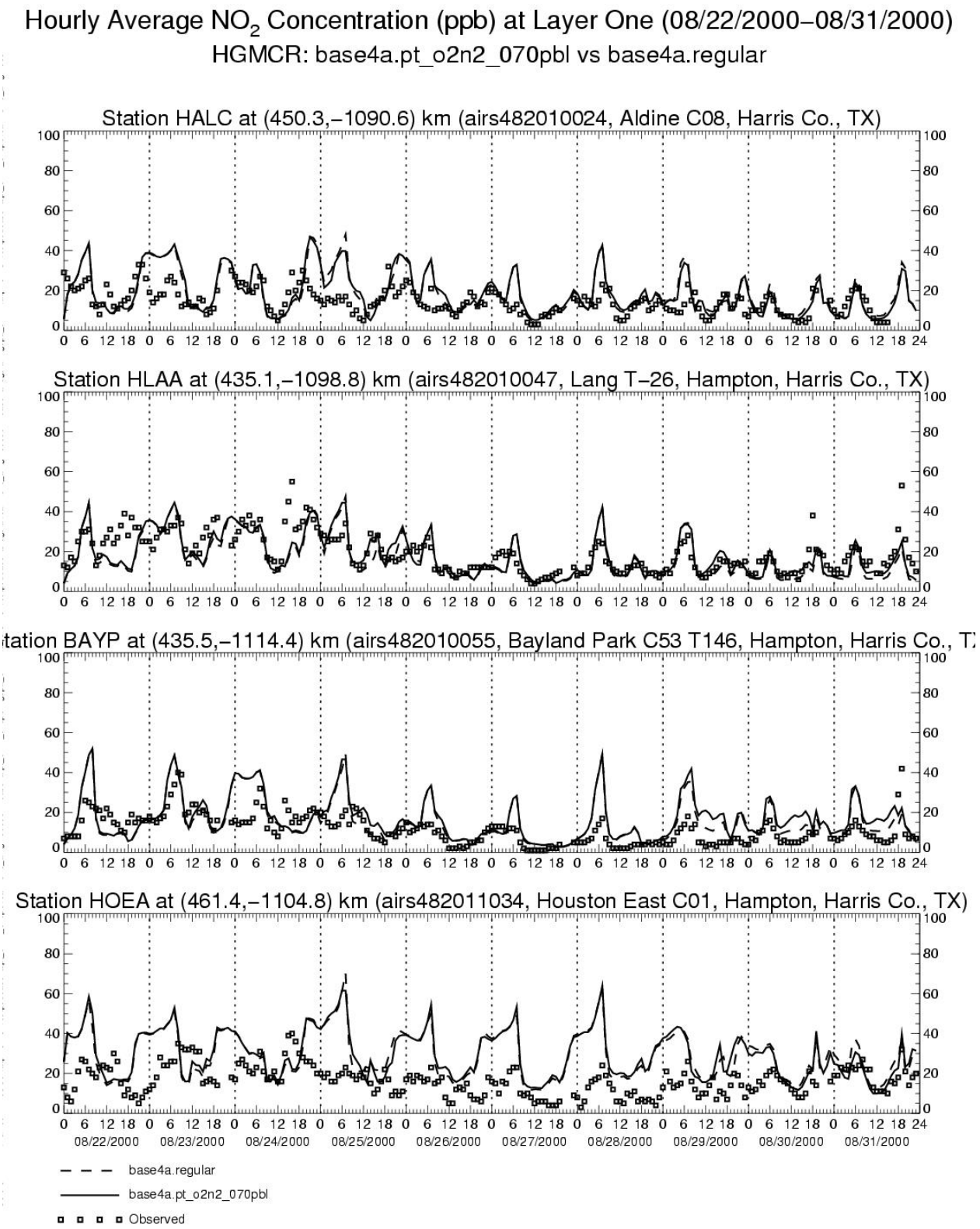

Hourly Average NO_2 Concentration (ppb) at Layer One (08/22/2000–08/31/2000)

HGMCR: base4a.pt_o2n2_070pbl vs base4a.regular

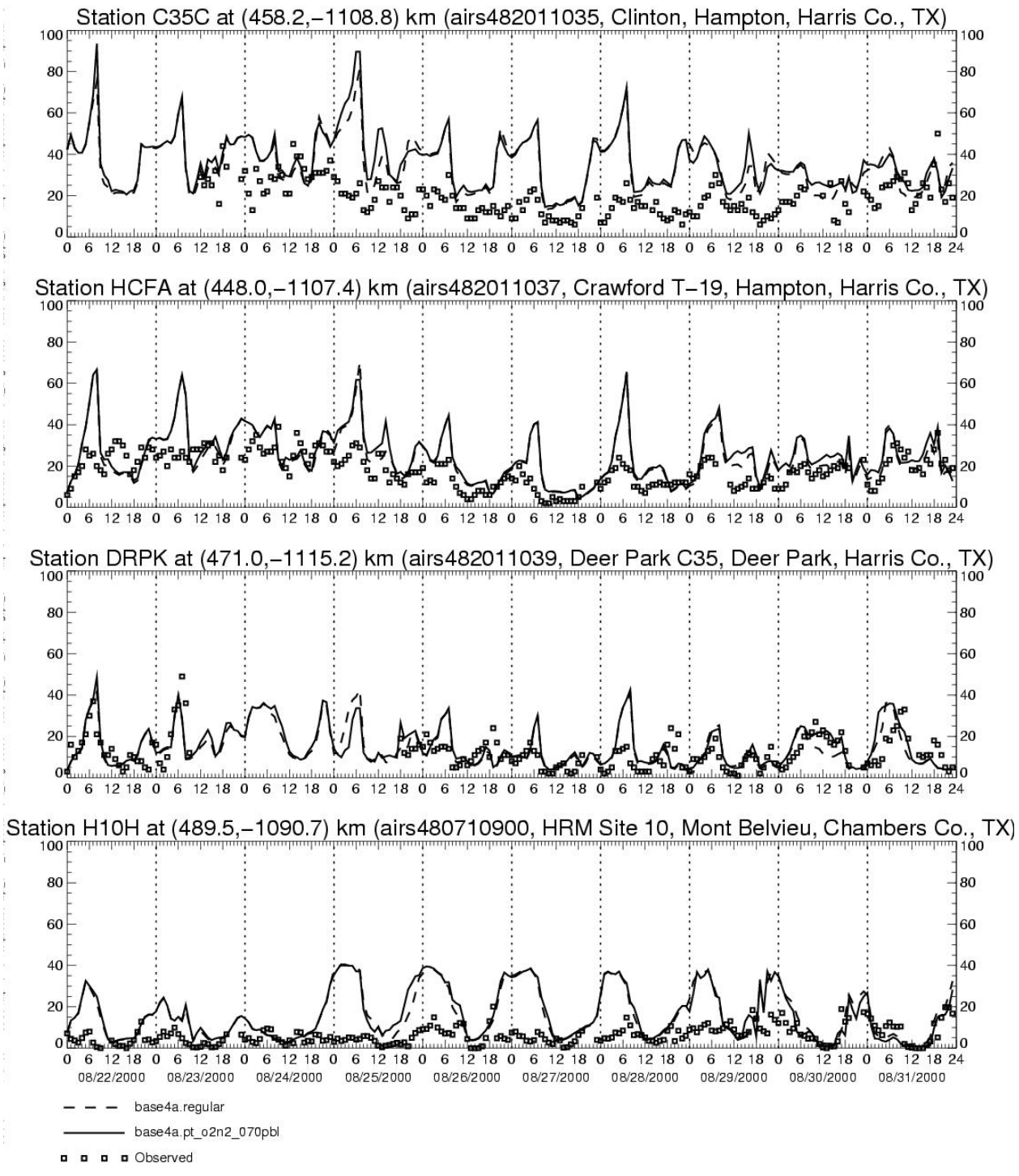

Hourly Average NO_2 Concentration (ppb) at Layer One (08/22/2000–08/31/2000)

HGMCR: base4a.pt_o2n2_070pbl vs base4a.regular

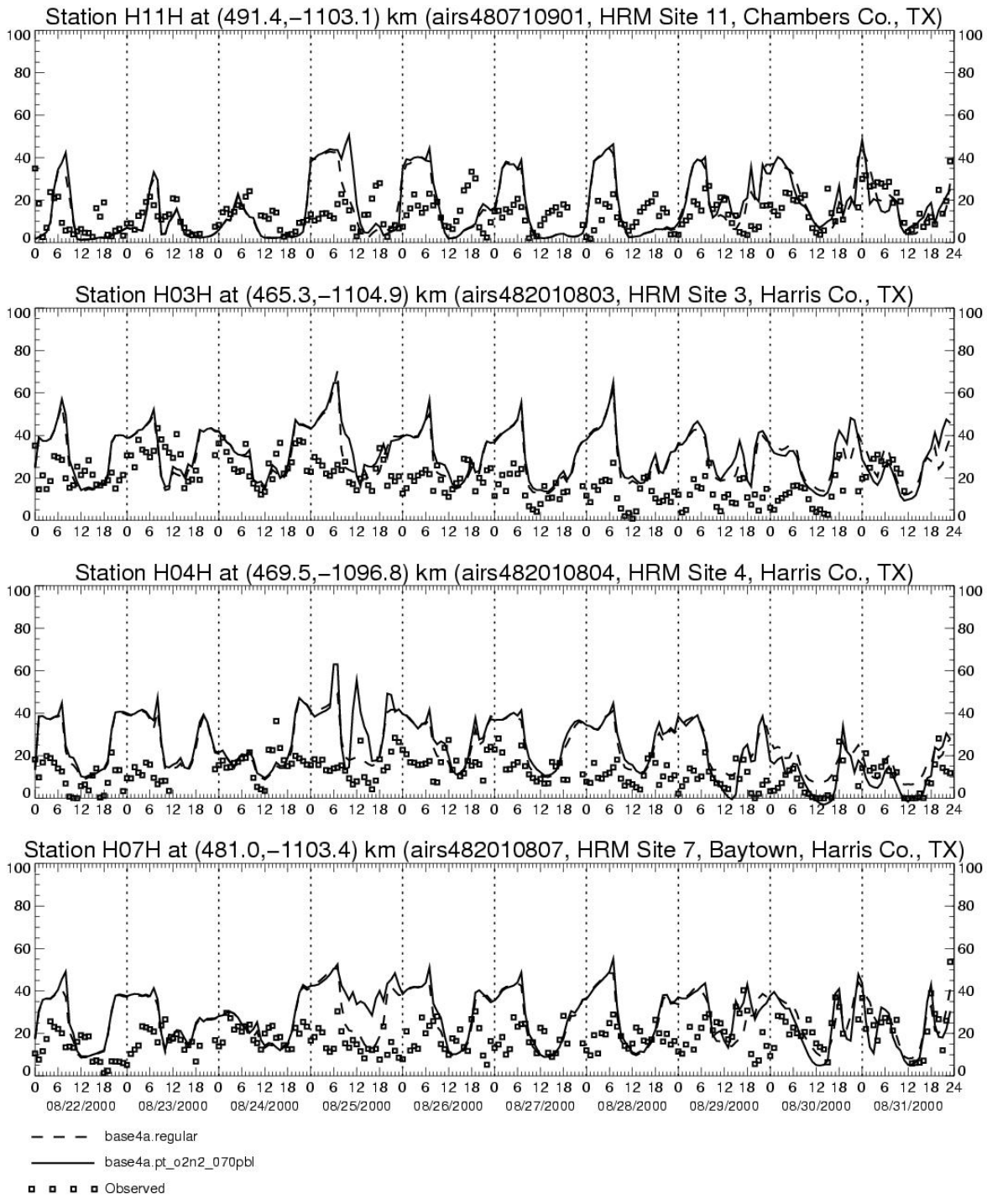

Hourly Average NO_2 Concentration (ppb) at Layer One (08/22/2000–08/31/2000)

HGMCR: base4a.pt_o2n2_070pbl vs base4a.regular

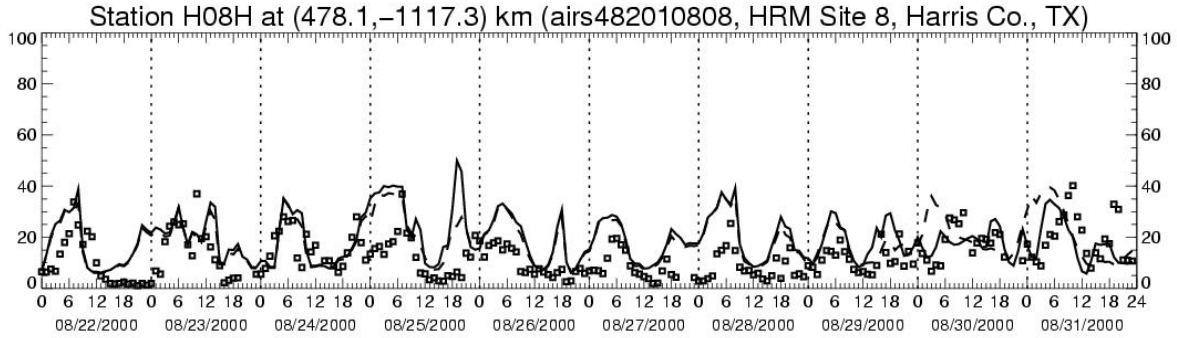

base4a.regular

base4a.pt_o2n2_070pbl

Observed

Hourly Average NO_2 Concentration (ppb) at Layer One (08/22/2000–08/31/2000)

HGMCR: base4a.pt_o2n2_070pbl vs base4a.regular

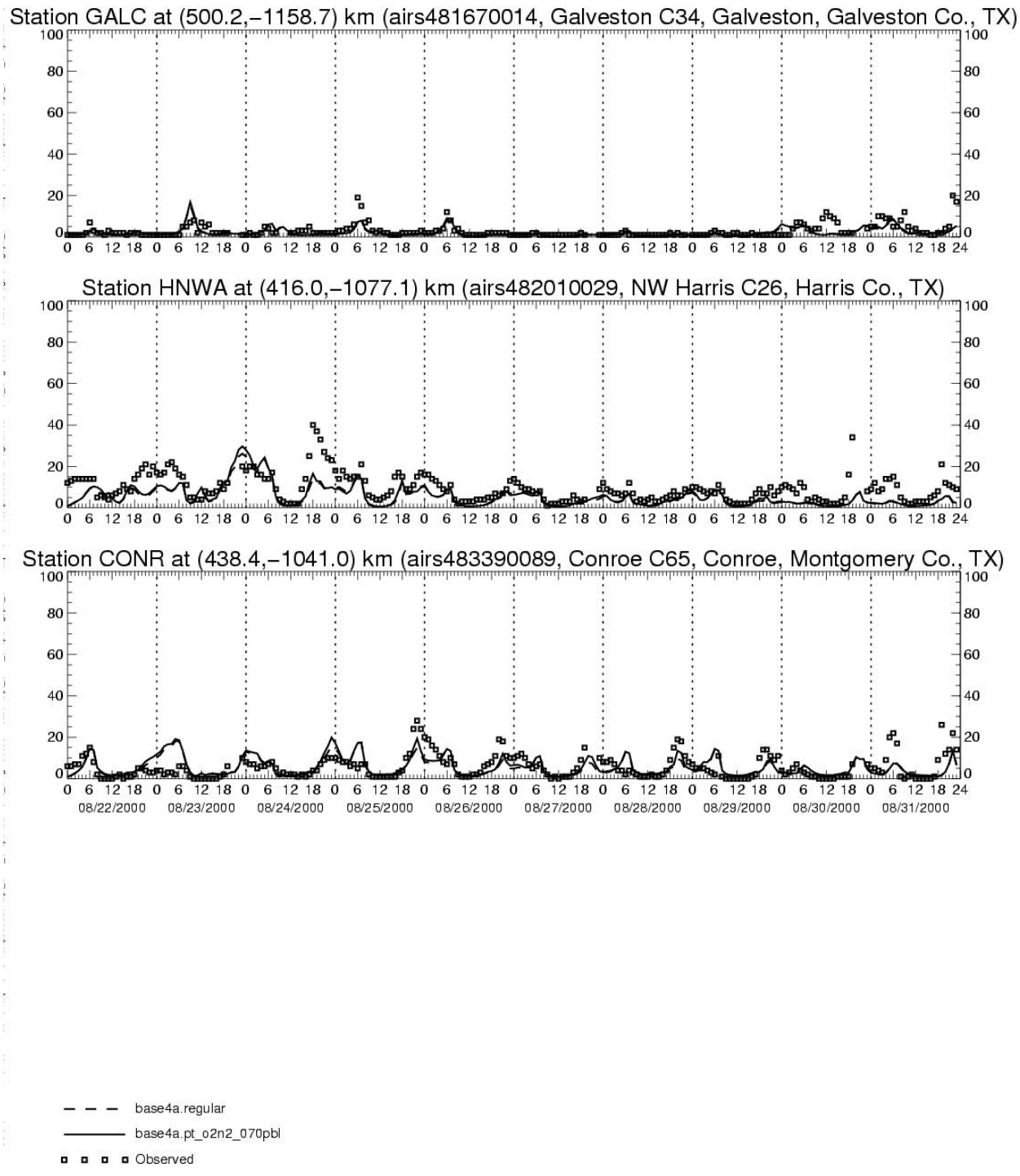

As was the case with NO, both base cases perform similarly for NO_2. Both cases tend to overpredict the ambient concentrations overnight and in the early morning, at urban locations, but generally midday predictions are reasonably accurate. Two possible causes for the overprediction are inadequate mixing and overestimation of NO_X emissions. The former cause may be mostly cosmetic, since the emissions will mix up during the day and will be available for ozone production during peak times. The latter possible cause could be related to a hypothesized over-estimation of NO_X emissions by MOBILE6, as discussed in the main body of the TSD. Some evidence in favor of the latter cause is the improved model performance seen when the on-road mobile source NO_X emissions were reduced by 25% in a sensitivity analysis.

In any case, it should be noted that the agreement between modeled and measured NO_2 concentrations improved towards the end of the episode, when the winds were generally westerly.

CO TIME SERIES

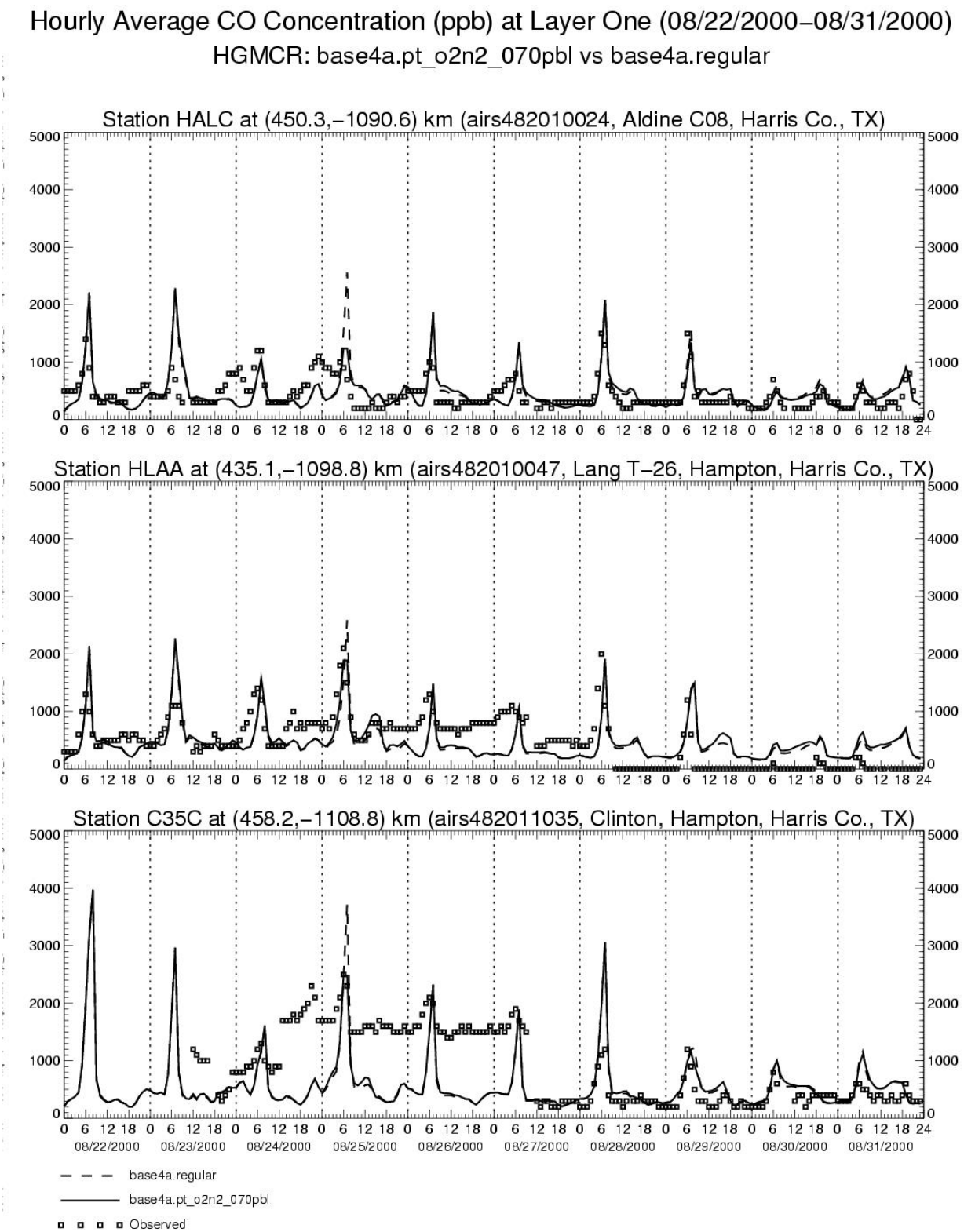

Hourly Average CO Concentration (ppb) at Layer One (08/22/2000–08/31/2000)

HGMCR: base4a.pt_o2n2_070pbl vs base4a.regular

Station HCFA at (448.0,–1107.4) km (airs482011037, Crawford T–19, Hampton, Harris Co., TX)

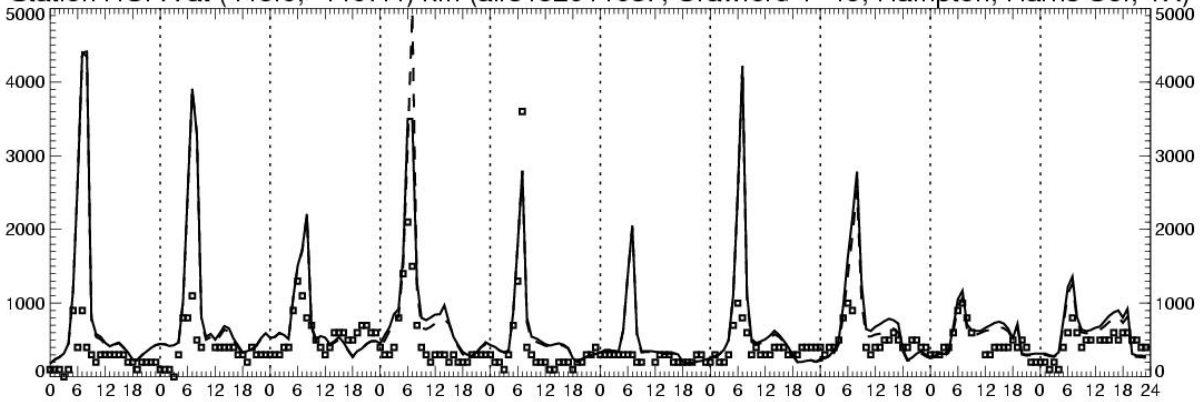

Station DRPK at (471.0,–1115.2) km (airs482011039, Deer Park C35, Deer Park, Harris Co., TX)

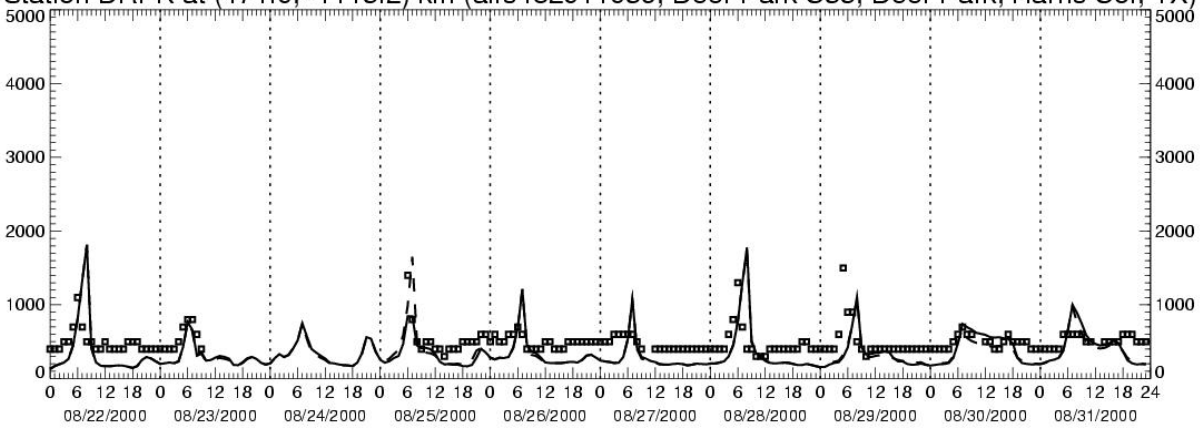

base4a.regular

base4a.pt_o2n2_070pbl

Observed

Both base cases again perform similarly with a couple of notable exceptions on August 25. The model generally predicts CO concentrations well, except for station HCFA where there is a general trend towards overprediction.

VOC TIME SERIES

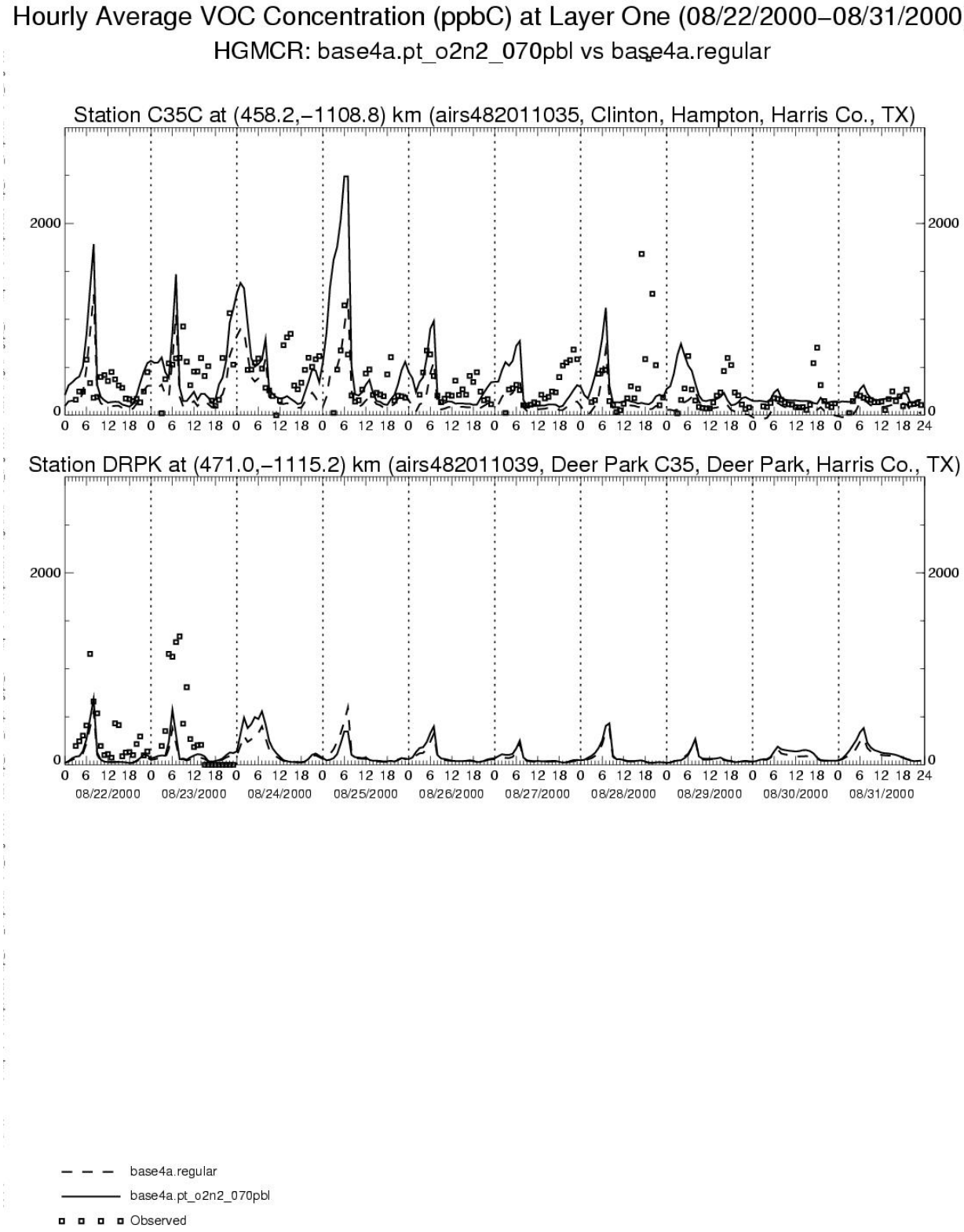

Very little ambient ground-level VOC data was collected during the episode period at the Deer Park site, due to an equipment malfunction. For the two ramp-up days available, both base cases appear to perform reasonably well, with some tendency towards underestimation. At the Clinton Drive site, both base cases actually performs reasonably well, given the variability in the ambient data. The model appears to have a tendency to overpredict VOC concentrations overnight and in the early morning, but to underpredict VOC concentrations during midday. The former tendency may be related to the model's reduced mixing during those hours, while the urban/industrial heat island might in fact generate considerable mixing overnight. While the adjusted base case clearly generated higher VOC concentrations than the unadjusted case, it is difficult to determine which matches the ambient data better.

It should be noted that the measured VOC concentrations are based on only the PAMS species, so do not represent the full suite of hydrocarbons. The modeled VOC concentrations, however, represent all emissions of VOCs. Thus the modeled VOC concentrations are biased high relative to the measurements.

Multi-pollutant Time Series at TexAQS Special Study Sites

During TexAQS, considerable amounts of ambient data were collected at the La Porte airport near the Ship Channel, and also on the 64th floor of the Williams Tower, located several miles west of downtown Houston. These rich data sets provide a rare opportunity to compare many modeled ozone precursors and intermediate species with ambient measurements. Note that ambient measurements were converted into Carbon Bond IV species whenever necessary for comparison. Also note that ozone is always shown on the first plot of each page in the following series. Only the adjusted base case is included in these plots.

WILLIAMS TOWER TIME SERIES (MODEL LAYER 4)

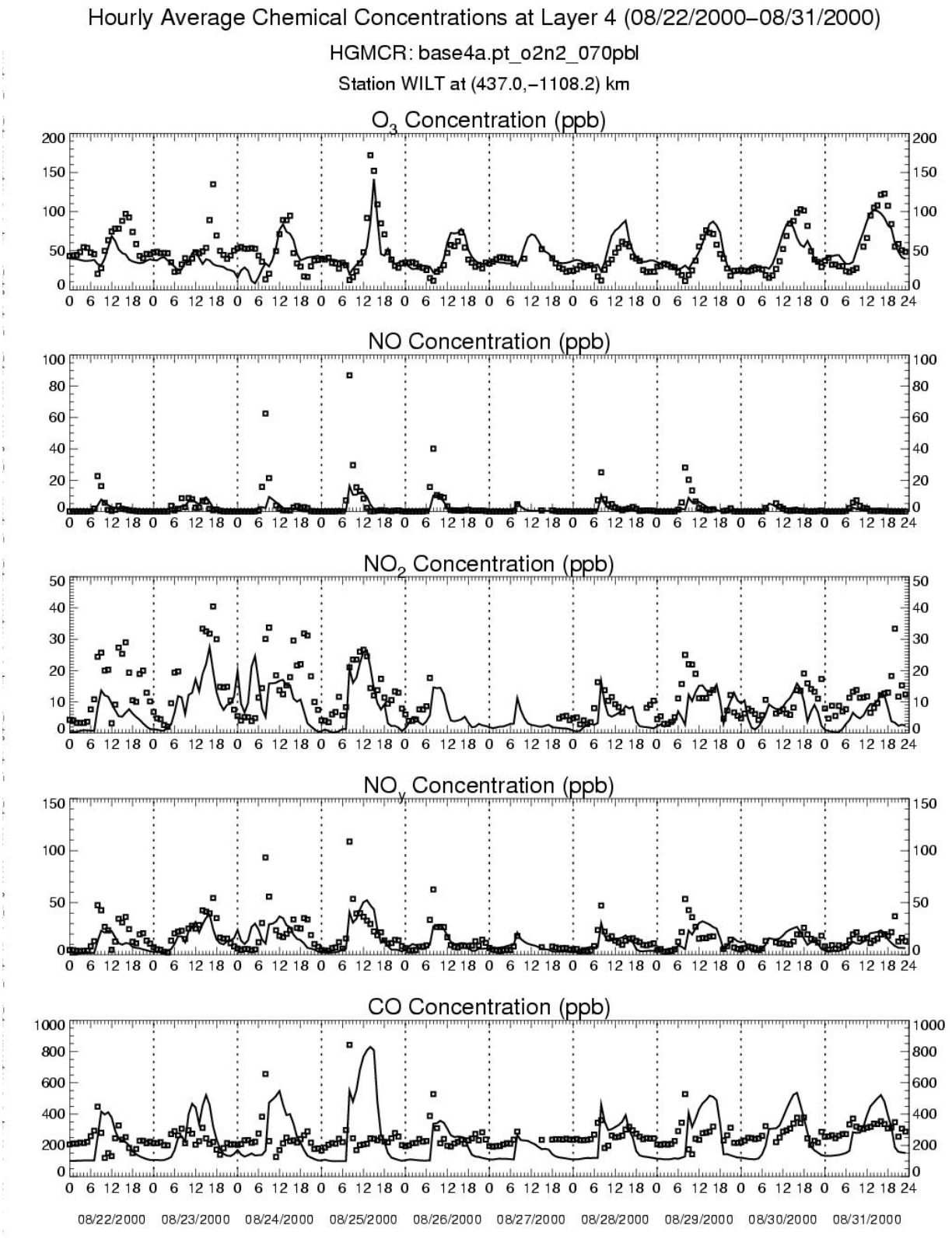

Hourly Average Chemical Concentrations at Layer 4 (08/22/2000–08/31/2000)

HGMCR: base4a.pt_o2n2_070pbl

Station WILT at (437.0,–1108.2) km

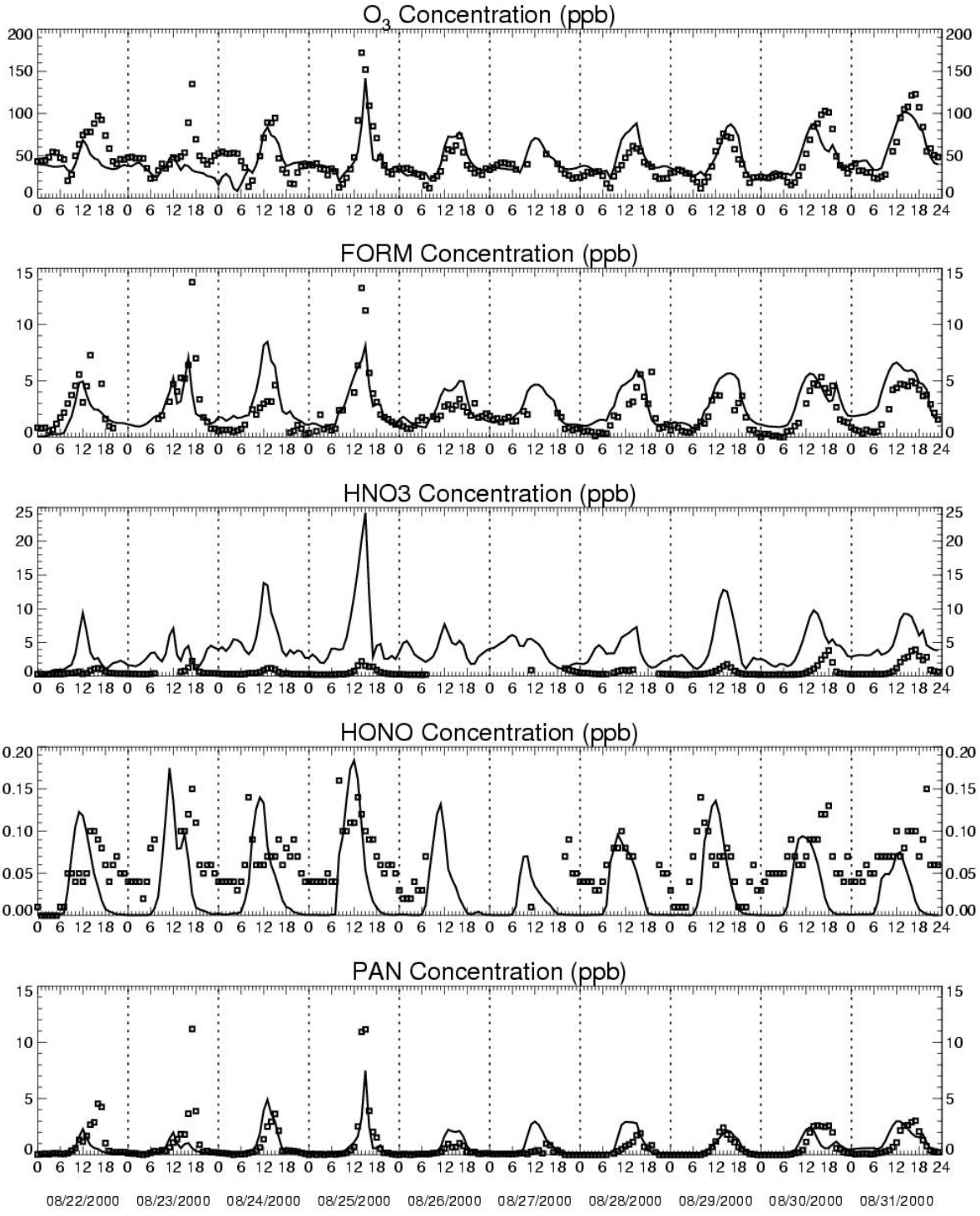

Station: airs000000000, Williams Tower, Harris Co., TX

For many species, the model performs quite well. Ozone, NO, NO_2, and NO_Y concentrations all compare favorably to measurements, except for some high measured NO and NO_Y concentrations. It is possible that the model is not mixing the morning peak motor vehicle emissions up fast enough. This hypothesis is consistent with the CO time series, which show a general underprediction overnight and in the early morning. However, during midday, the model appears to have a tendency to overpredict CO, especially on August 25.

Modeled concentrations of PAN and formaldehyde are in agreement with the measurements, and HONO agrees well during the daytime hours. However, overnight HONO concentrations are predicted to drop to zero in the model, a tendency not seen in the ambient data. The model seriously overpredicts concentrations of nitric acid. This overpredictation may not pose a problem, since nitric acid is a terminal product and, once formed, does not participate further in ozone photochemistry. If the model is simply failing to remove the nitric acid from the system, then no harm should result. If, however, the model is producing nitric acid to quickly, then it is removing radical sources from the system and retarding ozone formation. We will investigate the causes of the nitric acid overprediction during the course of the Phase II MCR modeling.

LA PORTE AIRPORT TIME SERIES

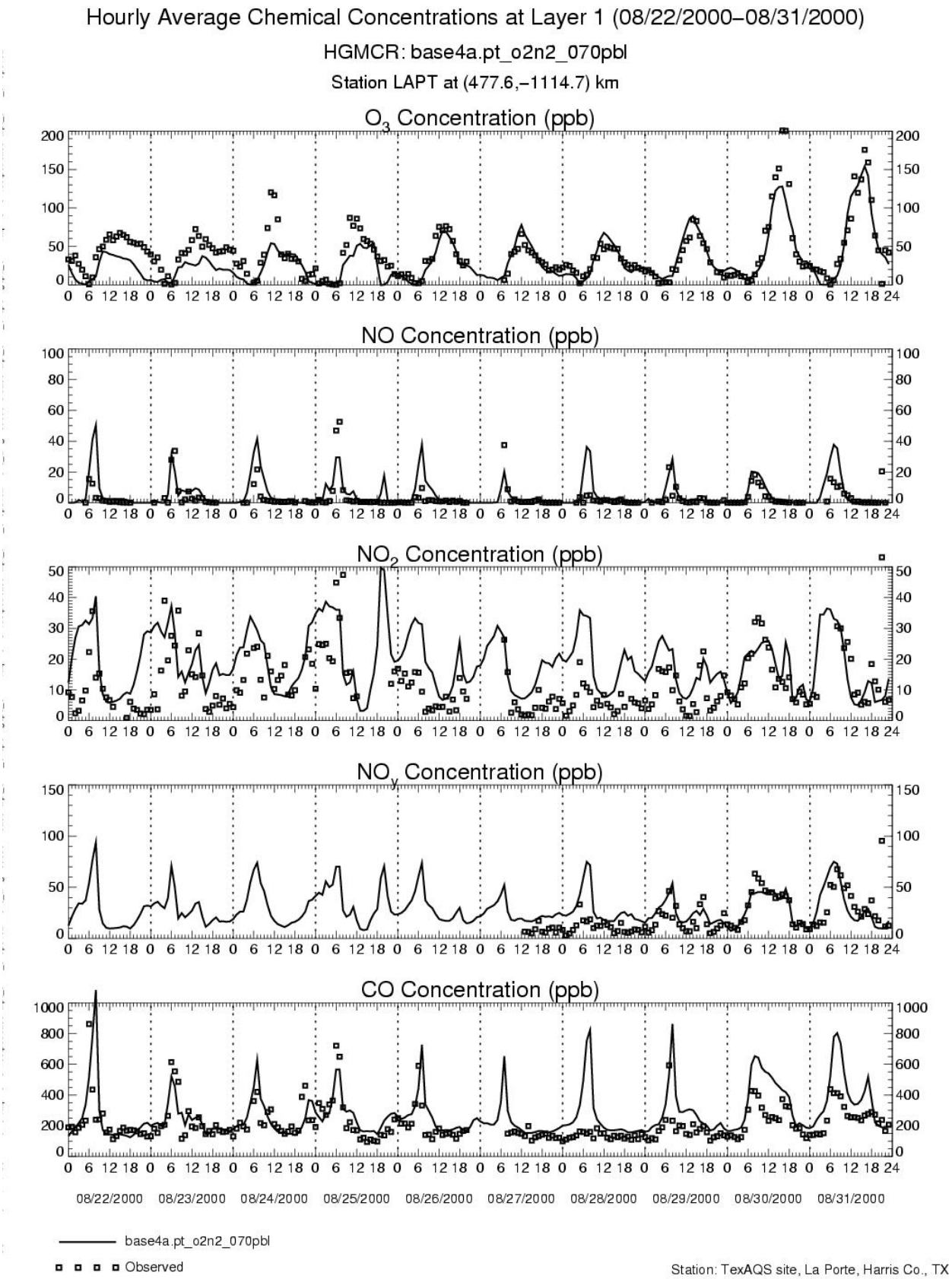

Hourly Average Chemical Concentrations at Layer 1 (08/22/2000–08/31/2000)

HGMCR: base4a.pt_o2n2_070pbl

Station LAPT at (477.6,–1114.7) km

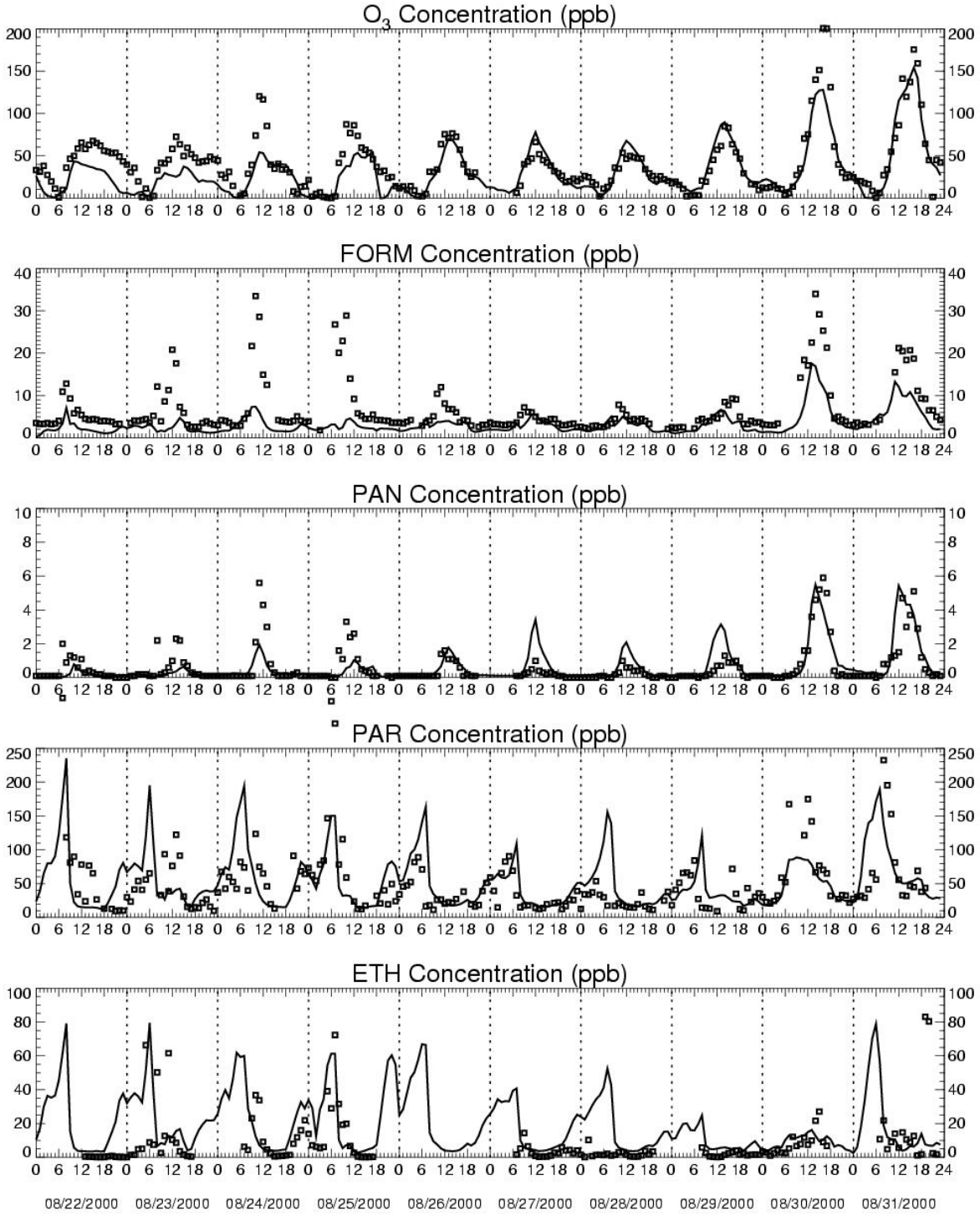

base4a.pt_o2n2_070pbl

Observed

Station: TexAQS site, La Porte, Harris Co., TX

Hourly Average Chemical Concentrations at Layer 1 (08/22/2000–08/31/2000)

HGMCR: base4a.pt_o2n2_070pbl

Station LAPT at (477.6,–1114.7) km

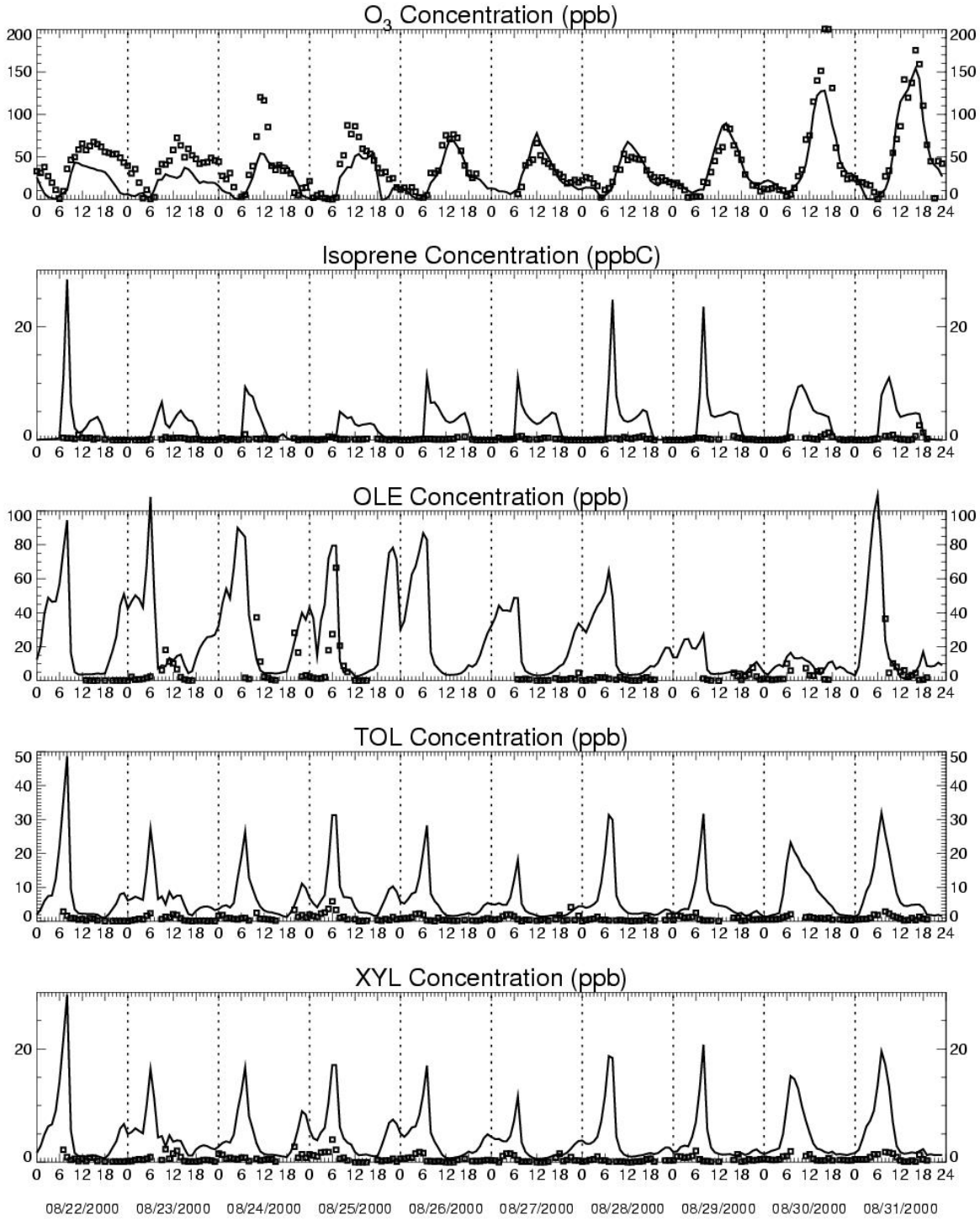

Station: TexAQS site, La Porte, Harris Co., TX

At the La Porte airport, the model appears to replicate the ozone, NO, NO_2, and NO_Y concentrations quite well. In addition, CO appears to be replicated well except for a couple of modeled morning peaks. Formaldehyde and PAN are replicated reasonably well by the model, except for a general underestimation during the first half of the episode.

The model performs remarkably well for the PAR and ETH (ethylene) species. It is interesting to note that the emissions adjustment added ETH (along with OLE), but did not add PAR to the modeled emissions. Predicted concentrations of OLE agree well with observations during the daytime, but tend to overpredict at night and in the morning (again may be due to too little vertical mixing in the model). The model significantly overpredicts daytime isoprene concentrations every day, indicating that the biogenic component is over-represented at this location (although the extremely hot and dry conditions prevalent throughout much of the episode may have inhibited normal plant metabolic processes as well).

Data for the CB-IV OLE species is fairly sparse, but the model replicated the ambient measurements extremely well on the evening of the 24th and morning of the 25th. However, a similar prediction on the 27th and 28th is not matched by the ambient data. Finally, TOL and XYL are generally overpredicted, especially in the early morning. Again note that these species were not adjusted in the model. The discrepancy between measured and modeled concentrations of these species may indicate that additional investigation into hydrocarbon speciation is warranted.

Model performance of the Base4a.pt_o2n2bs10a_m075n_070pbl sensitivity run

This section provides additional information on the performance of the sensitivity analysis described in section 2-4 of the Technical Support Document, compared with the performance of the "adjusted" base case base4a.pt_o2n2_070pbl. The comparisons presented here are all for the 1-km flexi-nest grid only, hence are only shown for the four days the flexi-nest was used (August 25 and 29-31). Note that in the ozone time series plots below there is actually a gap of 72 hours between the first 24-hour period (August 25) and the next (August 29).

After the time series plots, difference plots showing the geographic regions of higher or lower daily peak ozone concentrations are provided. Recall that on August 25, 29, and 31 the only difference between the two cases is a 25% reduction of on-road NO_X emissions, while on August 30 the sensitivity case also includes extra HRVOC emissions upwind from the NOAA canister taken that afternoon, as well as a 10 X increase in emissions from the smoking flare near Channelview. Note that the scale on the ozone difference plot for August 30 is different from that used for the other days, since the added HRVOC emissions dramatically increased daily peak ozone in some areas.

Time series comparison between Base4a.pt_o2n2bs10a_m075n_070pbl sensitivity run and Base4a.pt_o2n2__070pbl "adjusted" base case

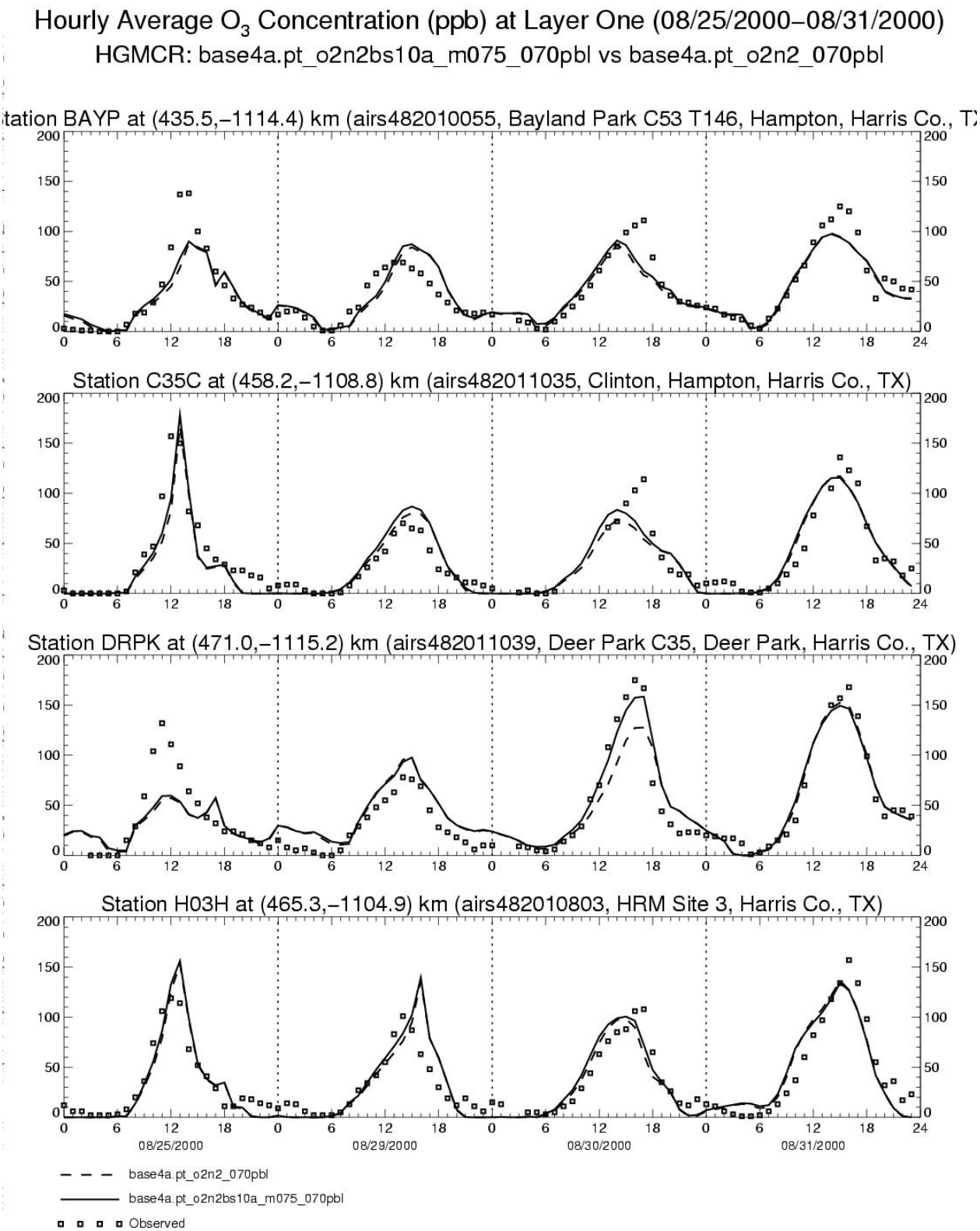

Hourly Average O_3 Concentration (ppb) at Layer One (08/25/2000–08/31/2000)

HGMCR: base4a.pt_o2n2bs10a_m075_070pbl vs base4a.pt_o2n2_070pbl

Station H04H at (469.5,–1096.8) km (airs482010804, HRM Site 4, Harris Co., TX)

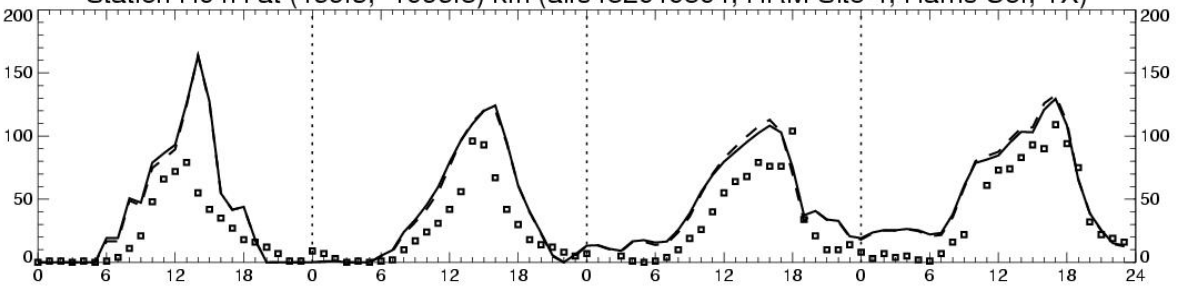

Station H07H at (481.0,–1103.4) km (airs482010807, HRM Site 7, Baytown, Harris Co., TX)

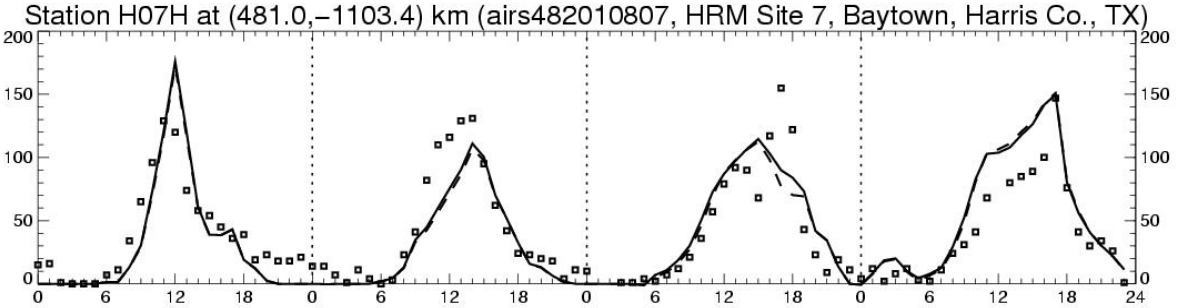

Station H08H at (478.1,–1117.3) km (airs482010808, HRM Site 8, Harris Co., TX)

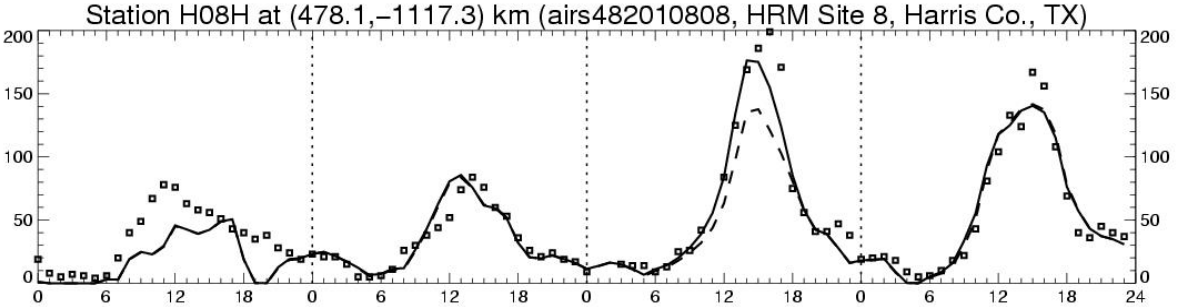

Station H10H at (489.5,–1090.7) km (airs480710900, HRM Site 10, Mont Belvieu, Chambers Co., TX)

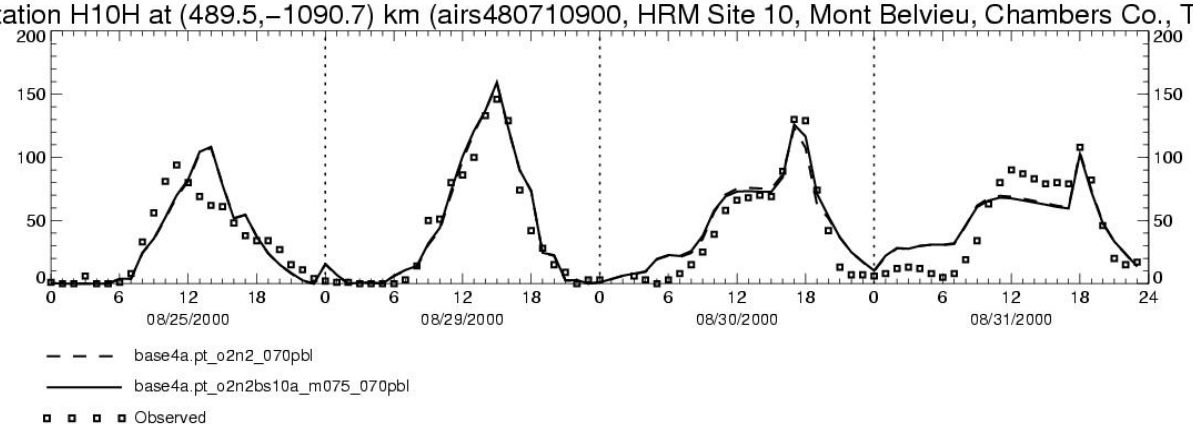

Hourly Average O_3 Concentration (ppb) at Layer One (08/25/2000–08/31/2000)

HGMCR: base4a.pt_o2n2bs10a_m075_070pbl vs base4a.pt_o2n2_070pbl

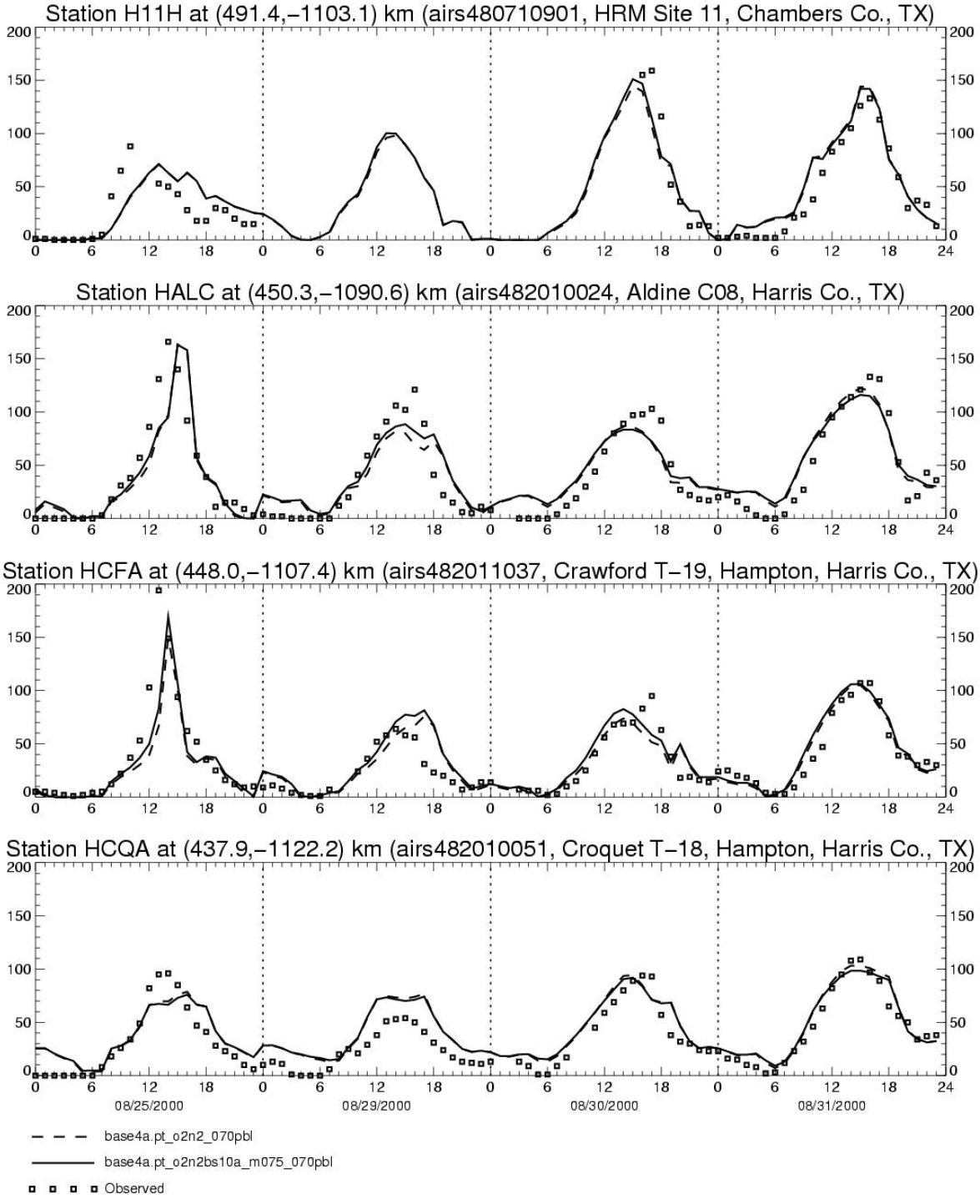

Hourly Average O_3 Concentration (ppb) at Layer One (08/25/2000–08/31/2000)

HGMCR: base4a.pt_o2n2bs10a_m075_070pbl vs base4a.pt_o2n2_070pbl

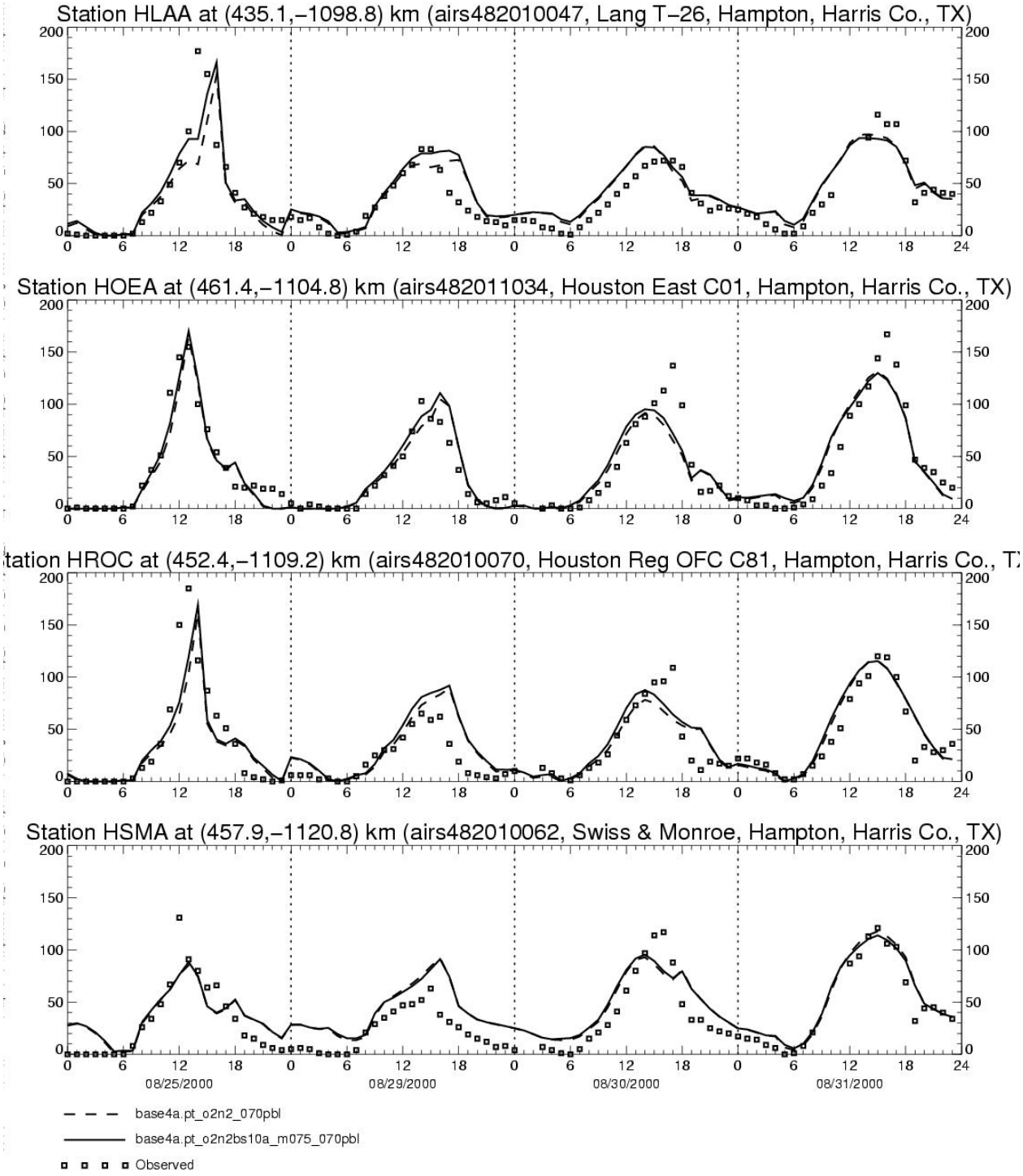

Hourly Average O_3 Concentration (ppb) at Layer One (08/25/2000–08/31/2000)

HGMCR: base4a.pt_o2n2bs10a_m075_070pbl vs base4a.pt_o2n2_070pbl

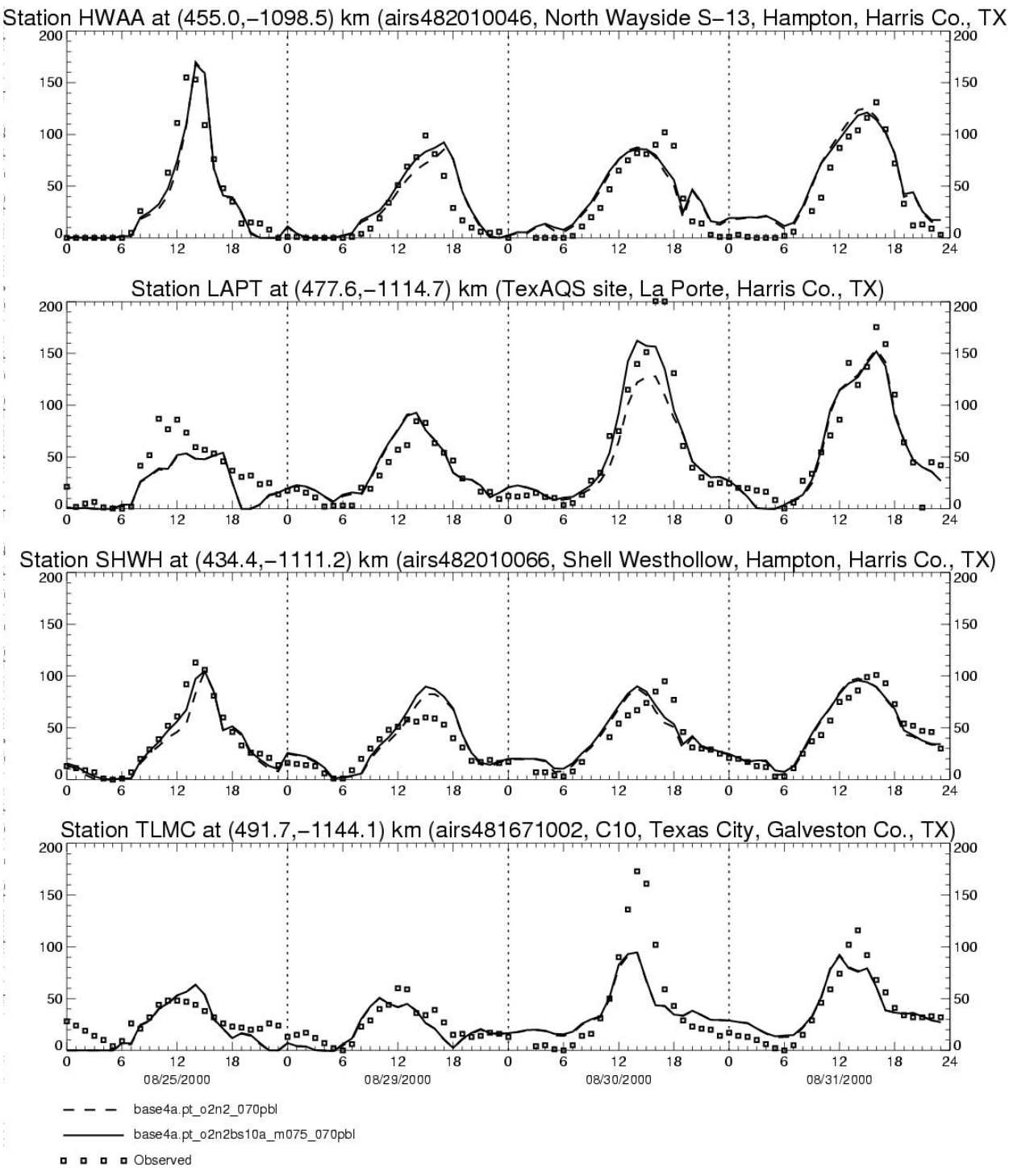

Over the first three days shown, the time series plots show a general increase in modeled ozone concentrations in the sensitivity case as compared with the base case, but the differences are fairly subtle except on August 30, where the two additional sources of HRVOC were included in the sensitivity run. It is interesting to note that on August 25 and 29, ozone concentrations generally increased as a result of reducing mobile source NO_X emissions. This phenomenon may be attributed to the scavenging of ozone by vehicular NO_X emissions, at least in the fine-grid area. On August 31, however, ozone concentrations are actually reduced slightly as a result of reducing vehicular NO_X emissions.

Daily peak ozone comparison between Base4a.pt_o2n2bs10a_m075n_070pbl sensitivity run and Base4a.pt_o2n2__070pbl "adjusted" base case

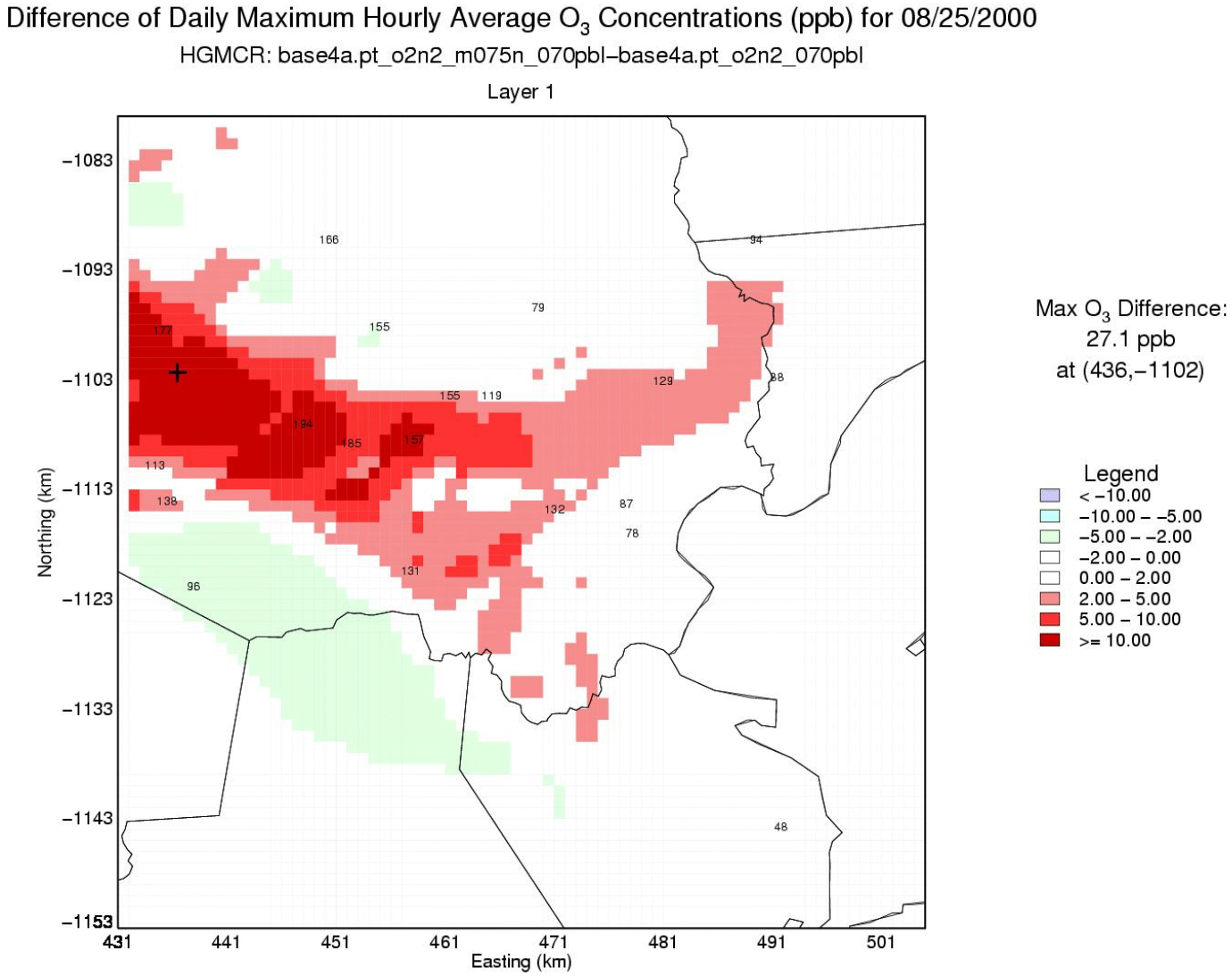

Difference of Daily Maximum Hourly Average O_3 Concentrations (ppb) for 08/29/2000

HGMCR: base4a.pt_o2n2_m075n_070pbl–base4a.pt_o2n2_070pbl

Layer 1

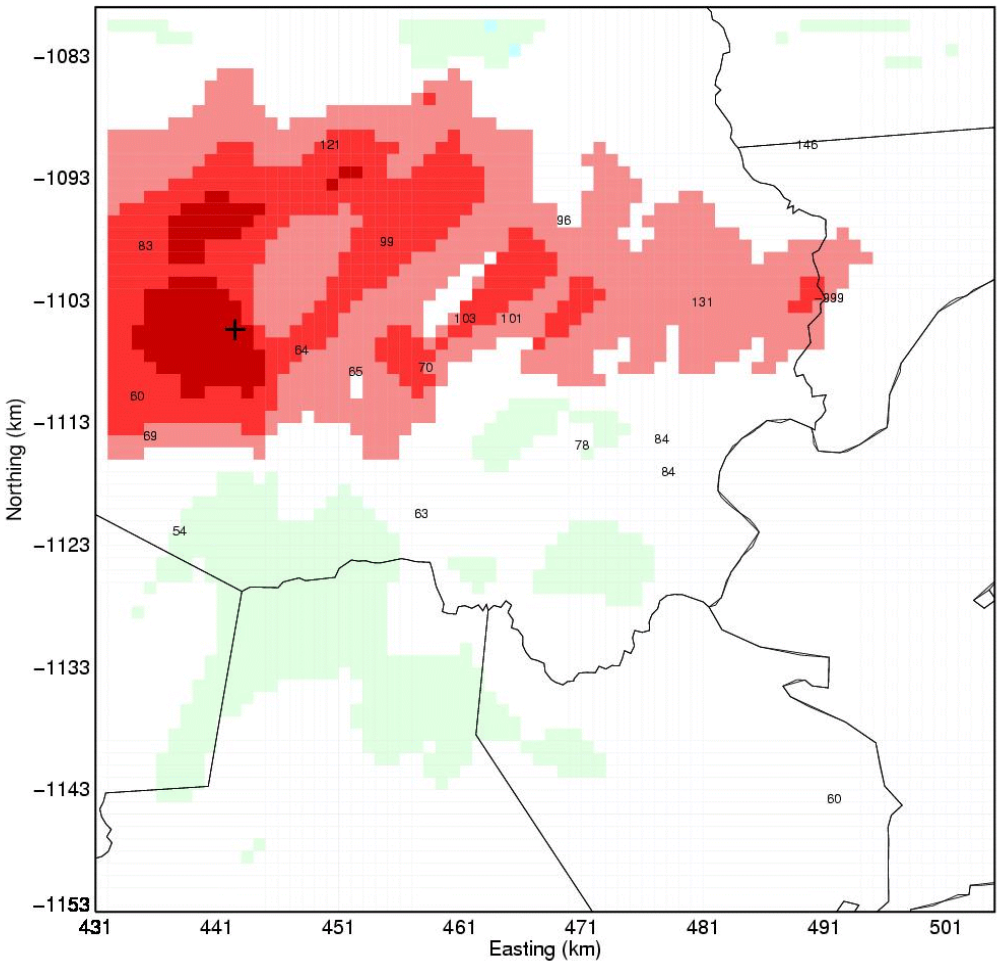

Max O_3 Difference:
13.5 ppb
at (442,−1105)

Legend
- < −10.00
- −10.00 – −5.00
- −5.00 – −2.00
- −2.00 – 0.00
- 0.00 – 2.00
- 2.00 – 5.00
- 5.00 – 10.00
- >= 10.00

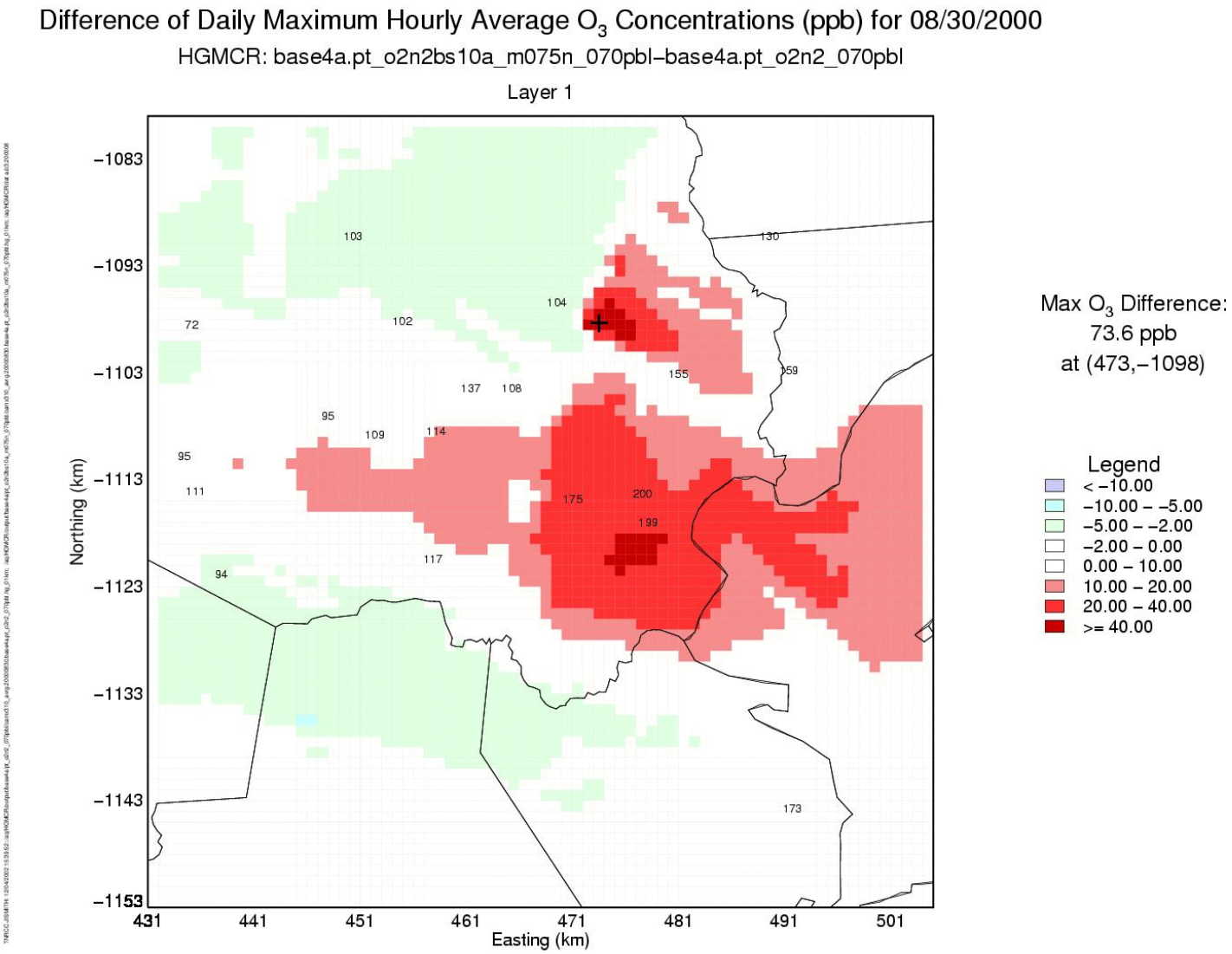

Note: The scaling on this plot differs from others in this series.

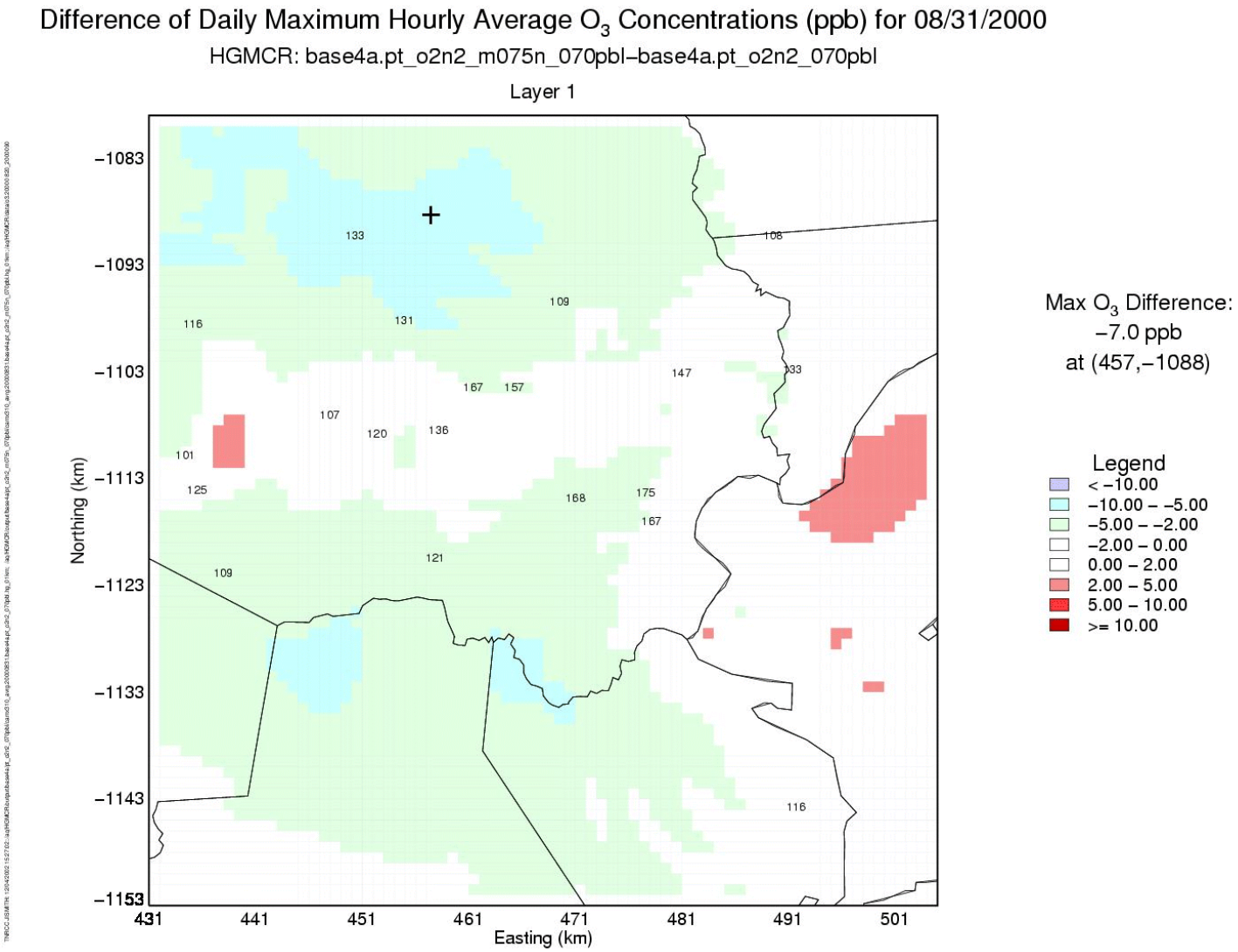

The difference plots in this section show that in all cases the reduction of on-road mobile source NO_X emissions led to increased ozone concentrations in some areas (although this effect is masked by the other changes on August 30). However, all days also show areas where reducing the NO_X emissions led to reduced peak ozone concentrations. As expected, the areas of ozone increase are generally near the urban core, while the reduced NO_X emissions led to lower ozone peaks in more rural areas. The exception to this observation occurs on August 31, where increased ozone peaks were seen in western Harris County and over the bay, while decreases occurred over a much broader area than on the other days. On August 30, the increased emissions of HRVOCs caused significant increases in peak ozone immediately downwind from the sources.